Charles University
Faculty of Science

Study programme: Genetics, Molecular Biology and Virology
Branch of study: Molecular Biology and Genetics of Eukaryota

B.Sc. Jitka Vojáčková

Functional analysis of the TSSC4 chaperone during snRNP formation
Analýza funkce chaperonu TSSC4 při formování snRNP částic

Diploma thesis

Supervisor: Assoc. Prof. David Staněk, Ph.D.

Prague, 2019

Prohlášení:

Prohlašuji, že jsem závěrečnou práci zpracovala samostatně a že jsem uvedla všechny použité informační zdroje a literaturu. Tato práce ani její podstatná část nebyla předložena k získání jiného nebo stejného akademického titulu.

V Praze, 29. 4. 2019

Jitka Vojáčková

Statement:

I hereby declare that I wrote the thesis independently and I cited all informational sources. This work or a substantial part of it was not presented to obtain another academic degree or equivalent.

In Prague, 29. 4. 2019

Jitka Vojáčková

Acknowledgements

Here, I would like to thank my supervisor, David Staněk, for great leading and support during my master studies. Many thanks also belong to all members of the Laboratory of RNA biology for a supportive and friendly working environment. Finally, I would like to thank my family for their endless support during my studies.

This work was supported by The Grant Agency of the Czech Republic from the project: Principles of snRNP sequestration into cellular structures, no. 18-10035S

Abstrakt

Sestřih je proces, během kterého jsou nekódující sekvence (introny) vystřiženy z pre-mRNA a exony spojeny. Celý tento proces je katalyzován multi-megadaltonovým sestřihovým komplexem, který se skládá z pěti malých jaderných ribonukleoproteinových částic (zkráceně snRNP částice), jenž každá obsahuje svoji vlastní malou jadernou RNA a sadu proteinů specifických pro každou částici. Během biogeneze snRNP částic jsou U4 a U6 snRNP částice spojeny za vzniku di-snRNP částice, která je dále asociována s U5 snRNP částicí a tím dává vzniku tri-snRNP. S pomocí hmotnostní spektrometrie jsme nalezly dříve necharakterizovaný protein interagující s U5 snRNP částicí, zvaný TSSC4. S použitím imunoprecipitace jsem potvrdila specificitu TSSC4 pro U5 snRNP a nalezla oblast TSSC4 zodpovědnou za interakci s U5 snRNP. Nezávisle na U5 snRNP částici, TSSC4 interaguje s PRPF19, komponentem komplexu, který se účastní katalytické aktivace sestřihového komplexu. Snížení koncentrace TSSC4 v HeLa buňkách způsobuje akumulaci di-snRNP specifických RNA a U5 snRNP částice v Cajalových tělískách, jaderných organelách důležitých pro biogenezi snRNP částic. Podobný fenotyp byl dříve pozorován po zastavení tvorby tri-snRNP částice. Abych otestovala důležitost TSSC4 pro vznik tri-snRNP, pomocí gradientové ultracentrifugace jsem rozdělila jednotlivé snRNP částice podle jejich sedimentačních vlastností. Po depleci TSSC4 v HeLa buňkách jsem pozorovala snížený obsah tri-snRNP částice. Neefektivní skládání tri-snRNP dále podporuje akumulace proteinu 52K v Cajalových tělískách, U5 snRNP specifického proteinu, který nebyl nalezen v tri-snRNP částici. Dále po snížení obsahu TSSC4 v HeLa buňkách ukazuji sníženou interakci mezi dvěma klíčovými proteiny U5 snRNP částice – PRPF8 a SNRNP200. Navrhuji tedy TSSC4 jako nový U5 snRNP specifický faktor důležitý pro skládání tri-snRNP částice.

Klíčová slova

Sestřihový komplex, male jaderné ribonukleoproteinové částice, TSSC4

Abstract

Splicing is a process, during which non-coding sequences (introns) are cleaved out of pre-mRNA, and exons are ligated. This whole process is catalysed by a multi-megadalton splicing complex, composed of five small nuclear ribonucleoprotein particles (shortly snRNPs), which each contains its own small nuclear RNA molecule and specific set of proteins. During the biogenesis of snRNPs, U4 and U6 snRNPs are assembled to form the di-snRNP, which further associates with U5 snRNP and gives rise to tri-snRNP. With the help of mass spectrometry, we have found previously uncharacterized protein interacting with U5 snRNP, called TSSC4. By immunoprecipitation, I confirmed TSSC4 as a U5 snRNP specific protein and identified the region of TSSC4 responsible for interaction with U5 snRNP. I also showed that TSSC4 interacts with PRPF19, a component of complex driving the catalytic activation of the spliceosome and that this interaction is U5 snRNP-independent. Knockdown of TSSC4 in HeLa cells results in accumulation of di-snRNAs and U5 snRNP in Cajal bodies, nuclear compartments involved in snRNP biogenesis. Similar phenotype was previously observed upon inhibition of tri-snRNP assembly. To analyse the importance of TSSC4 for tri-snRNP assembly, I separated individual snRNPs by glycerol gradient ultracentrifugation according to their sedimentation coefficient. Upon TSSC4 depletion in HeLa cells, I observed lower levels of tri-snRNP formation. Ineffective tri-snRNP assembly is further supported by the accumulation of 52K in Cajal bodies, which is U5 snRNP specific protein absent in tri-snRNP. I also show loosened interaction between two core components of U5 snRNP – PRPF8 and SNRNP200 upon TSSC4 depletion in HeLa cells. I thus propose TSSC4 as a novel U5 snRNP specific factor important for tri-snRNP assembly.

Keywords

Spliceosome, small nuclear ribonucleoprotein particles, TSSC4

Contents

Abbreviations

APS	Ammonium persulfate
BP	Branch point
BSA	Bovine serum albumin
CB	Cajal body
CBC	Cap-binding complex
cDNA	Complementary DNA
CRM1	Chromosome region maintenance 1
DAPI	4′,6-diamidino-2-phenylindole
DSE	Distal signal element
DTT	Dithiothreitol
EDTA	Ethylenediaminetetraacetic acid
EGFP	Enhanced green fluorescent protein
EGTA	Ethyleneglycoltetraacetic acid
FISH	Fluorescence *in situ* hybridisation
GFP	Green fluorescence protein
hnRNP	Heterogeneous nuclear ribonucleoprotein
IF	Immunofluorescence
Imp β	Importin β
IP	Immunoprecipitation
LSm	Like-Sm
m1Gppp	Monomethylguanosine cap
m3Gppp	Trimethylguanosine cap
Nt	Nucleotide
NTC	Nineteen complex
NTR	NTC-related complex
PBS	Phosphate buffered saline
PHAX	Phosphorylated adaptor for RNA export
pICln	Chloride ion current unducer protein
PIPES	Piperazine-N,N′-bis(2-ethanesulfonic acid)
PMSF	Phenylmethanesulfonyl fluoride
PNK	T4 Polynucleotide kinase
PPT	Polypyrimidine tract

PRMT5	Protein arginine methyltransferase 5
PRPF	pre-mRNA processing factor
PSE	Proximal sequence element
SART3	Squamous cell carcinoma antigen recognised by T-cells 3
scaRNA	Small Cajal body-specific RNA
SDS	Sodium dodecyl sulfate
siRNA	Small interfering RNA
SMN	Survival of motor neuron
SNAPc	snRNA-activating protein complex
snoRNP	Small nucleolar ribonucleoprotein
snRNA	Small nuclear RNA
snRNP	Small nuclear ribonucleoprotein
SPN1	Snurportin 1
ss	Splice site
SSC	Saline-sodium citrate
TBE	Tris-Borate-EDTA
TEMED	Tetramethylethylenediamine
TGS1	Trimethylguanosine synthetase 1
TSSC4	Tumour Suppressing Subtransferable Candidate 4
U2AF	U2 snRNP auxiliary factor
USP	Ubiquitin specific peptidase
WB	Western blot
γ-m-P_3	γ-monomethyl triphosphate

1 Introduction

In the process of gene expression in eukaryotic cells, the DNA is transcribed as pre-mRNA, which undergoes several processing steps and forms the mRNA molecule that can serve as a messenger for protein synthesis. One of these processing steps is splicing, during which the non-coding regions called introns are spliced out of the pre-mRNA molecule, and coding exons are ligated.

Splicing is catalysed by a multi-megadalton complex called spliceosome. The spliceosome is one of the most complex machineries in a cell, composed of five small nuclear ribonucleoprotein particles (shortly snRNPs), namely U1, U2, U4, U5 and U6 snRNPs. Each of these snRNPs contains an RNA molecule with the same name and a specific set of proteins.

Spliceosomal snRNPs are assembled in a complex pathway that includes a nuclear and cytoplasmatic stage. Considering the complexity of spliceosomal snRNPs, it is only logical, that there are several cofactors and chaperones involved in the assembly process. For example, in the assembly process of U5 snRNP, R2TP complex serves as an assembly chaperone (Malinova et al. 2017). Thanks to the high sensitivity of mass spectrometry and structural analysis of the spliceosomal complexes, there is an increasing number of previously unobserved proteins identified in interaction with spliceosomal snRNPs and thus increasing number of potential spliceosomal assembly factors. The function of many of these potential spliceosomal assembly factors is so far not understood.

The main aim of this thesis is to analyse a function of the previously undescribed factor TSSC4, which we recently found in a complex with U5 snRNP (Malinova et al. 2017). Understanding the function of this novel factor would help overall knowledge about U5 snRNP assembly.

2 Literature review

The catalytic splicing complex is assembled from five small nuclear ribonucleoprotein particles (snRNPs), which needs to be separately assembled to be able to form the spliceosome. The splicing complex is composed of U1, U2, U4, U5 and U6 snRNPs and is responsible for splicing of canonical introns. Minor spliceosome, containing U11, U12, U4atac, U6atac and U5snRNPs ensures splicing of non-canonical introns. Since this work is focused on the assembly of snRNPs in major spliceosome, I will not further discuss minor spliceosome and splicing.

Each snRNP consists of specific U-rich snRNA molecule (two in case of U4/U6 di-snRNP and three in case of U4/U6.U5 tri-snRNP), a common ring of Sm proteins (or LSm proteins in case of U6 snRNP) and a set of proteins specific for individual snRNP (shown in figure 2.1).

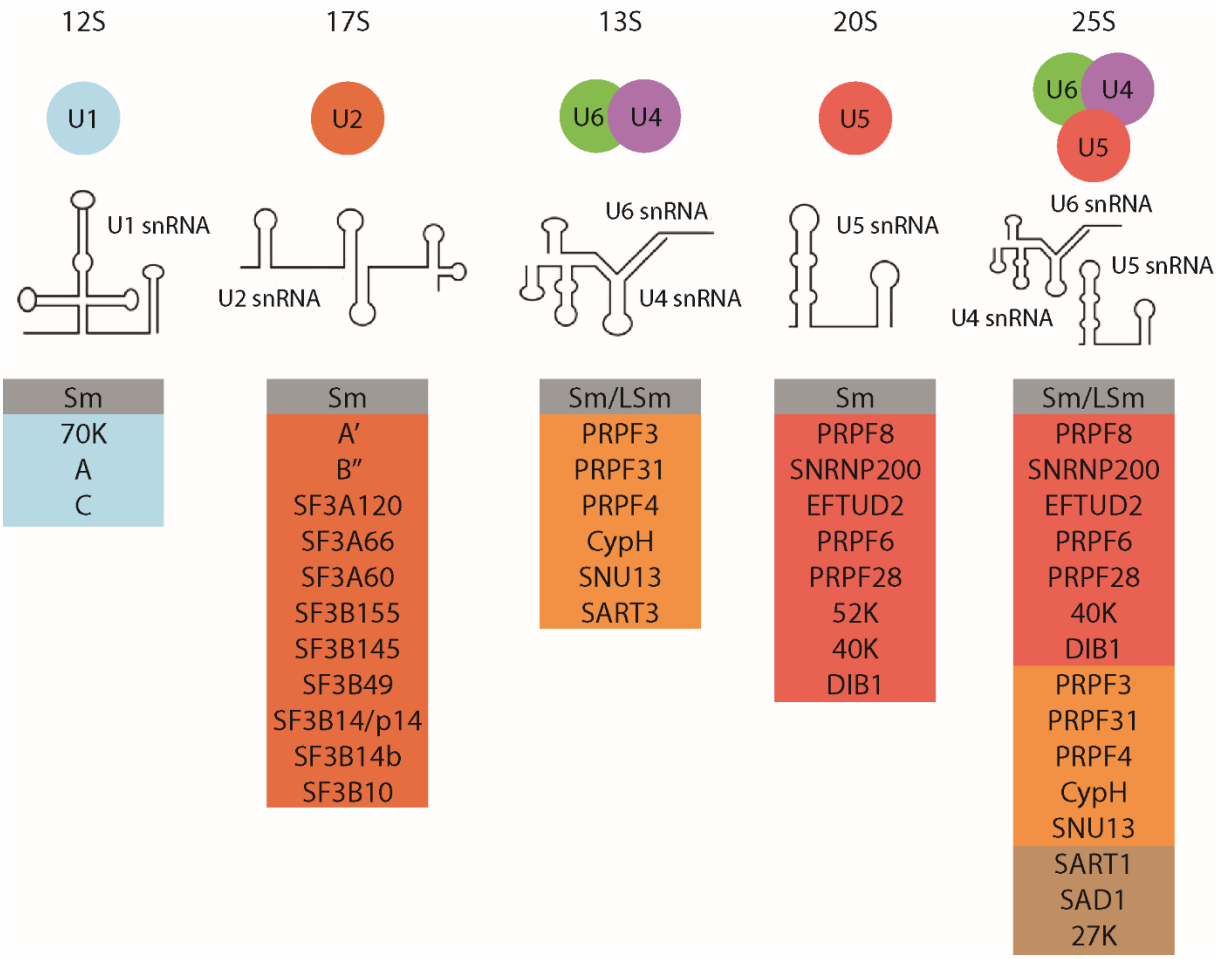

Figure 2.1 The components of snRNPs
The spliceosome is assembled from five small nuclear ribonucleoprotein particles, which are for simplicity shown here as colourful bubbles. Sedimentation coefficient, most probable secondary structure of snRNA, presence of either Sm or LSm ring and specific proteins for each snRNP are shown (adapted from Will & Luhrmann 2011).

2.1 Biogenesis of small nuclear RNPs

Small nuclear RNAs transcribed by RNA polymerase II, namely U1, U2, U4 and U5 snRNAs (see below) share a common biogenesis pathway, whereas biogenesis of U6 snRNA as an RNA polymerase III transcript differs (see chapter 2.1.6).

2.1.1 Transcription of small nuclear RNAs

Small nuclear RNAs (snRNAs) are transcribed by RNA polymerase II or, in case of U6 snRNA, by RNA polymerase III. The RNA polymerase III-transcribed U6 snRNA genes have a proximal sequence element (PSE) and a TATA-box sequence present in the basal promoter. The RNA polymerase II-transcribed snRNA genes have the same PSE but are lacking the TATA-box (figure 2.2). Both types of snRNA promoters can be recognised by a common snRNA-activating protein complex ($SNAP_c$) which drives the snRNA genes transcription initiation by both RNA polymerases (Sadowski et al. 1993). The TATA-box sequence is the decisive factor, which directs the recognition of the promoter by either RNA polymerase II or III (Lobo & Hernandez 1989, Mattaj et al. 1988). Promoter regions for both polymerases further contain distal sequence element (DSE), which enhances transcription efficiency (Schaub et al. 1997).

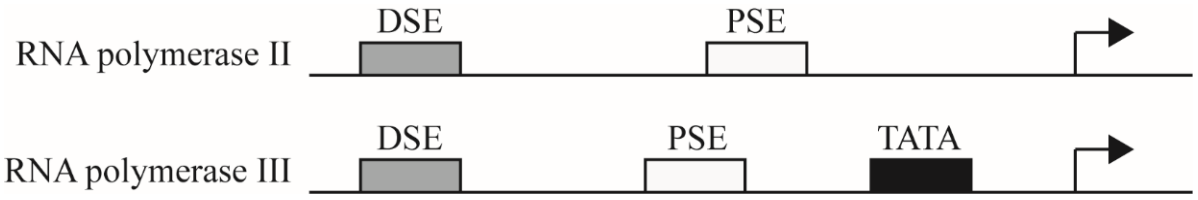

Figure 2.2 Scheme of snRNA genes promoter
Both types of snRNA promoters contain distal and proximal sequence elements. However, RNA polymerase III type promoter has additional TATA box. Arrows mark the transcription initiation position. DSE – distal sequence element, PSE – proximal sequence element, TATA – TATA box (adapted from Schaub et al. 1997)

Transcription termination and 3′ end processing of snRNA genes in yeast are driven by specific proteins, such as Ndr1 and nuclear exosome complex (Steinmetz et al. 2001, Vasiljeva & Buratowski 2006). In higher eukaryotes, snRNAs transcribed by RNA polymerase II are transcribed beyond the 3′ end of snRNA (Cuello et al. 1999, Madore et al. 1984). This prolonged snRNA transcript is bound by Integrator complex and catalytically cleaved at the 3′ end of snRNA (Baillat et al. 2005, O'Reilly et al. 2014). For U6 snRNA, as an RNA polymerase III transcript, T cluster in transcribed sequence serves as a signal for transcription termination and RNA polymerase III does not need any additional factors for termination (Bogenhagen & Brown 1981, Cozzarelli et al. 1983).

2.1.2 snRNA export to the cytoplasm

After transcription, snRNAs are transported to the cytoplasm. As an RNA polymerase II transcripts, Sm snRNAs are capped with 5′ monomethyl cap and bound by Cap binding complex (CBC), which is necessary for transport to the cytoplasm (Hamm & Mattaj 1990, Izaurralde et al. 1995). Sm snRNAs are further bound by phosphorylated adaptor for RNA export (PHAX), which contains leucine-rich nuclear export signal and thus serves as an adaptor between CBC/RNA complex and CRM1/RanGTP complex, common export receptor recognising the leucine-rich nuclear export signal (reviewed in Hutten & Kehlenbach 2007). In the cytoplasm, the PHAX complex is dephosphorylated by PP2A phosphatase and disassembled (Kitao et al. 2008, Ohno et al. 2000).

The export pathway to the cytoplasm is very similar as for mRNAs, which are also capped with 5′ monomethyl cap and bound by CBC. However, CRM1/RanGTP directly binds the CBC/RNA and the export pathway of mRNAs is independent on PHAX. It was shown, that length of RNA is the decisive factor that directs the export of RNA by either PHAX dependent or independent manner in a way, that shorter RNAs, such as snRNAs, are driven to PHAX dependent export pathway (Masuyama et al. 2004). As a molecular ruler that measures the length of RNA serves the heterogeneous nuclear ribonucleoprotein (hnRNP) C1/C2 tetramer that binds the unstructured RNA longer than 200-300 nt, such as mRNA (figure 2.3). C1/C2 hnRNP inhibits binding of PHAX complex, and mRNA is thus exported to the cytoplasm independently on PHAX complex (McCloskey et al. 2012).

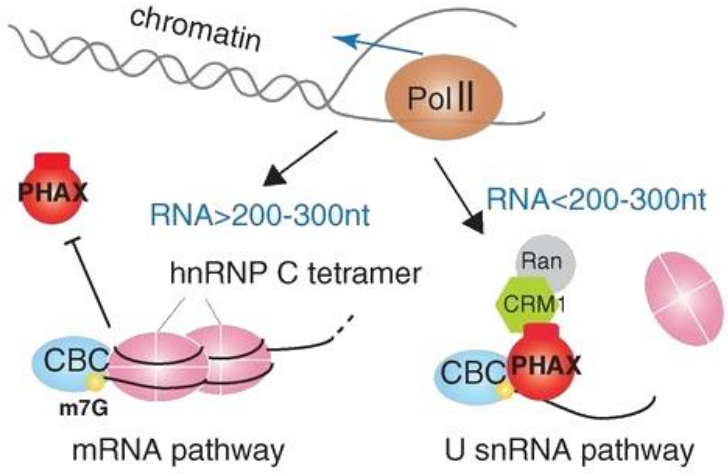

Figure 2.3 Mechanism of the C1/C2 hnRNP in RNA nuclear export
C1/C2 hnRNP is not bound on short snRNAs and thus enables binding of the PHAX complex, which drives nuclear export of snRNAs. PHAX – phosphorylated adaptor for RNA export, CBC – cap-binding complex, Pol II – RNA polymerase II, CRM1/Ran – export receptor, m7G – 7-methylguanosine cap (taken from McCloskey et al. 2012).

Cytoplasmic stage of snRNA biogenesis includes Sm ring assembly, snRNA 3′ end trimming and cap trimethylation (shown in figure 2.5).

2.1.3 Sm ring assembly

Sm ring is assembled from seven Sm proteins named SmB, SmD1, SmD2, SmD3, SmE, SmF and SmG. Sm proteins are part of Sm protein family (together with LSm proteins forming U6 snRNA Sm ring, see chapter 2.1.6) defined by two conserved regions (Hermann et al. 1995). Sm proteins can be non-specifically bound to RNA and it was shown for U1 snRNA, that the Sm ring is capable of forming *in vitro* (Raker et al. 1996). *In vivo*, the Sm ring assembly is secured by two protein complexes, the protein arginine methyltransferase 5 (PRMT5) complex and the survival of motor neuron (SMN) complex (Meister & Fischer 2002).

The PRMT5 complex containing pICln assembly chaperone dimethylates the arginines in GR repeat domains, present in SmB/B′, SmD1 and SmD3 (Meister et al. 2001). Sm proteins are further assembled in two pICln containing assembly intermediates, a ring-shaped 6S complex composed of SmD1, SmD2, SmE, SmF, SmG and pICln, where pICln acts as Sm mimic to complete the circle. The second Sm ring assembly intermediate is heterotrimer composed of SmB, SmD3 and pICln (Friesen et al. 2001, Chari et al. 2008). As mentioned, Sm proteins are able to spontaneously bind uridine-rich RNA, but interaction with pICln inhibits unspecific RNA interactions. Sm assembly intermediates containing pICln are further bound by the SMN complex, which ensures specific binding with snRNAs (Pellizzoni et al. 2002).

Apart from SMN protein, the SMN complex contains Gemins 2-8 and protein Unrip, that together forms the complex via a network of protein/protein interactions (Otter et al. 2007). The 6S assembly intermediate is bound to SMN and creates the 8S complex, in which the Gemin 2 is responsible for releasing of the pICln (Grimm et al. 2013). Gemin 5 directs the interaction of the SMN complex and snRNA (Yong et al. 2010), which is bound by the GW repeat domain of Gemin 5 at the specific sequence called Sm site (Lau et al. 2009). In the transition between the pICln containing complex and loading on the snRNA where the Sm ring is finished with SmB/B′ and SmD3, the 8S intermediate is thought to be stabilised by the TUDOR domain of SMN complex, which resembles the structure of Sm proteins (Selenko et al. 2001). The whole pathway of the Sm ring assembly is shown in figure 2.4.

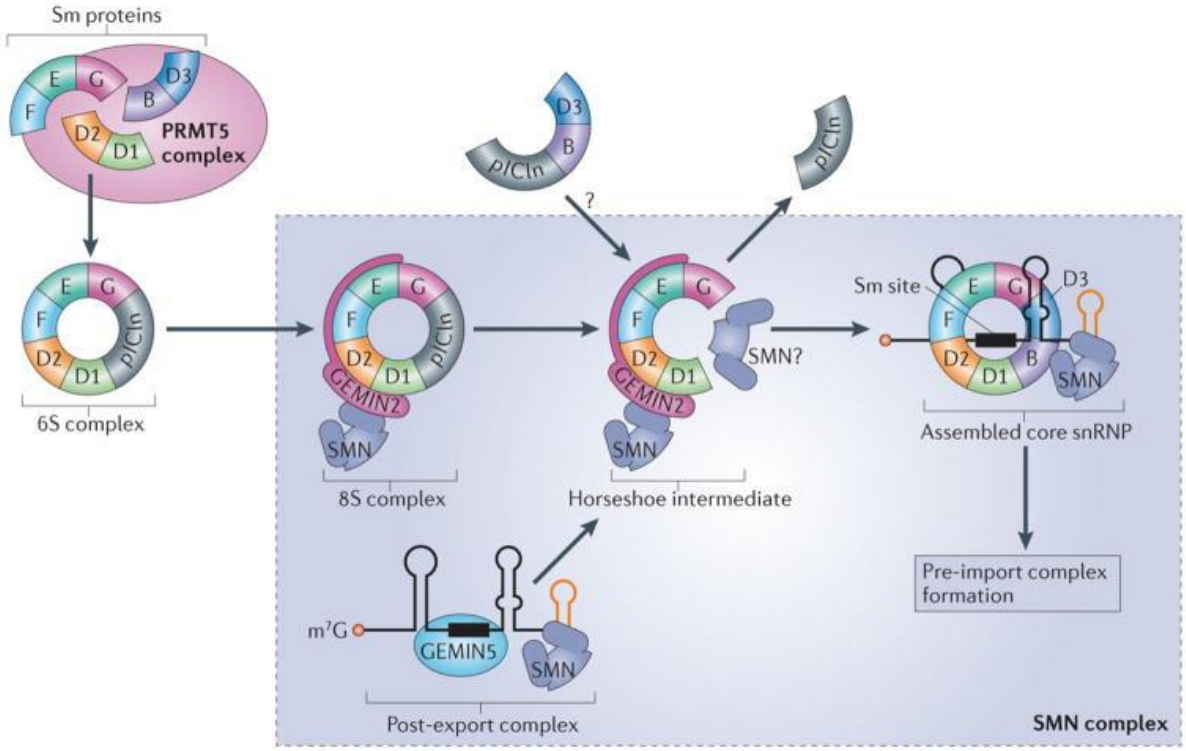

Figure 2.4 The Sm ring assembly pathway
PRMT5 dimethylates Sm proteins that contain GR repeat domains (SmB/B′, SmD1 and SmD3). Sm proteins further form assembly intermediates containing pICln. 6S Sm assembly intermediate is bound by SMN complex and by Gemin 5, present in SMN complex directed on snRNA, where it is closed by addition of SmB and SmD3. PRMT5 - protein arginine methyltransferase 5 complex, SMN - survival motor neuron complex (taken from Matera & Wang 2014).

2.1.4 snRNA 3′ end trimming, cap hypermethylation and re-import to the nucleus

After the Sm ring is assembled around the Sm site, the snRNA is stabilised, and subsequent cytoplasmic maturation steps are initiated. One of these steps is cap trimethylation (Plessel et al. 1994). Trimethylguanosine synthetase 1 (TGS1) binds directly to the SMN complex and ensures the formation of the 2,2,7-trimethylguanosine cap by transferring the methyl group from S-adenosylmethionine (Hausmann & Shuman 2005, Mouaikel et al. 2003).

As snRNAs are transcribed beyond the 3′ end of mature snRNA (Cuello et al. 1999, Madore et al. 1984), the prolonged 3′ end needs to be trimmed. Substrate for 3′ end trimming is the core snRNP, which means snRNA with the assembled Sm ring. It was shown in yeast, that 3′ end trimming of snRNAs is catalysed by the exosome (Allmang et al. 1999, van Hoof et al. 2000). In mammals, the exonuclease DIS3L2 was identified as the homolog of yeast exosome main catalytic subunit (Dziembowski et al. 2007, Tomecki et al. 2010). The exonuclease DIS3L2 was found to bind and degrade 3′ end of snRNAs suggesting, that DIS3L2 might play a role in snRNAs 3′ end trimming (Labno et al. 2016, Ustianenko et al.

2016). There is also some evidence about nuclear 3′ end processing of snRNAs. In this model, the cytoplasmic 3′ end trimming leaves additional 1-2 nucleotides which are further cleaved after re-transport of snRNAs to the nucleus (Yang et al. 1992). However, nuclear 3′ end processing of snRNAs needs to be further proved. It was shown for U2 snRNA in human cells, that the base pairing between the 3′ extension and inner sequence of U2 snRNA is important for 3′ end processing (Huang et al. 1997).

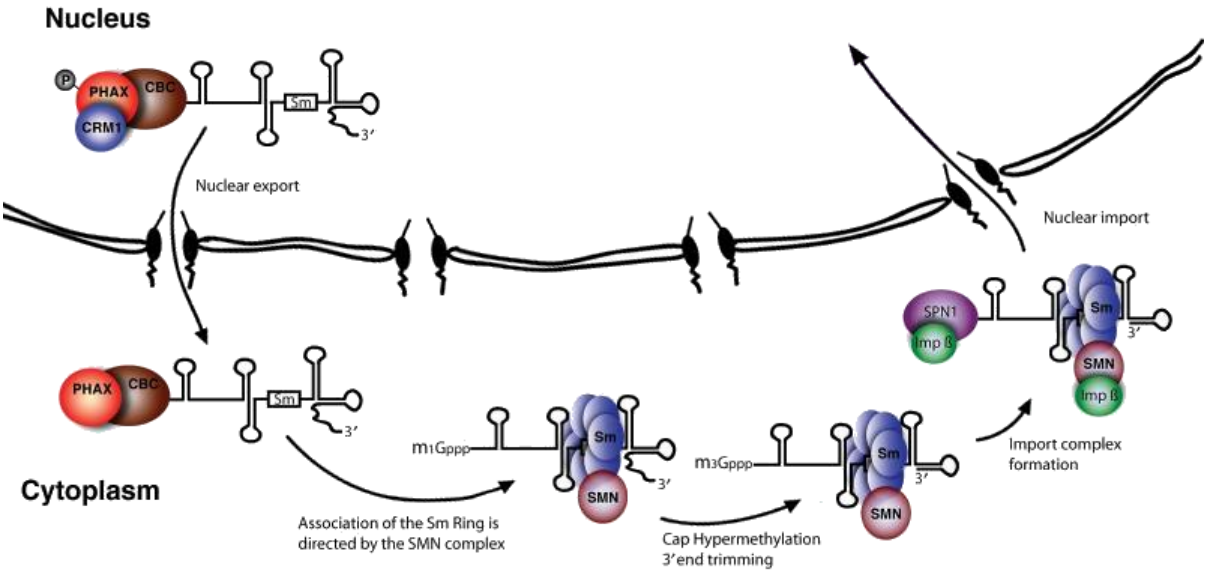

Figure 2.5 Cytoplasmic stage of biogenesis and nuclear import of snRNAs
After the snRNA is exported to the cytoplasm, the Sm ring is assembled on the Sm site, which is shown as a white box. Sm ring formation is followed by snRNA cap trimethylation and 3′ end trimming which together initiates the import complex formation. CBC – cap-binding complex, Imp β – importin β, m_1Gppp - monomethylguanosine cap, m_3Gppp – trimethylguanosine cap, PHAX - phosphorylated adaptor for RNA export, SMN - survival motor neuron complex, SPN1 – snurportin 1 (Adapted from Patel & Bellini 2008).

It was shown, that Sm ring is necessary for the transport of snRNAs back to the nucleus, but it is so far unclear, how the Sm proteins promote the nuclear import of snRNAs (Fischer et al. 1993). Cap tri-methylation of snRNAs serves as the additional signal for transport to the nucleus (Fischer & Luhrmann 1990, Neuman de Vegvar & Dahlberg 1990). It was shown, that Snurportin1 (SPN1) is recognising snRNAs and promoting nuclear import (Huber et al. 1998). SPN1 contains C-terminal tri-methylguanosine cap binding domain, which ensures the interaction with snRNAs that have already undergo cytoplasmic maturation steps, and N-terminal importin beta binding domain, necessary for interaction with importin β. Interaction of snRNAs with SPN1 and importin β is sufficient for snRNAs import to the nucleus, and this process is thus independent of importin α, which is common importin for proteins containing a nuclear localisation signal sequence (Palacios et al. 1997). Since the

SMN complex, as an mediator of cytoplasmic biogenesis of snRNAs, was found also in nucleus and direct interaction between SMN complex and importin β was shown, it was proposed, that SMN complex is transported to the nucleus together with snRNAs and may serve as an alternative NLS signal for snRNAs (Narayanan et al. 2004, Narayanan et al. 2002). The pathway of cytoplasmic biogenesis and nuclear import of snRNAs is shown in figure 2.5.

2.1.5 Cajal bodies and nuclear snRNP maturation

Cajal bodies (CBs) are nuclear non-membrane organelles (shown in figure 2.6), scaffolded by protein coilin (Raska et al. 1990). For the association of coilin with CB, the self-associating N-terminal part of coilin is necessary (Hebert & Matera 2000, Wu et al. 1994).

Since in zebrafish embryos the block of coilin translation results in lethality, which can be rescued by providing the mature snRNPs, the function of CB in snRNP formation was proposed (Strzelecka et al. 2010). In transcriptionally active cells, the protein components of snRNPs are present in CBs, as well as snRNAs (Carmo-Fonseca et al. 1992, Matera & Ward 1993) and CBs were thus identified as the place for the final step of snRNP assembly, during which they acquire the specific set of proteins (Nesic et al. 2004). After the snRNPs are imported to the nucleus, they are targeted and held in CB via interaction with Sm ring (Roithova et al. 2018). It was proposed for U2 snRNP, that once the specific proteins are loaded on snRNP, the Sm ring is covered which enables the release of snRNP from CB (Roithova et al. 2018). The assembly of snRNP specific proteins can be further accompanied by chaperones, as was shown for HSP90/RT2P complex that serves as the chaperone for U5 snRNP assembly (Malinova et al. 2017). The specific set of proteins for individual snRNPs is shown in figure 2.1.

Genes for snRNAs are often localised near CBs (Smith et al. 1995). It was shown, that coilin interacts with snRNA genes and nascent transcripts are connecting snRNA genes with CBs, suggesting the possibility of CBs functioning also in snRNA transcription regulation (Frey et al. 1999, Machyna et al. 2014).

Apart from the addition of a specific set of proteins, once the snRNP is in CB, the snRNAs are modified, which includes isomerisation of uridines to pseudouridines and 2′-O-ribose methylation. These modifications are driven by scaRNAs, which are explicitly found in CBs (Jady et al. 2003). It was shown, that *in vitro* transcribed U2 snRNA is not

incorporated in spliceosome, suggesting, that snRNAs modifications are necessary for proper spliceosome assembly (Yu et al. 1998). Once the snRNPs acquire their specific set of proteins in CBs, the assembly continues in tri-snRNP formation (see chapter 2.1.7), after which the snRNPs are released to the nucleoplasm to participate in the spliceosome assembly.

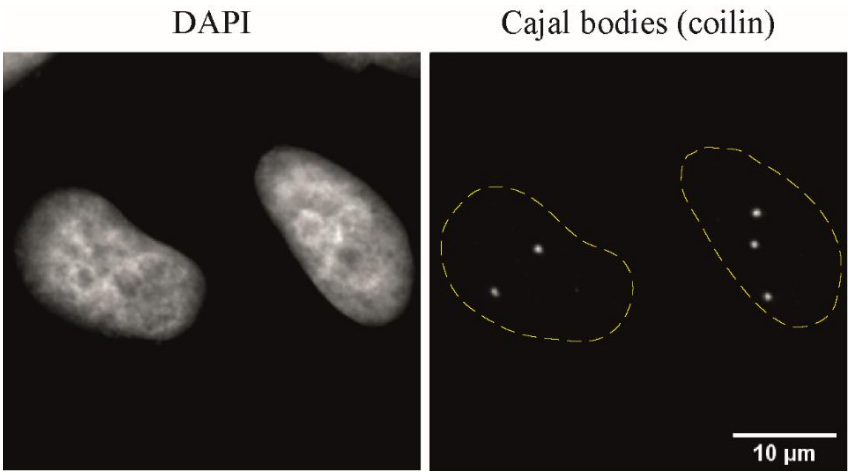

Figure 2.6 Cajal bodies
Cajal bodies are nuclear non-membrane organelles, in which the final maturation steps of snRNAs biogenesis take place. The marker of Cajal bodies used in this thesis is Cajal body scaffold protein coilin. HeLa cells were fixed and stained with a specific antibody against coilin. The dashed yellow line is illustrating the edge of the nucleus, based on DAPI staining.

2.1.6 U6 snRNP biogenesis

U6 snRNP is transcribed by RNA polymerase III and does not share the same biogenesis pathway. Whole biogenesis pathway of U6 snRNP takes place in the nucleus, and it was shown that before targeting to CBs, the U6 snRNA is localised in the nucleolus (Lange & Gerbi 2000).

U6 snRNA specific 3′ exonuclease (Booth & Pugh 1997) and polyU polymerase (U6-TUTase) were identified (Trippe et al. 2006, Trippe et al. 1998). Once the U6 snRNA is transcribed, its 3′ end is bound by La protein, which is common for RNA polymerase III transcripts as a mechanism for protection against exonucleases (Terns et al. 1992). However, during U6 snRNA maturation, its 3′ end is modified, cleaved by exonuclease Usb1 (Mroczek et al. 2012, Shchepachev et al. 2012) and carries cyclic 2′-3′ phosphate, which excludes the interaction with La protein (Lund & Dahlberg 1992, Terns et al. 1992). It was proposed a mechanism, during which the newly transcribed U6 snRNA, carrying the 3′ end extension of several templated uridines is bound by La protein and targeted to nucleolus for maturation. U6 snRNA is further polyuridinylated by U6-TUTase, and prolonged 3′ polyU tail of

U6 snRNA is cleaved and modified by cyclic 2′-3′ phosphate, which together with LSm ring (see below) protects the 3′ end of U6 snRNA from degradation. It is possible, that after the U6 snRNP is released from the spliceosome complex, it 3′ end needs to be cleaved, re-polyuridinylated and modified during the recycling of U6 snRNP (Booth & Pugh 1997, Lund & Dahlberg 1992, Shchepachev et al. 2012, Terns et al. 1992, Trippe et al. 1998).

Some RNA polymerase III transcripts, such as U6 snRNA, carries a 5′-triphosphate cap-like structure (Shumyatsky et al. 1990). The 5′ end of U6 snRNA is also bound by La protein, but during the maturation of U6 snRNP, the 5′ cap is methylated and resulting γ-m-P_3 cap inhibits La protein binding (Bhattacharya et al. 2002, Shimba & Reddy 1994).

Oppose the Sm ring present in RNA polymerase II-transcribed snRNAs (see chapter 2.1.3), U6 snRNP carries a ring of LSm 2-8 proteins (Like-Sm proteins). LSm ring is pre-assembled in the cytoplasm without the U6 snRNA present (Achsel et al. 1999, Zaric et al. 2005) and targeted to the nucleus by Lsm8 (Novotny et al. 2012). Although the U6 snRNA 3′ end formation of cyclic 2′-3′ phosphate inhibits binding of La protein, it enhances the binding of pre-assembled LSm ring (Achsel et al. 1999, Licht et al. 2008). As well as other snRNAs, U6 snRNA is also methylated and pseudouridinylated. For U6 snRNA, these modifications are guided by snoRNPs in the nucleolus (Ganot et al. 1999, Tycowski et al. 1998). The U6 snRNP biogenesis is shown in figure 2.7.

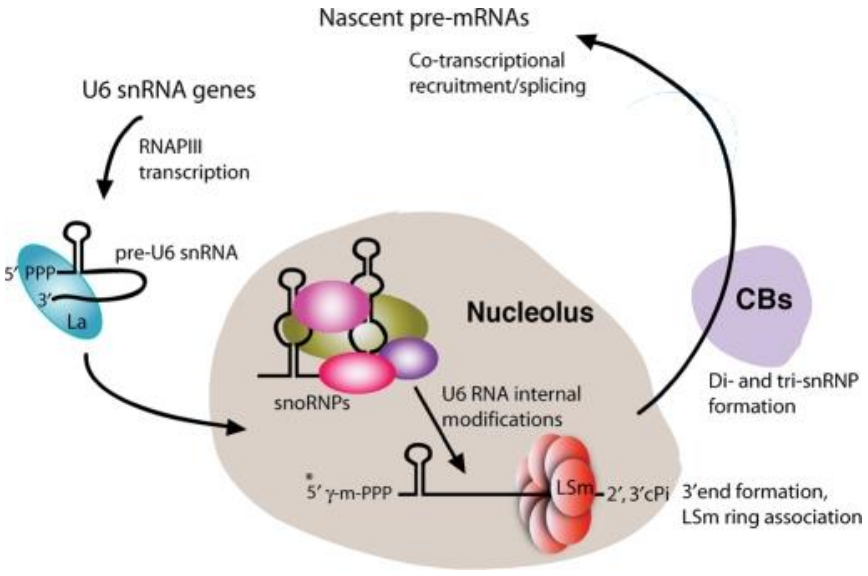

Figure 2.7 U6 snRNP biogenesis
U6 snRNA is transcribed by RNA polymerase III. In an interaction with La protein, it is located to the nucleolus, where it undergoes maturation steps, including U6 snRNA modifications, the formation of the 5′ cap-like structure, 3′ end processing and interaction with pre-assembled LSm ring. U6 snRNP is released from the nucleolus and transported to the Cajal body, where it forms di-snRNP and further tri-snRNP (adapted from Patel & Bellini 2008).

2.1.7 Di-snRNP and tri-snRNP formation

Once the U6 snRNP is assembled, it is bound in nucleoplasm by U6 snRNP specific protein SART3 (also known as p110) and targeted to CB (Stanek & Neugebauer 2004, Stanek et al. 2003), where the SART3, together with LSm ring initiates the base-pairing between U4 and U6 snRNAs and thus formation of U4/U6 di-snRNP (Achsel et al. 1999, Stanek et al. 2003). It was shown for yeast homolog of SART3, called Prp24, that it promotes unwinding of U6 snRNA internal loop and by that enables pairing with U4 snRNA (Didychuk et al. 2016, Martin-Tumasz et al. 2011). Since the Prp24 was found in interaction also with U4/U6 snRNA hybrid, the participation of Prp24 during U4/U6 snRNAs unwinding was also proposed (Ghetti et al. 1995). SART3 is not only responsible for the U4/U6 interaction during *de novo* di-snRNP assembly, but since the di-snRNP is during the splicing reaction disassembled, SART3 is also important for recycling of di-snRNP after splicing (Bell et al. 2002). U4/U6 di-snRNP is then completed by recruiting the di-snRNP specific proteins. The SNU13 binds the core U4/U6 snRNP and promotes the interaction of PRPF31 and preassembled SNRNP20/PRPF4/PRPF3 protein complex (Nottrott et al. 2002). The di-snRNP assembly can, without the CBs present, localise in the nucleoplasm. It is believed, that CBs ensures the proximity of all needed components and by mathematical modelling was predicted, that CBs enhance the association of U4 and U6 snRNPs up to 11-fold, with the optimum number of 3-4 CBs, which is the usual number of CBs in the cell (Klingauf et al. 2006).

Di-snRNP further associates with U5 snRNP via protein/protein interactions (the scheme of protein/protein interactions in tri-snRNP is shown in figure 2.8) in ATP dependent manner to form the tri-snRNP (Black & Pinto 1989). The di-snRNP specific PRPF31 interacts with U5 snRNP specific PRPF6 and thus provides the bridge between di-snRNP and U5 snRNP (Makarova et al. 2002). Since the depletion of either of these proteins results in the accumulation of di-snRNP in CBs, the tri-snRNP formation was localised to CBs (Schaffert et al. 2004). The efficiency of tri-snRNP formation was studied, and it was shown, that tri-snRNP formation in CBs is 10-fold faster than in the nucleoplasm (Novotny et al. 2011). U5 snRNP specific 52K (also known as CD2BP2) was found to interact with PRPF6. However, it is so far the only U5 snRNP specific protein not present in the tri-snRNP (Laggerbauer et al. 2005). It was proposed, that 52K is blocking the interaction of PRPF6 and PRPF31 and thus plays a role in the tri-snRNP assembly (Laggerbauer et al. 2005).

Another protein that may play a role in stabilising the tri-snRNP is di-snRNP specific PRPF3, also interacting with PRPF6 (Liu et al. 2015, Liu et al. 2006). There is some evidence, that PRPF3 is ubiquitinylated by PRPF19, a component of the nineteen complex (NTC, see chapter 2.2.1) which enables the interaction with PRPF8, core component of U5 snRNP (Song et al. 2010). It is thought, that the same mechanism of stabilised interaction with PRPF8 by PRPF19 driven ubiquitination is for interaction with PRPF31 as well (Das et al. 2017). There is a proposed model, in which the PRPF3 and PRPF31 are ubiquitinated during tri-snRNP assembly and in the process of splicing, when the tri-snRNP needs to be destabilised, these modifications are removed by deubiquitinases Usp4 for PRPF3 (Song et al. 2010) and Usp15 for PRPF31 (Das et al. 2017). Both of these deubiquitinases are brought to the spliceosome in association with SART3 (Das et al. 2017, Park et al. 2016, Zhang et al. 2016). There is also evidence showing the importance of other post-translational modifications in tri-snRNP assembly, for example SUMOylation of PRPF3 (Pozzi et al. 2017).

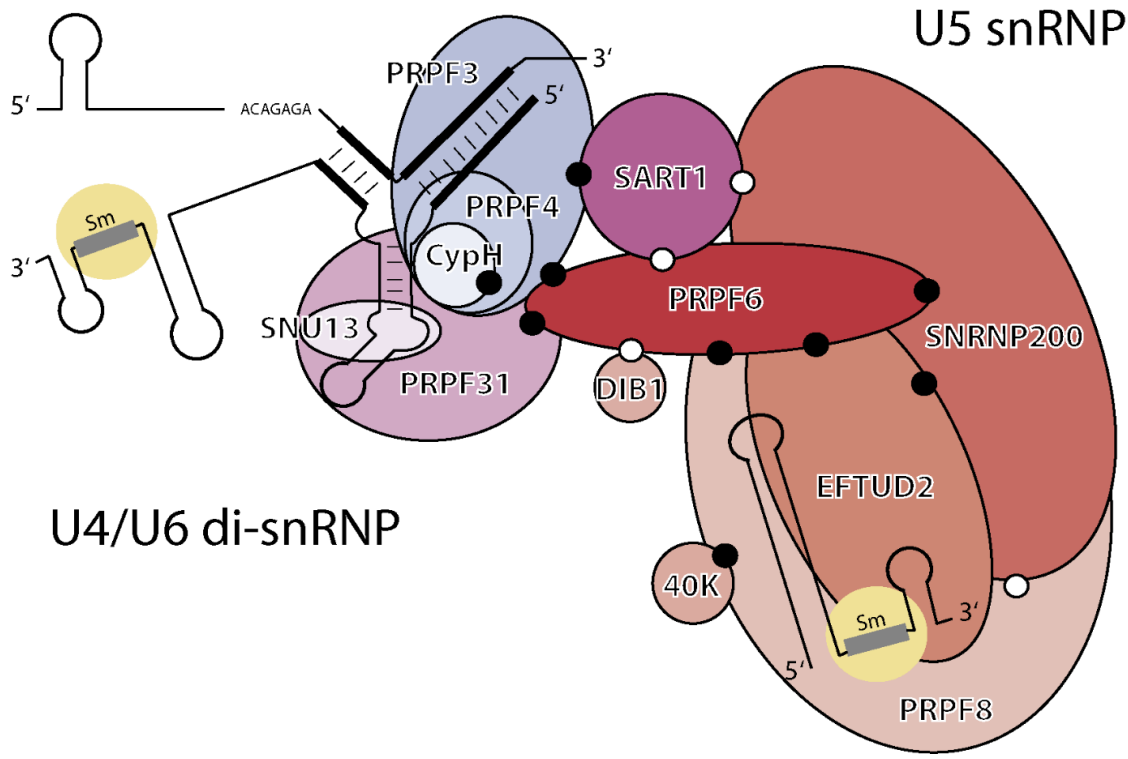

Figure 2.8 Scheme of protein/protein interactions in tri-snRNP
The di-snRNP is formed by complementary base-pairing between U4 and U6 snRNAs, which is further associated with U5 snRNP by protein/protein interactions and forms the tri-snRNP. All dots indicate protein/protein interactions for human orthologs tested by yeast 2 hybrid assay. White dots indicate interactions shown in yeasts orthologs (adapted from Liu et al. 2006).

Once the tri-snRNP is assembled, SART3 is destabilised from the complex and the tri-snRNP is released to the nucleoplasm, where, together with U1 and U2 snRNPs, it

participates in spliceosome assembly (Novotny et al. 2015). Assembly intermediate of tri-snRNP containing SART3 was found, but it is so far only uncertain evidence and needs to be further confirmed (Chen et al. 2017).

2.2 Splicing process

The splicing process was for the first time observed over fifty years ago in adenoviruses (Berget et al. 1977, Chow et al. 1977) and was confirmed year later in mouse (Konkel et al. 1978).

Each intron is defined by canonical sequences at the intron boundaries, called 5′ splice site (5′ ss) at the beginning of the intron and 3′ splice site (3′ ss) at the end. The branch point (BP), which is involved in lariat formation (see chapter 2.2.1) is localised near the 3′ ss and in higher eukaryotes followed by the polypyrimidine tract (PPT). These four canonical sequences together define the intron (shown in figure 2.9).

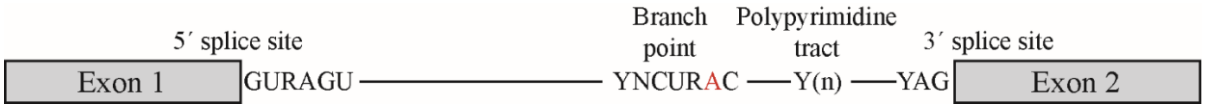

Figure 2.9 Exon-intron definition
Introns are defined by four canonical sequences, called 5′ splice site, 3′ splice site, branch point and polypyrimidine tract. Exons are shown as grey boxes, the intron is shown as a black line. The conserved sequences for 5′ splice site, 3′ splice site and branchpoint are shown. The red A in branch point sequence is illustrating the adenosine involved in lariat formation (adapted from Will & Luhrmann 2011).

Pre-mRNA of lower eukaryotes usually consist of long exons and short introns. In higher eukaryotes the situation is the opposite, meaning we can find short exons and long introns (Hawkins 1988).

2.2.1 Spliceosome assembly

Assembly of the spliceosome is a stepwise process, accompanied by many rearrangements in protein and RNA interactions. Most of the rearrangements are driven by DEAD-box helicases. Spliceosome assembly begins with the recognition of the 5′ splice site through complementary base pairing with U1 snRNA (Zhuang & Weiner 1986). The interaction of U1 snRNP with the 5′ splice site is ATP independent, and it is accompanied by non-snRNP protein interactions such as U1C, which was shown to be able to supplement the insufficient complementarity of U1 snRNA with 5′ splice site (Du & Rosbash 2002).

Next step is recognition of the 3′ splice site and the branch point, which is ensured by U2 snRNP and U2 snRNP auxiliary factor (U2AF). U2AF is a heterodimer containing two

subunits, U2AF35 and U2AF65 (Zamore & Green 1989). U1 snRNP promotes the interaction of U2AF35 with the 3′ splice site (Hoffman & Grabowski 1992), U2AF65 recognises the polypyrimidine tract and further promotes the interaction of U2 snRNP with the pre-mRNA (Valcarcel et al. 1996). This early stage, when U1 and U2 snRNPs are bound on pre-mRNA is called E complex, which is the only ATP-independent stage of spliceosome assembly. E complex undergoes rearrangements, which result in stabilisation of U2 snRNP at the branch point, and the intron boundaries are brought in proximity (Das et al. 2000). For the stabilisation of U2 snRNP at the branch point, PRPF5 is necessary (Xu et al. 2004). In this stage, called A complex, the branch point is bulged out from the sequence and by that its 2′ OH is available for the first catalytic step of splicing reaction.

Pre-assembled U4/U6.U5 tri-snRNP (see chapter 2.1.7) is bound afterwards and forms a pre-catalytic spliceosome, called B complex (Konarska & Sharp 1986). U5 snRNP specific PRPF28 drives the incorporation of tri-snRNP to spliceosomal B complex, and during this transition, it needs to be phosphorylated (Mathew et al. 2008). In the B complex, the complementary base-pairing between U1 snRNA and 5′ splice site needs to be disrupted and replaced by U6 snRNA (Kandels-Lewis & Seraphin 1993, Lesser & Guthrie 1993), which is also driven by U5 snRNP specific Prp28 (yeast homologs of human pre-mRNA processing factors are indicated by small letters) (Staley & Guthrie 1999). Another rearrangement step is unwinding the U4/U6 snRNAs. It was shown in yeast, that Brr2 (the yeast homolog of human SNRNP200) is responsible for U4/U6 snRNAs unwinding (Raghunathan & Guthrie 1998). SNRNP200 is able to unwind U4/U6 snRNAs *in vitro*, but with very low efficiency (Laggerbauer et al. 1998). Since the Brr2 is also involved in spliceosome disassembly (Small et al. 2006), it needs to be precisely regulated. The regulation of Brr2 is ensured by another U5 snRNP specific proteins, namely Snu114 (the yeast homolog of human EFTUD2) (Bartels et al. 2002, Small et al. 2006) and Jab1 domain of Prp8 (Maeder et al. 2009). Once the U4/U6 snRNAs are unwind, U6 snRNA establishes a new base-pairing interaction with U2 snRNA (Madhani & Guthrie 1992, Sun & Manley 1995), which, together with presence of Prp8 ensures the U6 snRNA conformation capable of recruiting the catalytic metal ligands and catalysing the splicing reaction (Fica et al. 2013).

Except for the spliceosomal snRNPs, the B complex was found to interact with NTC complex (Fabrizio et al. 2009), which was named after its core component Prp19 (Cheng et al. 1993). NTC complex was shown to stabilise U5 and U6 snRNPs within the spliceosome after the U4 snRNP is released (Chan et al. 2003), but the mass spectrometry analysis shows NTC

complex present already in B complex together with U4 snRNP (Fabrizio et al. 2009). It is so far not clear, whether NTC complex is bound before or after the U4 snRNP is released from the spliceosome. Once the NTC complex is bound to the spliceosome, it stays associated until the post-catalytic state of the spliceosome and thus must be recycled by so far unknown mechanism (Ilagan et al. 2013).

The loss of U1 and U4 snRNPs results in extensive rearrangements in RNA/RNA interactions and protein composition, including loss of U4/U6 di-snRNP specific proteins and recruitment of NTC complex, generating activated spliceosome, called B^{ACT}. There is also a proposed function of U5 snRNP specific Dib1 (the yeast homolog of human DIB1) during this transition (Schreib et al. 2018).

B^{ACT} complex undergoes another round of rearrangements, driven by Prp2, which result in catalytic spliceosome complex, called B^{*} (Kim & Lin 1996). During this remodelling, the reactants needed for the first catalytic steps of splicing, namely the 5′ splice site and branch point adenosine, become accessible (Bao et al. 2017). After the structural rearrangements, Prp2 is dissociated (Kim & Lin 1996) and B* complex catalyses first transesterification reaction, during which the 5′ splice site is cleaved, and intron lariat is formed (Ruskin et al. 1984). First catalytic step results in the formation of C complex. C complex is remodelled by Prp16 (Schwer & Guthrie 1992) and the cooperation of Slu7, Prp18 and Prp22 facilitate the second transesterification reaction (Ansari & Schwer 1995, Horowitz & Abelson 1993, Schwer & Gross 1998).

2.2.2 Spliceosome disassembly

The second catalytic step of splicing results in the formation of post-catalytic spliceosome called P complex, in which the exons are ligated, but pre-mRNA and intron lariat are still bound to the spliceosome. The transition of spliceosome to P complex is accompanied by structural rearrangements, that allows binding of Prp22 on mRNA (Schwer 2008), which ensures the release of the mRNA from the post-catalytic spliceosome (Company et al. 1991, Wagner et al. 1998).

For the release of the intron lariat from the spliceosome, as well as disassembly of the spliceosomal core, Prp43 is necessary (Arenas & Abelson 1997, Martin et al. 2002, Tsai et al. 2005). It was shown in yeast, that Prp43, together with Ntr1 and Ntr2 forms so-called NTR complex (Tsai et al. 2005). The NTR complex is targeted to the spliceosome through the interaction of Ntr2 with Brr2 (the yeast homolog of human SNRNP200) (Tsai et al. 2007),

and the activity of Prp43 is stimulated by Ntr1 (Tanaka et al. 2007). Since the Brr2, as the U5 snRNP specific protein, is part of the spliceosome already in early stages, the interaction of NTR complex with spliceosome needs to be regulated. It was shown, that presence of Prp16 and Slu7 in the spliceosome inhibits the NTR complex binding and that the NTR complex is active only after the spliceosomal rearrangement catalysed by Prp22, which together ensures the activity of NTR complex only in post-catalytic spliceosome (Chen et al. 2013). Another factor participating in spliceosome disassembly is Brr2 that unwinds U2/U6 snRNA duplex, which is regulated by Snu114 (the yeast homolog of EFTUD2) (Small et al. 2006), but this stage was found to be independent on Brr2 ATPase activity (Fourmann et al. 2013). It is thus possible that Brr2 has only auxiliary function during this process (Fourmann et al. 2013). Since the human homolog of Ntr1 was found (Yoshimoto et al. 2009), the same mechanism of snRNPs release from intron lariat is expected. The whole pathway of the splicing reaction is shown in figure 2.10.

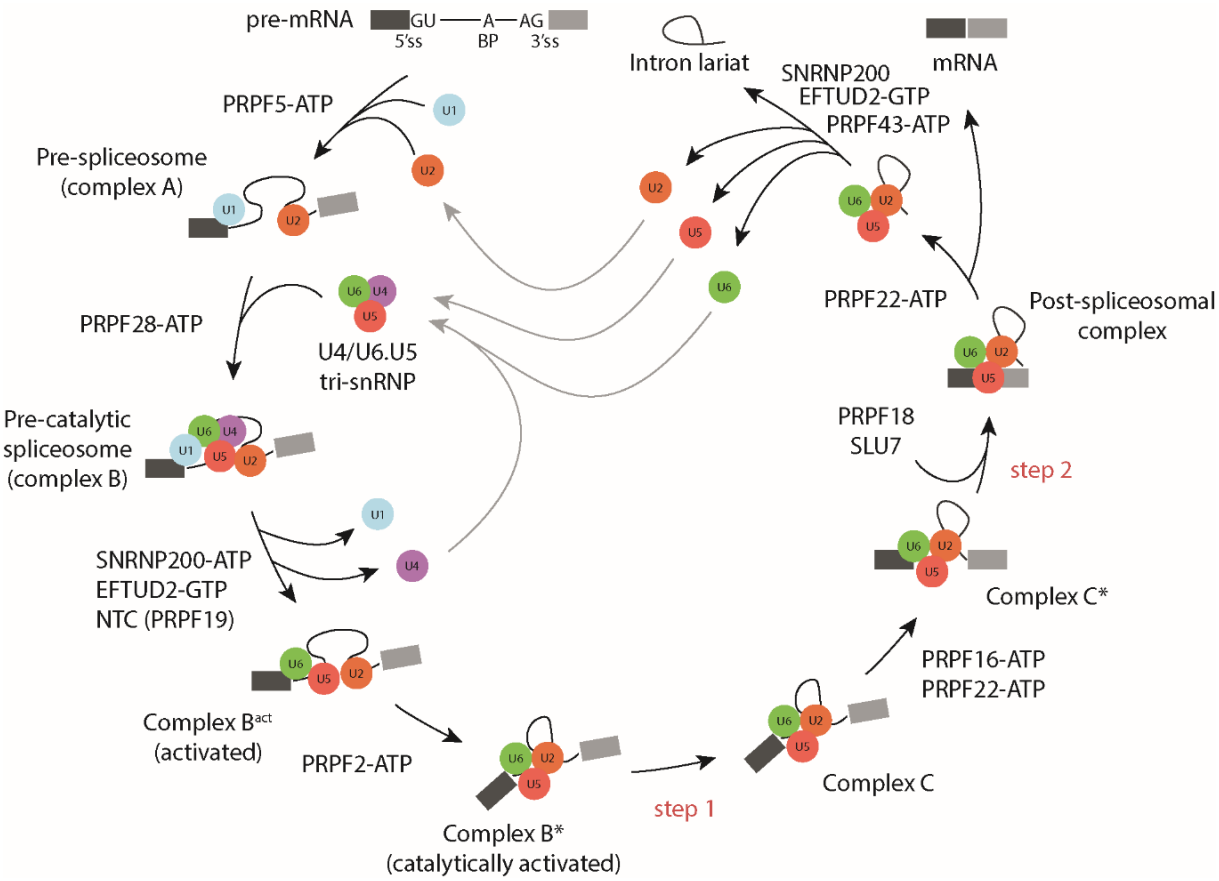

Figure 2.10 Splicing process
Pre-mRNA is recognised by the U1 and U2 snRNPs. Pre-assembled tri-snRNP is bound, and the resulting complex is activated, during which the NTC complex is associated with the spliceosome. The spliceosome is remodelled by the activity of several helicases and catalyses two transesterification reactions resulting in spliced out intron lariat and ligated exons of mRNA. Spliceosomal snRNPs are further released from the intron lariat and recycled for another round of splicing reaction (adapted from Will & Luhrmann 2011).

Once the snRNPs are released from intron lariat, they are transported to Cajal bodies for recycling and tri-snRNP reassembly (Stanek et al. 2008), but there is so far not much known about the mechanism of spliceosomal snRNPs recycling.

2.3 U5 snRNP

Since this thesis is focused on U5 snRNP, this chapter will provide additional information about assembly and recycling of U5 snRNP.

The structure of yeast spliceosome shows that U5 snRNP specific proteins, specifically Prp8, Brr2 and Snu114 form the central part of the spliceosome, where Prp8 anchors the catalytic centre of the spliceosome (Yan et al. 2015).

There was an assembly precursor of U5 snRNP found in yeast (Gottschalk et al. 2001). From the U5 snRNP specific proteins, this 16S U5 snRNP, in contrast to mature 20S snRNP and 35S post-catalytic U5 snRNP (Makarova & Makarov 2015), consist of only Sm ring, Prp8 and Snu114 but contains an additional factor named Aar2 (the yeast homolog of human AAR2), which is not found in tri-snRNP (Gottschalk et al. 2001). Mature U5 snRNP contains additional specific proteins but lacks the Aar2 (Stevens et al. 2001). Nuclear localisation signal of Prp8 was identified, and it was found, that its absence results in accumulation of Aar2/U5 snRNP in the cytoplasm, but at the same time, Brr2 keeps its nuclear localisation (Boon et al. 2007). Based on this finding the maturation model of U5 snRNP was proposed. In this model, Prp8 is bound with Aar2 and Snu114 already in the cytoplasm. After transport to the nucleus, this complex is bound with the core U5 snRNP consisting of U5 snRNA and Sm ring. Phosphorylation of Aar2 then promotes the release of Aar2 from the complex, and even if Aar2 and Brr2 interact with different parts of Prp8, loss of Aar2 enables the interaction of Brr2 with Prp8 (shown in figure 2.11) (Boon et al. 2007, Weber et al. 2011).

In human cells, assembly intermediate of U5 snRNP proteins, containing PRPF8, EFTUD2, SNRNP200 and assembly chaperones AAR2 and HSP90/R2TP complex was found. It was shown that PRPF8 and EFTUD2 associate with HSP90/R2TP complex in the cytoplasm. There is a proposed model, in which this cytoplasmic assembly intermediate is further associated with SNRNP200 and lately U5 snRNA in the nucleus (Malinova et al. 2017). The interaction of HSP90/R2TP complex with U5 snRNP is probably mediated by R2TP cofactor ZNHIT2 (Cloutier et al. 2017). Several previously poorly characterised proteins were found to co-precipitate with U5 snRNP specific proteins and HSP90/R2TP

cofactor ZNHIT2, namely TTC27, EAPP, NCDN, ECD and TSSC4. It was thus proposed, that these proteins may serve as U5 snRNP assembly factors (Cloutier et al. 2017, Malinova et al. 2017).

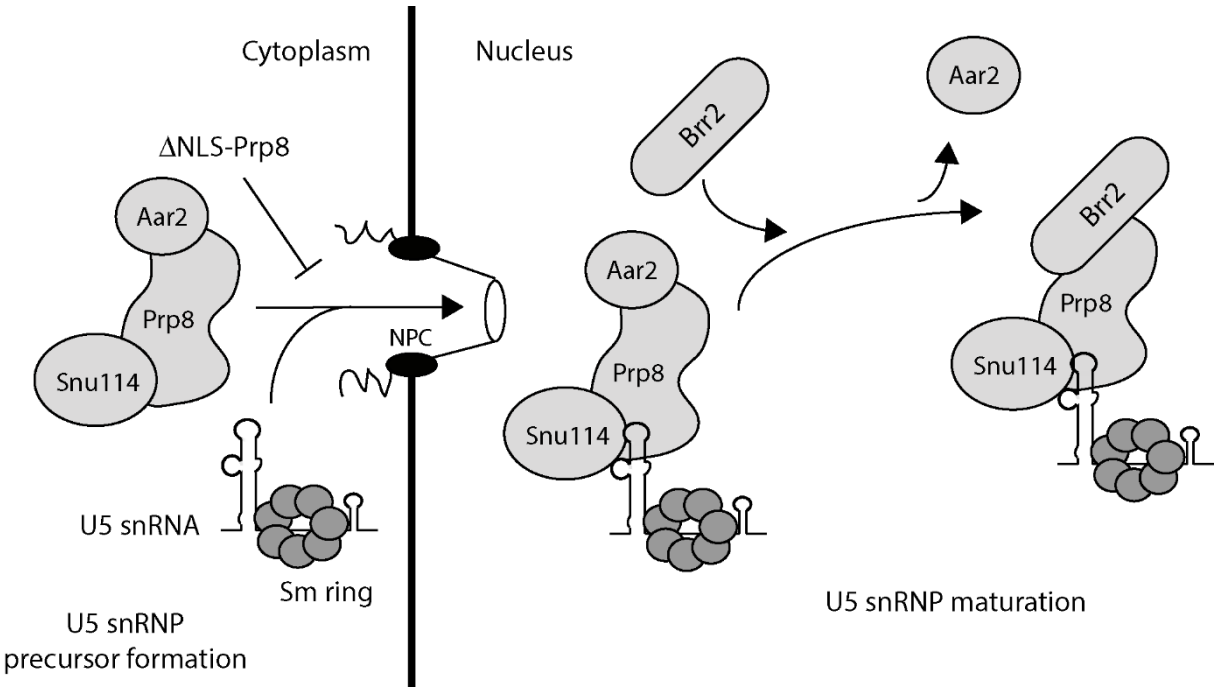

Figure 2.11 Model of U5 snRNP maturation in yeast
Prp8 forms a cytoplasmic complex together with Snu114 and Aar2. This complex is transported to the nucleus, where it is bound by U5 snRNP core. Further, the Aar2 is released from U5 snRNP which enables binding of Brr2. NLS – nuclear localisation signal, NPC – nuclear pore complex (adapted from Boon et al. 2007)

After the disassembly of the spliceosome, U5 snRNP is released associated with the NTC complex as 35S U5 snRNP (Makarova & Makarov 2015). However, using purified yeast spliceosome components *in vitro*, the post-catalytic 18S U5 snRNP and interaction of NTC complex with U2 snRNP and intron lariat were found (Fourmann et al. 2013). It is possible, that snRNP recycling pathway differs between yeast and human cells, and 18S U5 snRNP might be specific for yeast, whereas 35S U5 snRNP for human cells. However, this is so far only speculation, which would need to be further confirmed.

It was suggested, that the interaction of NTC complex with the spliceosome results in loss of several U5 snRNP proteins (Makarov et al. 2002). In comparison with mature 20S U5 snRNP, the post-catalytic 35S U5 snRNP lacks PRPF6, PRPF28, DIB1 and 52K, which is lost during tri-snRNP assembly (Laggerbauer et al. 2005, Makarov et al. 2002). The recycling mechanism of U5 snRNP and whether it is one step transition from 35S to 20S U5 snRNP or if it is transiently dissociated to a smaller complex, such as 18S U5 snRNP found in yeast

(Fourmann et al. 2013), is still unknown. The splicing cycle from the U5 snRNP point of view is shown in figure 2.12.

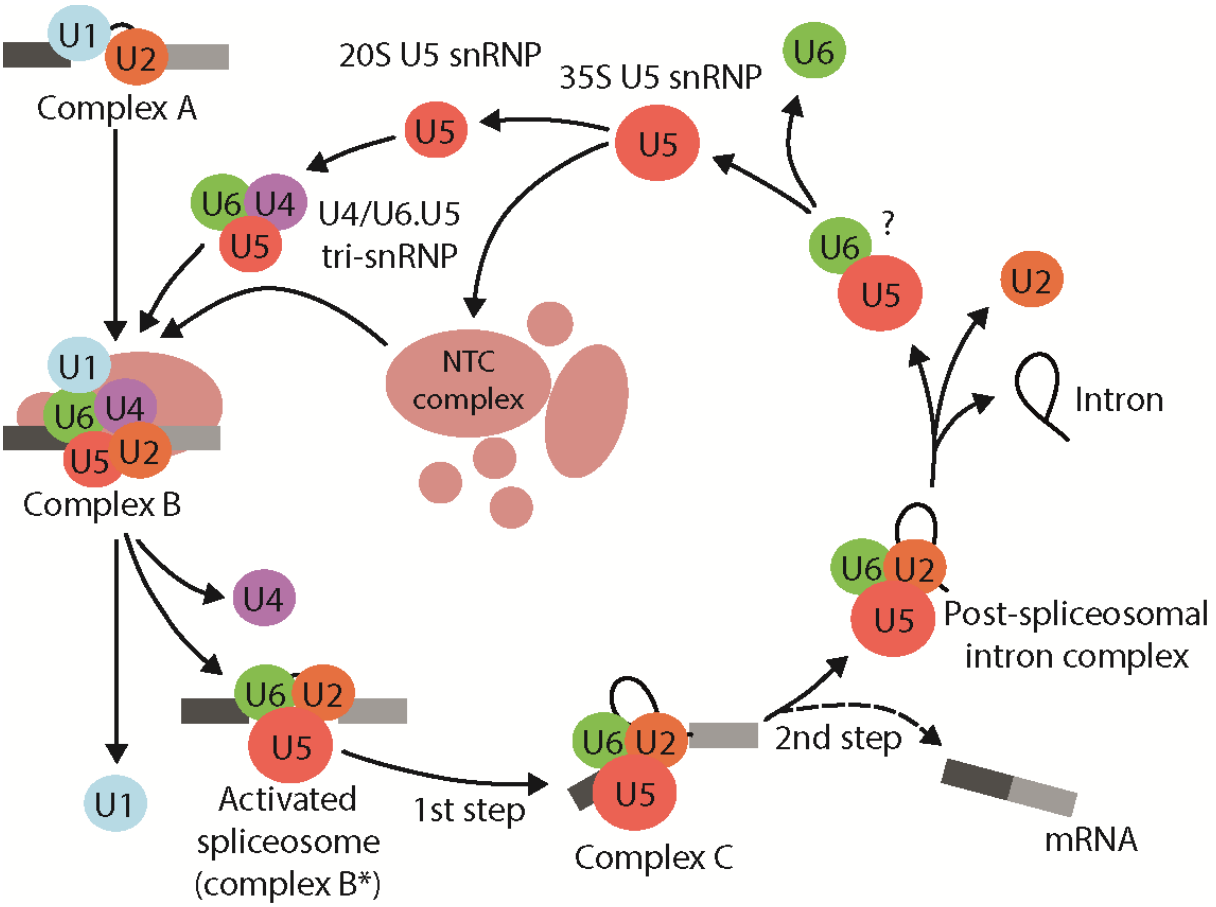

Figure 2.12 U5 snRNP remodelling during the splicing cycle
Mature 20S U5 snRNP in incorporated in tri-snRNP and the spliceosome. Upon the activation of the spliceosome, NTC complex is associated with the spliceosome, which results in loss of several U5 snRNP proteins. Post-catalytic U5 snRNP stays associated with the NTC complex and forms 35S U5 snRNP. The recycling mechanism of U5 snRNP is still unknown. NTC – nineteen complex (adapted from Wahl et al. 2009).

During the U5 snRNP remodelling, the PRPF8 structure is modified to harbour the snRNA in the position suitable for splicing catalysis, as can be seen in the structures of individual spliceosome complexes (Agafonov et al. 2016, Fica et al. 2019, Plaschka et al. 2017, Zhan et al. 2018a, Zhan et al. 2018b). Also, the extensive movement of SNRNP200 within U5 snRNP is striking (shown in figure 2.13). In tri-snRNP, SNRNP200 can be found near the body of the U5 snRNP structured by PRPF8 (Agafonov et al. 2016). During the transition to B-complex, SNRNP200 is positioned near U4 snRNP Sm ring (Zhan et al. 2018b). From the structural insight, SAD1 was proposed to tether SNRNP200 in tri-snRNP position, remote from U4/U6 snRNA duplex. Dissociation of SAD1 during the transition to B complex would then allow SNRNP200 to shift and bound the U4/U6 snRNA duplex

(Agafonov et al. 2016). Since the position of Prp28 is overlapping with B-complex specific proteins, it was proposed, that once the interaction of U1 snRNP with the spliceosome is disrupted, Prp28 is released and enables binding of B-complex specific proteins, as well as repositioning of Brr2 (the yeast homolog of human SNRNP200) (Plaschka et al. 2017). After the two catalytic steps of splicing, SNRNP200 in P-complex seems to be destabilised from the spliceosome body and is bound only by interaction with PRPF8 (Fica et al. 2019).

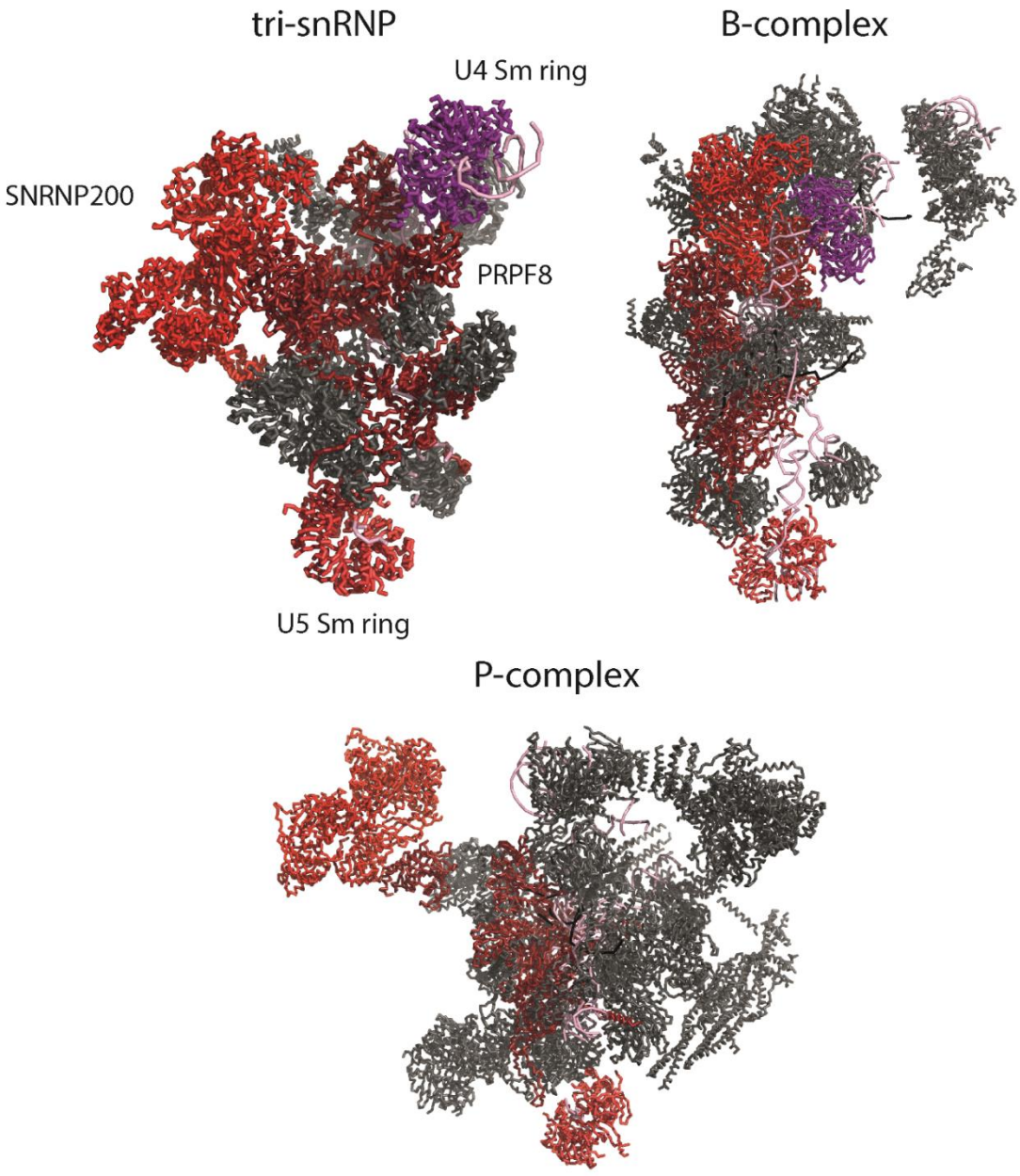

Figure 2.13 SNRNP200 position in different spliceosome complexes
SNRNP200 in tri-snRNP is positioned near the U5 snRNP body. During the transition to B complex, SNRNP200 is shifted and positioned near U4 Sm ring, thus U4/U6 snRNA duplex. In the post-catalytic P-complex, SNRNP200 is destabilised from the spliceosome body. Red – SNRNP200, light red – U5 Sm ring, brown - PRPF8, purple – U4 Sm ring, light pink – spliceosomal snRNAs, black – pre-mRNA, rest of the spliceosome is for simplicity shown as grey (Adapted from PDB ID: 3JCR, 6AHD, 6QDV).

3 Aims of the thesis

We previously found the interaction of TSSC4 with U5 snRNP (Malinova et al. 2017), which was later independently confirmed (Cloutier et al. 2017). However, TSSC4 is not found in mature U5 snRNP (Bach et al. 1989), and it was thus proposed as a putative U5 snRNP assembly factor. TSSC4 is previously undescribed protein with unknown function, and the only available connections of TSSC4 with U5 snRNP are mass spectrometry analysis. The aim of this thesis was to confirm the interaction of TSSC4 with U5 snRNP, determine whether TSSC4 has a role during U5 snRNP assembly and to characterise its potential function.

To address the main aim, we set a series of partial goals:

- confirm the interaction of TSSC4 with U5 snRNP
- determine the region of TSSC4 responsible for U5 snRNP interaction
- analyse the effect of TSSC4 depletion on U5 snRNP protein composition
- analyse the effect of TSSC4 depletion on the effectivity of tri-snRNP assembly

4 Material and methods

4.1 Material

4.1.1 Instruments

37°C incubator Raven2	LTE scientific, UK
37°C shaker ORBI-SAFE	SANYO, JPN
Analytical weight KERN EG420-NM	Kern&Shon GmbH, DEU
Automatic pipette Pipetman	Gilson, FRA
Centrifuge 5417R	Eppendorf, DEU
Centrifuge 5430R	Eppendorf, DEU
Centrifuge Biofuge pico	Heraeus, DEU
CO_2 incubator	SANYO, JPN
Dry bath incubator	Major Science, USA
Flow box	Clean Air Techniek B.V., NLD
Heat-stir CB162	P-LAB a.s., CZE
Hoefer S6100 gradient mixer	AP Czech s.r.o., CZE
Horizontal electrophoresis	BioRad, USA
Imager Universal Hood II	BioRad, USA
L-70 ultracentrifuge	Beckman Coulter, USA
LAS-3000 Imager	Fujifilm, JPN
Mini Rocker MR-1	Biosan, USA
MJ Mini Personal Thermal Cycler	BioRad, USA
Olympus IX70 microscope with DeltaVision system	Applied Precision, SVK
Orbital shaker OS-100	Biosan, USA
Power supply PowerPac Universal	BioRad, USA
Sample mixer	Invitrogen, USA

Schoeller Biohazard Box EFIS 4BSC	Schoeller instruments, DEU
Shaking CO_2 incubator New Brunswick	Eppendorf, DEU
Sonicator U50 Control	IKA Labortechnik, DEU
Spectrophotometer NanoDrop 2000	Thermo Fisher Scientific, USA
T100^{TM} Thermal Cycler	BioRad, USA
Thermomixer Comfort	Eppendorf, DEU
TS-100C Thermo shaker	Biosan, USA
Vertical electrophoresis for RNA gels	EMBL workshop, DEU
Vertical electrophoresis Mini-Protean Tetra Cell	BioRad, USA
Vortex Genie2	Scientific Industries, USA
Water bath	Julabo, USA

4.1.2 DNA probes for fluorescence *in situ* hybridisation

Table 4.1 List of DNA probes used for FISH

DNA Probe	Sequence (5′ to 3′)
U2_snRNA	[A488]GAACAGATACTACACTTGATCTTAGCCAAAAGGCCGAGAAGC
	Cy3-GAACAGATACTACACTTGATCTTAGCCAAAAGGCCGAGAAGC
U4_snRNA	[A488]TCACGGCGGGGTATTGGGAAAAGTTTTCAATTAGCAATAATCGCGCCT
	Cy3-TCACGGCGGGGTATTGGGAAAAGTTTTCAATTAGCAATAATCGCGCCT
U5_snRNA	[A488]CTCTCCACGGAAATCTTTAGTAAAAGGCGAAAGATTTATACGATTTGAAGAG
	[Atto565]CTCTCCACGGAAATCTTTAGTAAAAGGCGAAAGATTTATACGATTTGAAGAG
U6_snRNA	Cy3-CACGAATTTGCGTGTCATCCTTGCGCAGGGGCCATGCTAATC

4.1.3 Primers

Table 4.2 List of used oligonucleotides

Primer		Sequence (5′ to 3′)	Used for
TSSC4	F	GGAAGATCTCATGGCTGAGGCAGGAACAGGTGAGCCG	Cloning by restriction
	R	TCCCCGCGGGACCTCAGCACCTGGGTCCTC	
TSSC4_repair	F	AAGCCAGACACGAGAGGAAGAGGGTC	Site-directed mutagenesis
	R	CGACCCCTCGGACTGGTT	
TSSC4_Δ1-50	F	CCGATGGGGCTGCCTGGG	Site-directed mutagenesis
	R	GAGATCTTCCAGATCTGAGTACTTGTACAGCTC	
TSSC4_Δ51-100	F	GAGGGGGCGGCCAGACGG	Site-directed mutagenesis
	R	GGACAGTGCTTCCACTTCAGCACCAC	
TSSC4_Δ101-150	F	CCGGTCCCCGACTACGTG	Site-directed mutagenesis
	R	CAGGCAGTCAAAGATGTCACGG	
TSSC4_Δ151-200	F	TTCAACCAGGATCCCTCCAG	Site-directed mutagenesis
	R	AGGCACCCTTGGTGAGGC	
TSSC4_Δ201-250	F	GGCGAGGGCCCTGTGGAG	Site-directed mutagenesis
	R	GGAGGACACGCAGTCAGTGG	
TSSC4_Δ251-300	F	ACTGTTGGCTTCCATGGC	Site-directed mutagenesis
	R	CCTGTCTGTGGCAGGATTC	
TSSC4_Δ301-330	F	CCGCGGGGACCGCGGGCC	Site-directed mutagenesis
	R	TTCCACCGGCGGGAGACCTGGCAC	
P235 pEGFP-N-5′		AAATGTCGTAACAACTCCGC	Sequencing
P233 pEGFP-C-3′		TTTATGTTTCAGGTTCAGGG	Sequencing
Random hexamers		NNNNNN	Reverse transcription

4.1.4 Primary antibodies

Table 4.3 List of used primary antibodies
IF – immunofluorescence, IP – immunoprecipitation, WB – Western blot

Antibody	Origin	Producer	Used for
anti-coilin	Mouse	M. Carmo-Fonseca (Almeida et al. 1998)	IF
anti-EFTUD2	Rabbit	L. Lührmann (Fabrizio et al. 1997)	IF, WB
anti-FLAG	Rabbit	Sigma-Aldrich, USA (F7425)	IP
anti-FLAG	Mouse	Sigma-Aldrich, USA (F1804)	WB
anti-GFP	Goat	D. Drechsel, MPI-CBG, Dresden	IP
anti-GFP	Mouse	Santa Cruz Biotechnology, Inc., USA (SC-9996)	WB
anti-PRPF19	Mouse	Santa Cruz Biotechnology, Inc., USA (SC-514338)	IF, WB
anti-PRPF31	Rabbit	Sigma-Aldrich, USA (HPA041939)	WB
anti-PRPF4	Rabbit	L. Lührmann (Lauber et al. 1997)	WB
anti-PRPF6	Mouse	Santa Cruz Biotechnology, Inc., USA (SC-166889)	WB
anti-PRPF8	Mouse	Santa Cruz Biotechnology, Inc., USA (SC-55533)	WB
anti-SmD1	Rabbit	Abcam, GBR (ab79977)	WB
anti-SNRNP200	Rabbit	Sigma-Aldrich, USA (HPA029321)	WB
anti-TSSC4	Rabbit	Proteintech, USA (14531-1-AP)	IF, WB
anti-Tubulin	Mouse	P. Draber, IMG CAS, CZE	WB
anti-U2A′	Rabbit	Abcam, GBR (ab128937)	WB

4.1.5 siRNAs

Table 4.4 List of used siRNAs

siRNA	Sequence of sense strand (5′ to 3′)	Producer
NC5 (Silencer Negative Control 5 siRNA)	Scrambled sequence (no significant sequence similarity to human gene sequences)	Ambion, USA
SNRNP200 (Silencer select siRNA)	GUGAUUCAGAUUGAGUCCUtt	Ambion, USA
TSSC4 (Silencer select Pre-designed siRNA)	CGGUGGUGCUGAAGUGGAAtt	Ambion, USA

4.1.6 Cell cultures

Bacterial culture: competent bacterial cells *Escherichia coli*, strain DH5α

Human cell culture: HeLa cells, WT

HeLa cells, PRPF8-GFP (Malinova et al. 2017) – stable HeLa cell line expressing PRPF8 tagged with GFP

HeLa cells, SNRNP200-GFP (Cvackova et al. 2014) – stable HeLa cell line expressing SNRNP200 tagged with GFP

4.2 Methods

4.2.1 Cell culture

HeLa cells were cultured in high-glucose (4.5 g/l) Dulbecco's modified Eagle's medium (DMEM, Sigma-Aldrich, USA), supplemented with 10 % fetal bovine serum, 1 % penicillin and streptomycin. Cells were grown at 37 °C and 5 % CO_2 atmosphere.

4.2.2 Cloning by restriction and site-directed mutagenesis

For cloning by restriction, the cloned insert was amplified by PCR from HeLa wt cDNA. Cloned insert and target vector were digested with required restrictases and cleaned with DNA Clean & Concentrator^{TM}-5 Kit (Zymo Research, USA) according to the manufacturer's protocol. The insert was phosphorylated, vector dephosphorylated, and both again cleaned with DNA Clean & Concentrator^{TM}-5 Kit (Zymo Research, USA) according to the manufacturer's protocol. Vector and insert were mixed and ligated, dephosphorylated

vector alone was used as a negative control for ligation. The construct was transfected to DH5α competent cells and the cells cultivated at 37 °C overnight. Next day, the set of 8-16 grown colonies were screened by colony PCR with primers used for insert amplification and DNA was isolated from positive colonies with QIAprep® Spin Miniprep Kit (Qiagen, DEU) according to the manufacturer's protocol. Isolated vectors were further analysed by restriction digestion, and the positive colonies were sequenced for final control.

TSSC4 was cloned to pEGFP-N1 and TripleFlag-C3 (a modified version of pEGFP-C3) using BglII and SacII restriction enzymes.

Since the cloning of TSSC4-GFP-N1 introduced unwanted point-mutation, site-directed mutagenesis was used to repair the mutation, as well as for the preparation of deletion mutants of TSSC4. For the preparation of deletion mutants of TSSC4, TSSC4-GFP-N1 was used as a template for PCR amplification and primers around the deleted sequence were used for introducing the deletion. The sample was resolved on 0.5 % agarose/TBE, and DNA in requested length was isolated from the gel with ZymocleanTM Gel DNA Recovery Kit (Zymo Research, USA) according to the manufacturer's protocol. Since the small difference in length of the template vector and requested amplicon, DpnI restrictase was used to disrupt the template vector (DpnI cleaves only methylated recognition site). DNA was cleaned with DNA Clean & Concentrator^{TM}-5 Kit (Zymo Research, USA) according to the manufacturer's protocol and ligated. Selection of positive colonies was done in the same manner as for cloning by restriction. Scheme of cloning by restriction and site-directed mutagenesis is shown in figure 4.1.

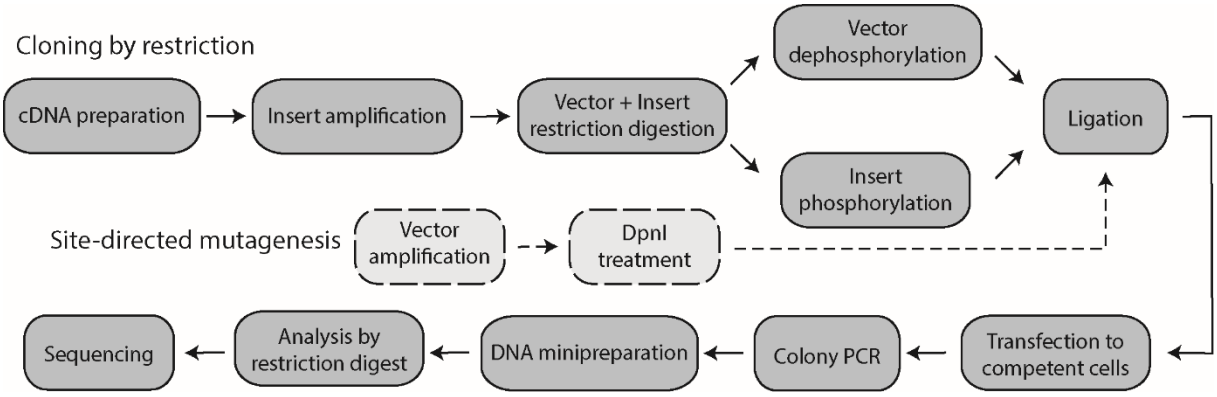

Figure 4.1 Workflow scheme for cloning by restriction and site-directed mutagenesis
The cloned insert was amplified from HeLa wt cDNA. Ends of the insert, as well as the target site of the vector were modified. After ligation, positive colonies were screened by colony PCR, restriction digestion and sequencing. For site-directed mutagenesis, the cloned vector was used as a template for amplification. Template DNA was disrupted by DpnI restriction and amplicon ligated. Screening for positive colonies was done in the same manner, as for cloning by restriction.

4.2.3 RNA isolation by TRIzol reagent

Cells were cultured ideally to 100 % confluency, the medium was removed, and cells were washed with PBS buffer. TRIzol reagent (Ambion, Inc., USA) was added according to table 4.5. Cells in TRIZOL reagent were transferred to a microcentrifuge tube and after 5 min of incubation in room temperature, chloroform was added according to table 4.5. The mixture was vigorously vortexed for at least 1 min, incubated 3 min in room temperature and centrifuged at 20 000 g, 4 °C for 15 min.

An upper colourless aqueous phase was transferred to a new tube (lower organic phase was stored in 4 °C until protein isolation, if needed), mixed with isopropanol and carrier (glycogen) and the RNA was precipitated in -20 °C for at least 1 h. After precipitation, samples were centrifuged at 20 000 g, 4 °C for 20 min and the supernatant was removed. Pellet was washed with 70 % BioUltra Ethanol and centrifuged at 20 000 g, 4 °C for 5 min. The supernatant was removed, the sample spun at small table centrifuge to remove the residual supernatant, and the pellet was dissolved in 10 µl 1x RNA buffer for PAGE-Urea polyacrylamide RNA gel or in 10 µl RNase-free water for cDNA preparation.

Table 4.5 Used volumes of chemicals for RNA isolation by TRIzol reagent for different types of samples

	12 Well plate	10 cm Petri dish	Gradient fractions
TRIzol	400 µl	3 ml	600 µl
Chloroform	80 µl	600 µl	120 µl
Glycogen	3 µl	4 µl	6 µl
Isopropanol	200 µl	1.5 ml	1 ml

1x RNA buffer: 20 mM Tris (pH 8.0), 8 M Urea, Xylene blue

PBS buffer: 137 mM NaCl, 2.7 mM KCl, 10 mM Na_2HPO_4, 1.8 mM KH_2PO_4, pH 7.4

4.2.4 DNase treatment

10 µl of RNA isolated from HeLa cells by TRIzol reagent were supplemented with DNase TURBO buffer to final concentration 1x and 1 µl DNase TURBO (Invitrogen, USA). Samples were incubated at 37 °C for 30 min – 1 h. RNase-free water to the final volume of 50 µl was added, and the sample was mixed with 25 µl ammonium acetate and 125 µl 100 % BioUltra ethanol. The samples were precipitated at -80 °C for at least 1 h and centrifuged at

20 000 g, 4 °C for 20 min. Pellet was 2x washed with 70 % BioUltra ethanol, the supernatant was removed, and the pellet was resuspended in 10 µl RNase-free water.

4.2.5 Reverse transcription

5 µg of DNase treated RNA were mixed with 1 µl 10 mM dNTPs (deoxynucleotide triphosphates) and 1 µl of 140 µM random hexamers. RNase-free water was added to the final volume of 14.5 µl. Samples were incubated 5 min at 65 °C and 5 min on the ice afterwards.

4 µl of 5x first-strand buffer (Invitrogen, USA), 1 µl of 100 mM DTT and 0.5 µl of SuperScript III (Invitrogen, USA) were added. Samples were incubated at 55 °C for 2 h and 70 °C for 15 min afterwards. The resulting cDNA was cleaned with DNA Clean & Concentrator^{TM}-5 Kit (Zymo Research, USA) according to the manufacturer's protocol and used as a template for PCR amplification of inserts for cloning by restriction.

5x first-strand buffer: 250 mM Tris-HCl (pH 8.3), 375 mM KCl, 15 mM $MgCl_2$

4.2.6 Polymerase chain reaction

High fidelity Phusion polymerase (New England Biolabs, USA) was used for cloning insert amplification and site-directed mutagenesis. Programme for PCR amplification by Phusion polymerase is shown in table 4.6. Set of 8 reactions per 10 µl were prepared for each set of primers according to table 4.7, and the optimal annealing temperature was tested. In case of ineffective of insufficient amplification, the buffer for GC rich sequences was used instead of high-fidelity buffer (New England Biolabs, USA). Determined optimal annealing temperature and used buffers are shown in table 4.8.

Table 4.6 Programme for PCR amplification by Phusion polymerase

Initial denaturation	98 °C	30 s	1 cycle
Denaturation	98 °C	10 s	30 cycles
Annealing	54-65 °C gradient or determined optimal temperature per primer set	15 s	
Elongation	72 °C	1 min per 1000 bp	
Final elongation	72 °C	5 min	1 cycle

Table 4.7 Composition of PCR reaction for amplification by Phusion polymerase

	10 µl reaction for primer test	20 µl reaction for insert amplification
5x Phusion buffer	2 µl	4 µl
10 mM dNTPs	0.2 µl	0.4 µl
5 µM primer F	1 µl	2 µl
5 µM primer R	1 µl	2 µl
DMSO	0.3 µl	0.6 µl
Phusion DNA polymerase	0.1 µl	0.2 µl
Template DNA	1 µl	2 µl
10 M Betaine	1 µl	2 µl
ddH_2O	3.4 µl	6.8 µl

Table 4.8 Determined annealing temperature and used buffers for each set of primers used for PCR amplification by Phusion polymerase

Primer set	Determined annealing temperature	Buffer used for amplification
TSSC4	62 °C	GC
TSSC4_repair	63 °C	GC
TSSC4_Δ1-50	64 °C	HF
TSSC4_Δ51-100	64 °C	HF
TSSC4_Δ101-150	64 °C	HF
TSSC4_Δ151-200	64 °C	HF
TSSC4_Δ201-250	64 °C	HF
TSSC4_Δ251-300	64 °C	HF
TSSC4_Δ301-330	64 °C	HF

4.2.7 Agarose electrophoresis

Horizontal agarose electrophoresis was used for separation of DNA molecules according to length in 1 % agarose/TBE. For visualisation of DNA molecule, Gelstar (Thermo Fisher Scientific, USA) was mixed into agarose gel before agarose solidification in dilution 1:10 000. Samples were mixed with 6x loading dye to final concentration 1x before loading. In case of preparation of DNA molecules for isolation from agarose gel, 0.5 % agarose/TBE was used.

TBE buffer: 89 mM Tris base (pH 8.2), 89 mM boric acid, 2 mM EDTA

6x loading dye: 10 mM Tris-HCl (pH 7.6), 60 % (v/v) glycerol, 0.03 % (w/v) bromfenol blue, 0.03 % (w/v) xylenkyanol, 60 mM EDTA

4.2.8 Restriction digestion

Restriction digestion was used for the preparation of vectors and inserts for cloning by restriction and screening for positive colonies after cloning. The reaction was prepared according to table 4.9 and incubated at 37 °C for at least 1 h. Afterwards, the reaction was heat inactivated, according to supplier instructions and restricted DNA was cleaned with DNA Clean & Concentrator^{TM}-5 Kit (Zymo Research, USA) according to the manufacturer's protocol.

Table 4.9 Composition of restriction reaction

	Vector and insert restriction for cloning	Screening for positive colonies
Template DNA	18 µl	1 µg
Restriction enzyme	0.2 µl	0.2 µl
Buffer recommended for used restrictase	2 µl	2 µl
ddH_2O	0 µl	Fill to 20 µl

4.2.9 Dephosphorylation

Vectors used for cloning by restriction were after restriction dephosphorylated. 18 µl of the cleaned restricted vector were mixed with 2 µl 10x FastAP buffer and 1 µl FastAP (Thermo Fisher Scientific, USA). The reaction was incubated at 37 °C for at least 30 min,

heat inactivated at 75 °C for 5 min and cleaned with DNA Clean & Concentrator^{TM}-5 Kit (Zymo Research, USA) according to the manufacturer's protocol.

4.2.10 Phosphorylation

Inserts used for cloning by restriction were after restriction phosphorylated. 18 µl of the cleaned restricted insert were mixed with 2 µl 10x T4 DNA ligase buffer (New England Biolabs, USA) and 1 µl PNK (Thermo Fisher Scientific, USA). The reaction was incubated in 37 °C for at least 30 min and cleaned with DNA Clean & Concentrator^{TM}-5 Kit (Zymo Research, USA) according to the manufacturer's protocol.

4.2.11 Ligation

Dephosphorylated vector and phosphorylated insert were ligated for cloning with T4 DNA ligase (Thermo Fisher Scientific, USA). The ligation reaction was prepared according to table 4.10 and incubated at 16 °C overnight.

Table 4.10 Composition of the ligation reaction

T4 DNA ligase buffer	2 µl
Vector DNA	50 ng
Insert DNA	37.5 ng
T4 Ligase	1 µl
Nuclease-free water	Fill to 20 µl

4.2.12 Transfection to DH5α cells

Competent bacterial *E. coli* cells DH5α were used to grow up the plasmids. Cells were thawed on ice, 50 µl of cell culture were mixed with 1 µl plasmid DNA (in case of cloning and site-directed mutagenesis, the whole ligation reaction was used), mixed gently by pipetting and incubated 20 min on ice. Heat shock was introduced at 42 °C for 30 s. Immediately after the heat shock, 350 µl SOC medium were added, and the cells were incubated in 37 °C, 600 rpm for 1 h. Cells were further plated on agar plates with LB medium with requested selection antibiotics and cultivated in 37 °C overnight.

SOC medium: 0.2 % (w/v) tryptophan, 0.05 % (w/v) yeast extract, 1 mM NaCl, 0.25 mM KCl, 1 mM $MgCl_2$, 1 mM $MgSO_4$, 2 mM glucose

LB medium: 1 % (w/v) tryptophan, 0.5 % (w/v) yeast extract, 1 % NaCl, pH 7.0

4.2.13 Colony PCR

Colony PCR was used to select positive clones after cloning by restriction and site-directed mutagenesis. Taq Polymerase (Invitrogen, USA) was used for colony PCR. The reaction was mixed according to table 4.11. Instead of template DNA, part of bacterial DH5α colony was scratched from the agar plate with the pipette tip and resuspended in PCR reaction. Same primers and same annealing temperatures as for cloning were used.

Table 4.11 Composition of PCR reaction for amplification by Taq polymerase

	5 µl reaction for colony PCR
Taq polymerase buffer without $MgCl_2$	0.5 µl
10 mM dNTPs	0.1 µl
25 mM $MgCl_2$	0.3 µl
5 µM primer F	0.5 µl
5 µM primer R	0.5 µl
Taq polymerase	0.075 µl
ddH_2O	2.525 µl
Cells (template)	rougly 0.5 µl

Table 4.12 Programme for PCR amplification by Taq polymerase

Initial denaturation	94 °C	3 min	1 cycle
Denaturation	94 °C	45 s	30 cycles
Annealing	Determined optimal temperature per primer set	30 s	
Elongation	72 °C	1 min per 1000 bp	
Final elongation	72 °C	10 min	1 cycle

4.2.14 DNA and siRNA transfection to HeLa cells

Transfection of DNA plasmids to HeLa cells was used for fluorescence microscopy and immunoprecipitation of GFP-tagged proteins.

For fluorescence microscopy, Lipofectamine® LTX reagent (Invitrogen, USA) was used. Cells were seeded in 24 well plate on microscopy coverslips and transfected day after seeding, in 60-70 % confluency. 200 µl of DMEM medium (Sigma-Aldrich, USA) without serum and antibiotics were mixed with 1.5 µl Lipofectamine LTX and 1 µg transfected DNA. The reaction was incubated 20 min in room temperature, 200 µl of the medium were removed from the cell culture, and the transfection reaction was added. After 24 h, cells were fixed and used for immunostaining and fluorescence microscopy.

For immunoprecipitation, Lipofectamine® 3000 reagent (Invitrogen, USA) was used. Cells were seeded in 10 cm petri dish and transfected day after seeding, in 60-70 % confluency. 250 µl of Opti-MEM were mixed with 5 µl Lipofectamine® 3000 reagent (reaction 1) and separately, 300 µl of Opti-MEM were mixed with 7.5 µl P3000™ reagent and 3 µg transfected DNA (reaction 2). Reactions 1 and 2 were mixed, cultivated 15 min in room temperature and added to cell culture. The cells were harvested 24 h after transfection.

For siRNA interference, Oligofectamine™ (Invitrogen, USA) was used. For fluorescence microscopy, cells were cultured in 24 well plate and transfected day after seeding. 17.5 µl of Opti-MEM were mixed with the requested amount of siRNA, according to the final concentration (reaction 1) and incubated 5 min in room temperature. Separately, 5 µl of Opti-MEM were mixed with the same amount of Oligofectamine™ as siRNA (reaction 2). Reaction 1 and 2 were mixed, incubated 15 min in room temperature and added to cell culture. Cells were fixed after 48 h. For immunoprecipitation or gradient ultracentrifugation, cells were cultured in 10 cm petri dish, 210 µl of Opti-MEM were used in reaction 1 and 60 µl in reaction 2. Cells were harvested after 72 h (cultured in 6 ml of medium for 24 h, 10 ml of medium for next 24 h and in 10 ml of fresh medium for another 24 h).

The optimal concentration for each used siRNA was tested. For best results, 50 nM concentration of siRNA was used for both, TSSC4 and SNRNP200 siRNA.

4.2.15 Immunoprecipitation

Hela cells were cultured in 10 cm Petri dish till ideally 100 % confluency. Cells were 3x washed with ice cold PBS buffer, harvested into 1 ml ice cold PBS buffer and transferred to microcentrifuge tubes.

Cells were centrifuged at 1 000 g, 4 °C for 5 min and the cell pellet was resuspended in 500 µl NET2 buffer, supplemented with 1 µl RNAsin (Promega, USA) and 2 µl Protease Inhibitor Cocktail Set III (MilliporeSigma, USA). Cells were then sonicated on ice bath by

2x 45 pulses (0.5 s pulses at 40 % amplitude) and the resulting lysate was centrifuged at 20 000 g, 4 °C for 10 min. The supernatant was transferred into a new microcentrifuge tube, and input samples were saved (1x 30 µl for protein input and 1x 15 µl for RNA input, kept in 4°C till further use, isolated together with immunoprecipitated samples). Rest of the supernatant was incubated on a rotator for 1 h at 4 °C with 10 µl Protein G PLUS-Agarose beads (Santa Cruz Biotechnology, Inc., USA) for pre-cleaning.

For immunoprecipitation step, 30 µl Protein G PLUS-Agarose beads were 3x washed with ice cold NET2 buffer and incubated in 500 µl NET2 buffer supplemented with 6 µg/µl goat anti-GFP antibody (or rabbit anti-Flag antibody) on a rotator for at least 1 h at 4 °C in siliconized microcentrifuge tubes. Afterwards, beads with bound antibodies were 3x washed with ice cold PBS and incubated with pre-cleaned cell lysates on a rotator at 4 °C overnight.

Next day, lysates were discarded, beads were 3x washed with ice cold NET2 buffer and divided into equal fractions for RNA and protein isolation. NET2 buffer was discarded from the beads.

For protein isolation, beads were mixed with the same volume of 2x Sample buffer, as the volume of the beads (30 µl for immunoprecipitated samples, 15 µl for input samples), incubated 5 min at 95 °C and stored at -20 °C until further use. Proteins were resolved and analysed by Western blotting. RNA was isolated by TRIzol reagent and analysed by silver-stained PAGE-Urea polyacrylamide RNA gel.

PBS buffer: 137 mM NaCl, 2.7 mM KCl, 10 mM Na_2HPO_4, 1.8 mM KH_2PO_4, pH 7.4

NET2 buffer: 150 mM NaCl, 0.05 % (v/v) NP-40, 50 mM Tris-HCl (pH 7.4)

2x sample buffer: 250 mM Tris-HCl, 20 % (v/v) glycerol, 4 % (w/v) SDS, 0.02 % (v/v) β-mercaptoethanol, 0.02 % (w/v) bromphenol blue

4.2.16 PAGE-Urea polyacrylamide RNA gel

PAGE-Urea was used for resolving the snRNA molecules. 40 ml of 10 % polyacrylamide Urea gel/TBE was prepared according to table 4.13.

Urea was first dissolved in 10x TBE and 30 % polyacrylamide at 80 °C. Water to final volume was added, and the mixture cooled to room temperature. TEMED and 10 % APS were added, and the gel poured. Once the gel solidified, it was pre-ran at 500 V for at least 15 min in TBE buffer. For analysis of immunoprecipitation experiment, only half volume of input

samples was loaded compared to immunoprecipitated samples. Gel ran at 500 V in TBE buffer for 2h 40 min and stained by silver afterwards.

For silver staining, the gel was fixed in 40% MeOH, 10 % Acetic acid for 30 min, treated with potassium dichromate (3.4 mM $K_2Cr_2O_7$, 3.2 mM HNO_3) for 10 min and washed 3x for 30 s in dH_2O. After washing, the gel was stained with silver (12 mM $AgNO_3$) for 30 min and again washed 3x for 30 s in dH_2O. Image was developed with sodium carbonate [280 mM Na_2CO_3, 0.02 % (v/v) formaldehyde] until clear image and development was stopped with 1 % acetic acid.

Table 4.13 Composition of PAGE-Urea polyacrylamide gel

Urea	19.2 g
10x TBE	4 ml
30 % acrylamide/N,N'-methylenebisacrylamide (19:1)	13.3 ml
10 % APS	400 µl
TEMED	25 µl
ddH_2O	Fill to 40 ml

10x TBE buffer: 890 mM Tris base (pH 8.2), 890 mM boric acid, 25 mM EDTA

TBE buffer: 89 mM Tris base (pH 8.2), 89 mM boric acid, 2.5 mM EDTA

4.2.17 SDS-PAGE Polyacrylamide gel electrophoresis

SDS-PAGE was used for separating the proteins in polyacrylamide gel according to protein weight. 10 % or 8 % (in case of resolving big proteins as SNRNP200 or PRPF8) separating gels were used. Separating and stacking gels were mixed according to tables 4.14 and 4.15 and ran in 80 V for 30 min and then at 100 V 1 h – 1 h 20 min (until sufficient separation) in SDS buffer. 4 µl of PageRuler Plus prestained protein ladder (Thermo Fisher Scientific, USA) were used as a protein marker.

Table 4.14 Composition of separating gels used for SDS-PAGE

	8 % separating gel (5 ml)	10 % separating gel (5 ml)
ddH_2O	2.3 ml	2.0 ml
30 % acrylamide/N,N'-methylenebisacrylamide (37.5:1)	1.3 ml	1.7 ml
1.5 M Tris (pH 8.8)	1.3 ml	1.3 ml
10 % SDS	0.05 ml	0.05 ml
10 % APS	0.05 ml	0.05 ml
TEMED	0.003 ml	0.002 ml

Table 4.15 Composition of stacking gel used for SDS-PAGE

	Stacking gel (5 ml)
ddH_2O	3.4 ml
30 % acrylamide/N,N'-methylenebisacrylamide (37.5:1)	1.0 ml
1.0 M Tris (pH 6.8)	0.75 ml
10 % SDS	0.06 ml
10 % APS	0.06 ml
TEMED	0.006 ml

SDS buffer: 25 mM Tris-HCl, 192 mM glycine, 0.1 % (w/v) SDS

4.2.18 Western Blotting

After electrophoresis, proteins were transferred to a 0.45 µm nitrocellulose membrane (GE Healthcare, USA). Blotting sandwich was folded with two sponges, 2x 3 pieces of 3 mm Whatman™ chromatography paper (GE Healthcare, USA) and SDS-PAGE polyacrylamide gel with nitrocellulose membrane inside. All the components were soaked in transfer buffer.

Western blotting ran at a constant current of 360 mA for 2 h. After blotting, the membrane was washed in PBST and stained with 0.1 % Ponceau/1 % acetic acid for control unspecific protein visualisation. Ponceau was washed with PBST and membrane was blocked by incubation in 10 % (w/v) low-fat milk (NutriStar, FRA)/PBST for 1h. After blocking, the membrane was washed in 1 % (w/v) low-fat milk/PBST and stained by primary antibody diluted in 1 % (w/v) low-fat milk/PBST to required concentration for 1h. Afterwards, the membrane was washed 2x 10 min in 1 % (w/v) low-fat milk/PBST, 1x 10 min in PBST, stained by secondary antibody diluted in 1 % (w/v) low-fat milk/PBST for 1 h and washed 3x 10 min in PBST. For all experiments, AffiniPure goat secondary antibodies conjugated with horseradish peroxidase (Jackson ImmunoResearch, GBR) diluted 1:10 000 were used. The membrane was afterwards incubated with SuperSignal™ West chemiluminescent substrate (Thermo Fisher Scientific, USA) for 2 min and the image was developed in LAS-3000 imager.

Transfer buffer: 25 mM Tris-HCl, 192 mM glycine, 20 % (v/v) methanol

PBST: 137 mM NaCl, 2.7 mM KCl, 10 mM Na_2HPO_4, 1.8 mM KH_2PO_4, 0.05 % (v/v) Tween® 20 (Sigma-Aldrich, USA), pH 7.4

4.2.19 Immunofluorescence and fluorescence *in situ* hybridisation

Cells were grown on microscope coverslips, 3x washed with PBS buffer, fixed in 4 % paraformaldehyde/PIPES for 10 min and again 3x washed in PBS buffer. Cells were permeabilized by 0.5 % (v/v) Triton®X-100 (SERVA Electrophoresis GmbH, DEU)/PBS for 5 min, 3x washed with PBS buffer, blocked by 5 % (v/v) normal goat serum (SouthernBiotech, USA)/PBS for 10 min and again 3x washed with PBS buffer.

For immunostaining, coverslips were incubated with primary antibody/PBS diluted to required concentration for 1h, 3x washed with PBS buffer, incubated with secondary antibody/PBS diluted 1:500 and again 3x washed with PBS buffer. AffiniPure goat secondary antibodies conjugated with Alexa Fluor™ 488, 555 or 647 (Invitrogen, USA) were used. If only immunostaining was needed for sample preparation, coverslips were washed with dH_2O and mounted to microscope slides by DAPI Fluoromount-G® (SouthernBiotech, USA).

For fluorescence *in situ* hybridisation, immunostained cells were again fixed by 4 % paraformaldehyde/PIPES and 3x washed with PBS buffer. Coverslips were then treated with 0.1 M glycine, 0.2 M Tris-HCl (pH 7.4) for 10 min, washed in PBS buffer, treated with 50 % (v/v) formamide/2x SSC, again washed in PBS buffer and incubated in moister chamber

with probe mix supplemented with 0.3 µl of probe in 37 °C for 1h. Coverslips were then washed with 50 % (v/v) formamide/2x SSC in 37 °C for 20 min, 2x SSC in 37 °C for 20 min, 1x SSC in room temperature for 20 min and mounted to microscope slides by DAPI Fluoromount-G® (SouthernBiotech, USA).

Images were taken by DeltaVision microscopic system (Applied Precision Ltd., SVK) coupled to Olympus IX70 microscope with oil immersion objective (60x/1.4 NA). For every image, 15 Z-stacks with 200 nm spacing were collected and restored by SoftWorx deconvolution system (Applied Precision Ltd., SVK), as described previously (Novotny et al. 2011).

PBS: 137 mM NaCl, 2.7 mM KCl, 10 mM Na_2HPO_4, 1.8 mM KH_2PO_4, pH 7.4

4 % paraformaldehyde/PIPES: 4 % (w/v) paraformaldehyde, 100 mM PIPES (pH 6.9), 2 mM $MgCl_2$, 1.25 mM EGTA (pH 8.0)

20x SSC: 3M NaCl, 300 mM sodium citrate, pH 7.0

Probe mix: 50 % (v/v) formamide, 5 % (w/v) dextran sulphate, 0.5 % (w/v) BSA, 2x SSC

4.2.20 Gradient ultracentrifugation

Gradient ultracentrifugation in linear 10-30 % glycerol gradient was used to separate U5 snRNP, di-snRNP and tri-snRNP. 10 % and 30 % glycerol solutions were prepared according to table 4.16. Equal fractions of prepared 10 % and 30 % glycerol solutions (5.5 ml) were poured to ultracentrifugation tubes compatible with used SW-40 rotor using gradient mixer. Glycerol gradient was let at 4 °C to equilibrate for 1h.

Table 4.16 Composition of glycerol solutions used for gradient pouring

	10 % glycerol (20 ml)	30 % glycerol (20 ml)
10x G buffer	2 ml	2 ml
Glycerol	2 ml	6 ml
Protease Inhibitor Cocktail Set III (MilliporeSigma, USA)	20 µl	20 µl
1 M DTT	10 µl	10 µl
0.1 M PMSF	100 µl	100 µl
ddH_2O	15.87 ml	11.87 ml

Cells were grown ideally to 100 % confluency in 10 cm petri dish, and the nuclear extract was prepared using NE-PER Nuclear and Cytoplasmic Extraction Reagents (Thermo Fisher Scientific, USA) according to the manufacturer's protocol. 15 µl of nuclear and cytoplasmic extract were saved for testing the separation of the nuclear from the cytoplasmic phase (by staining for SmD1 and tubulin) and efficiency of knockdown by Western blot. Nuclear extract was poured on top of the glycerol gradient and the weight of the tubes was evened with 1x G buffer.

The rotor was pre-cooled to 4 °C and ultracentrifugation ran at 130 000 g (32 000 rpm for used SW-40 rotor), 4 °C for 17 h. Immediately after centrifugation, the gradient was fractioned from the top by 500 µl using a pipette to total 23 fractions. Pellet was dissolved in 500 µl ddH_2O and used as the 24th fraction.

From each fraction, RNA was isolated by TRIzol reagent (Ambion, Inc., USA) as described above. The organic phase of TRIzol was used for protein isolation.

10x G buffer: 200 mM HEPES/KOH (pH 8.0), 1.5 M KCl, 15 mM $MgCl_2$

4.2.21 Protein isolation by TRIzol reagent

Protein isolation by TRIzol reagent (Ambion, Inc., USA) was used for isolating the proteins from gradient ultracentrifugation fractions. Organic phase after RNA isolation was mixed with 180 µl of 100 % BioUltra ethanol, samples were vortexed for 1 min, incubated 3 min at room temperature and centrifuged at 2000 g, 4 °C for 5 min. The supernatant was transferred into a new microcentrifugation tube, mixed with 450 µl of isopropanol, incubated at room temperature for 10 min and centrifuged at 12 000 g, 4 °C for 10 min. Pellet was washed with 80 % BioUltra ethanol and again centrifuged at 12 000 g, 4 °C for 10 min. Pellet was dried at 37 °C and resuspended in 48 µl NEST-2 buffer, 50 °C at 900 rpm. Once resuspended, samples were mixed with 12 µl 5x sample buffer, incubated in 95 °C for 5 min and resolved with SDS-PAGE and Western blotting.

NEST-2 buffer: 50 mM Tris-HCl (pH 6.8), 20 mM EDTA, 5 % (w/v) SDS

5x sample buffer: 625 mM Tris-HCl, 50 % (v/v) glycerol, 10 % (w/v) SDS, 0.05 % (v/v) β-mercaptoethanol, 0.05 % (w/v) bromphenol blue

5 Results

5.1 TSSC4 is a nuclear protein specific for U5 snRNP

As a first step, I wanted to confirm the interaction of TSSC4 with U5 snRNP (Malinova et al. 2017). I constructed TSSC4-GFP and TSSC4-tripleFlag expressing vectors and used them to determine TSSC4 cell localisation and analysed protein and RNA interactions.

For cell localisation, I transfected HeLa cells with TSSC4-GFP and empty GFP vector as a negative control, fixed the cells and compared the localisation of GFP signal by fluorescence microscopy (figure 5.1). I observed diffuse nuclear localisation of TSSC4-GFP without accumulation in any nuclear bodies.

To rule out the possibility of the artefact introduced by GFP-tagging, the result was confirmed by staining with primary antibody against endogenous TSSC4 (figure not shown).

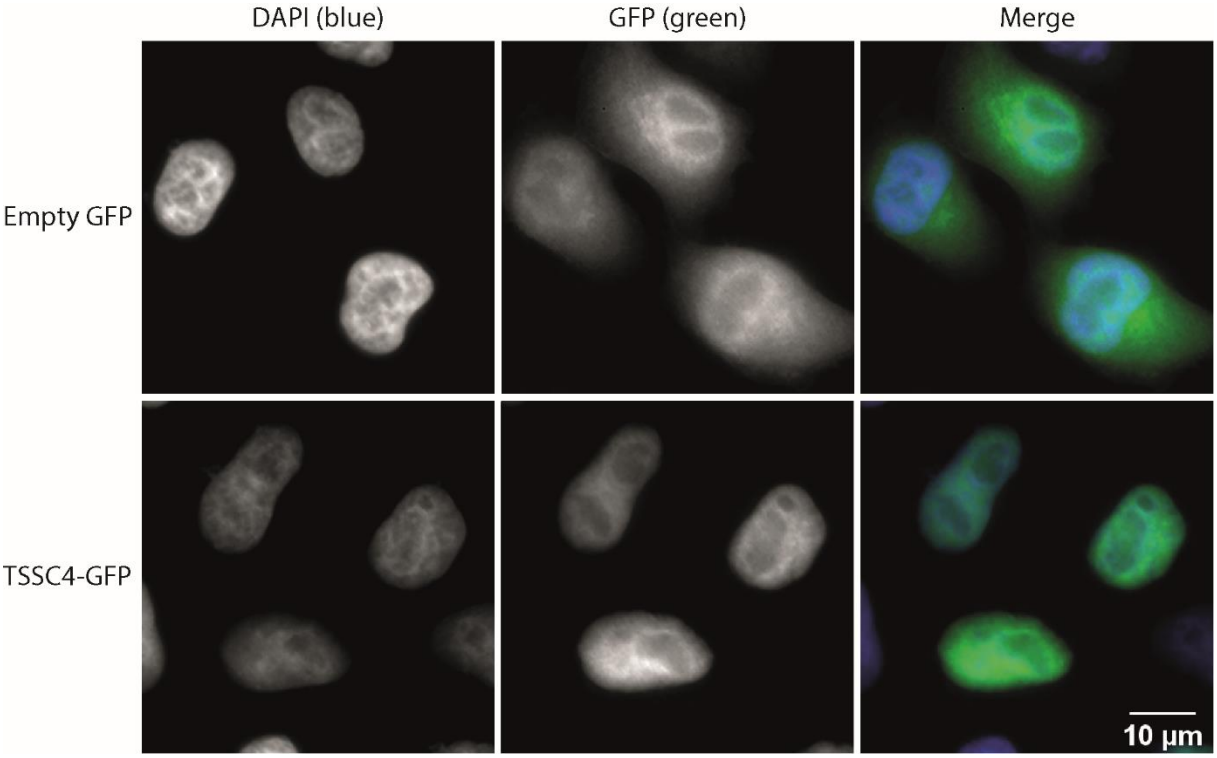

Figure 5.1 Cell localisation of TSSC4
HeLa cells were transfected with TSSC4-GFP expressing vector and empty GFP vector as a negative control. Cells were fixed and mounted with Fluoromount containing DAPI. Images were resolved by fluorescence microscopy.

To identify the interacting proteins and RNAs with TSSC4, I used TSSC4-GFP and TSSC4-tripleFlag for immunoprecipitation by anti-GFP or anti-Flag antibody, respectively.

I analysed the co-precipitating proteins by Western blotting (figure 5.2) and RNA by silver-stained PAGE-Urea polyacrylamide gel (figure 5.3).

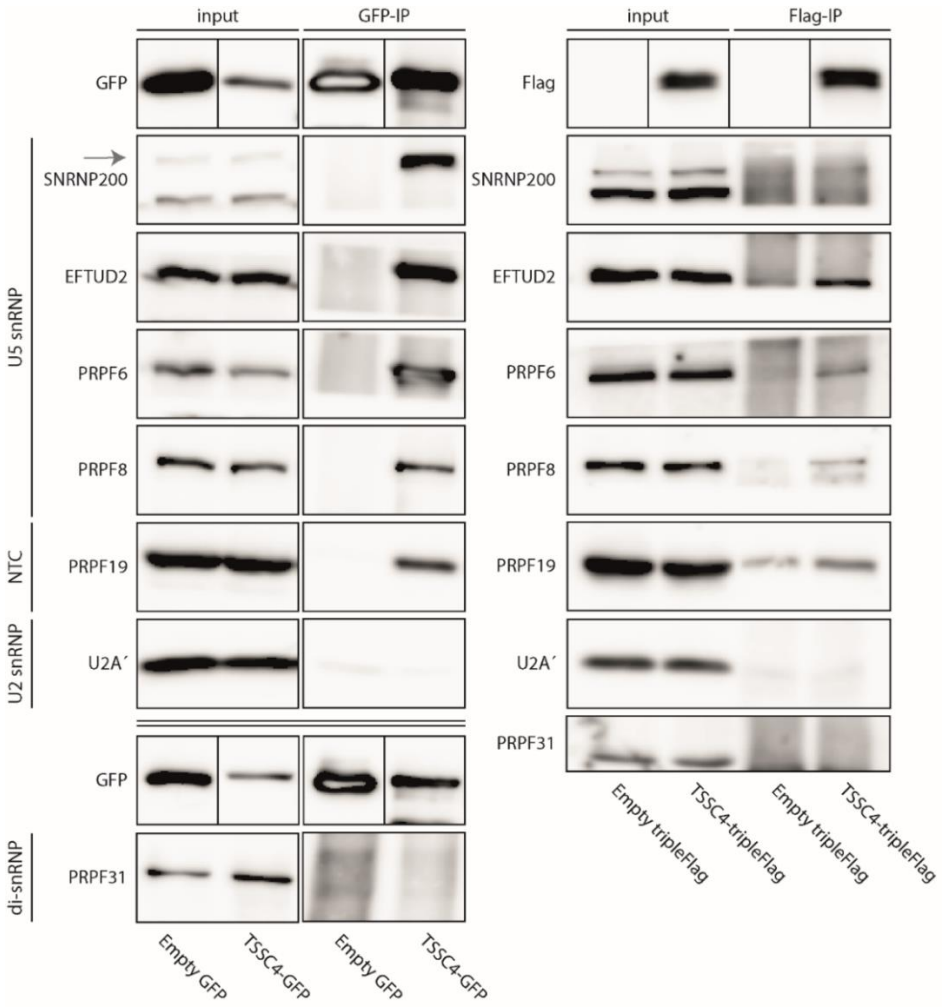

Figure 5.2 Proteins co-precipitated with TSSC4-GFP/tripleFlag
HeLa cells were transfected with TSSC4-GFP/tripleFlag, empty GFP/tripleFlag vector was used as a negative control. Cell lysates were prepared and used for immunoprecipitation. Proteins were isolated and analysed by Western blotting. Staining for SNRNP200 shows close unspecific band, the specific SNRNP200 band is marked by the grey arrow. NTC – nineteen complex

The results show the interaction of TSSC4 with U5 snRNP specific proteins and U5 snRNA, as well as interaction with PRPF19, a component of NTC complex which drives the catalytic activation of the spliceosome (Chan et al. 2003). The interactions can be identified using both, GFP and Flag-tagged constructs. However, the interactions detected by Flag-tagged construct are weaker. This could be explained by either less efficient Flag-immunoprecipitation or stabilisation of TSSC4 interactions introduced by GFP tagging. I did not observe interaction with di-snRNP specific PRPF31, neither U4 snRNA, suggesting that TSSC4 is specific for U5 snRNP and is not present in tri-snRNP. I did not observe either interaction of TSSC4 with U2 snRNP specific U2A′. However, on RNA level, weak

interaction of TSSC4 with U2 and U6 snRNAs can be detected, suggesting, that TSSC4 might associate with these snRNAs as well.

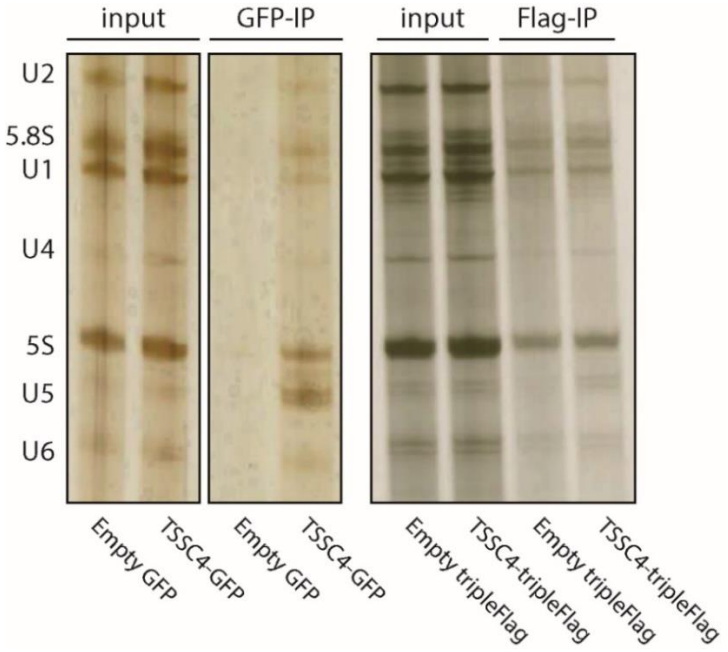

Figure 5.3 RNA co-precipitated with TSSC4-GFP/tripleFlag
HeLa cells were transfected with TSSC4-GFP/tripleFlag, empty GFP/tripleFlag was used as a negative control. Cell lysates were prepared and used for immunoprecipitation. RNA was isolated by TRIzol reagent and resolved on PAGE-Urea polyacrylamide gel, which was for visualisation of RNA molecules stained by silver. The position of individual snRNAs, together with 5.8S and 5S is shown on the left.

5.2 Deletion mutants of TSSC4

Apart from the evolutionarily conserved domain in the middle part of the protein belonging to TSSC4 superfamily, TSSC4 does not contain any specific protein motif (figure 5.4, determined by protein to protein BLAST, https://blast.ncbi.nlm.nih.gov/Blast.cgi and https://www.genome.jp/tools/motif/).

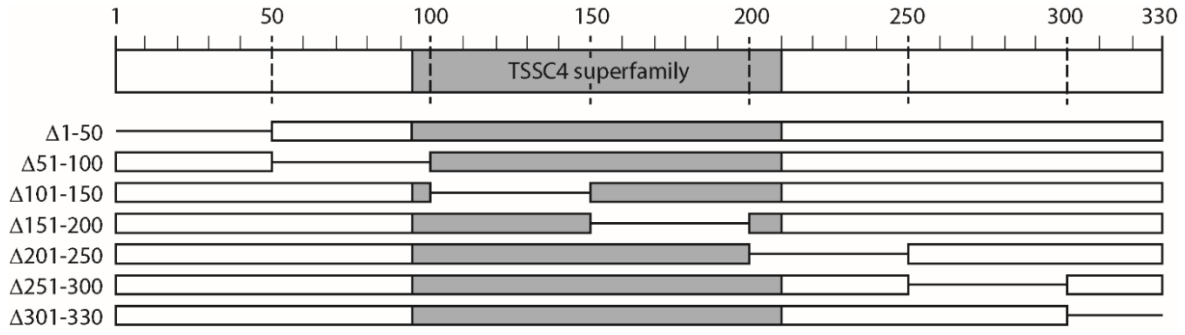

Figure 5.4 Scheme of prepared deletion mutants of TSSC4
TSSC4-GFP vector was used as a template for preparation of TSSC4 deletion mutants by site-directed mutagenesis. The evolutionarily conserved domain of TSSC4 is shown as a grey box, the rest of the protein is shown as a white box. The amino acid position is shown above the scheme of the protein. Crossed lines are marking the boundaries of the deletions. The lines in the scheme of deletion mutants are indicating deleted regions.

To determine which region of the TSSC4 is responsible for interaction with U5 snRNP, I prepared a series of deletion mutants by deleting 50 amino acids along the TSSC4 sequence, except the mutant 301-330, where I removed the last C-terminal 30 amino acids. All mutants were tagged by GFP at the C-terminus (the scheme is shown in figure 5.4). Unfortunately, I was not able to prepare deletion mutant TSSC4_Δ1-50-GFP, and the product of TSSC4_Δ301-330-GFP was repeatedly degraded in cells. I transfected these TSSC4 deletion mutants to HeLa cells, performed immunoprecipitation with anti-GFP antibody and analysed co-precipitating proteins (figure 5.5) and RNA (figure 5.6). I used an empty GFP vector as a negative control and the full-length TSSC4-GFP as a positive control.

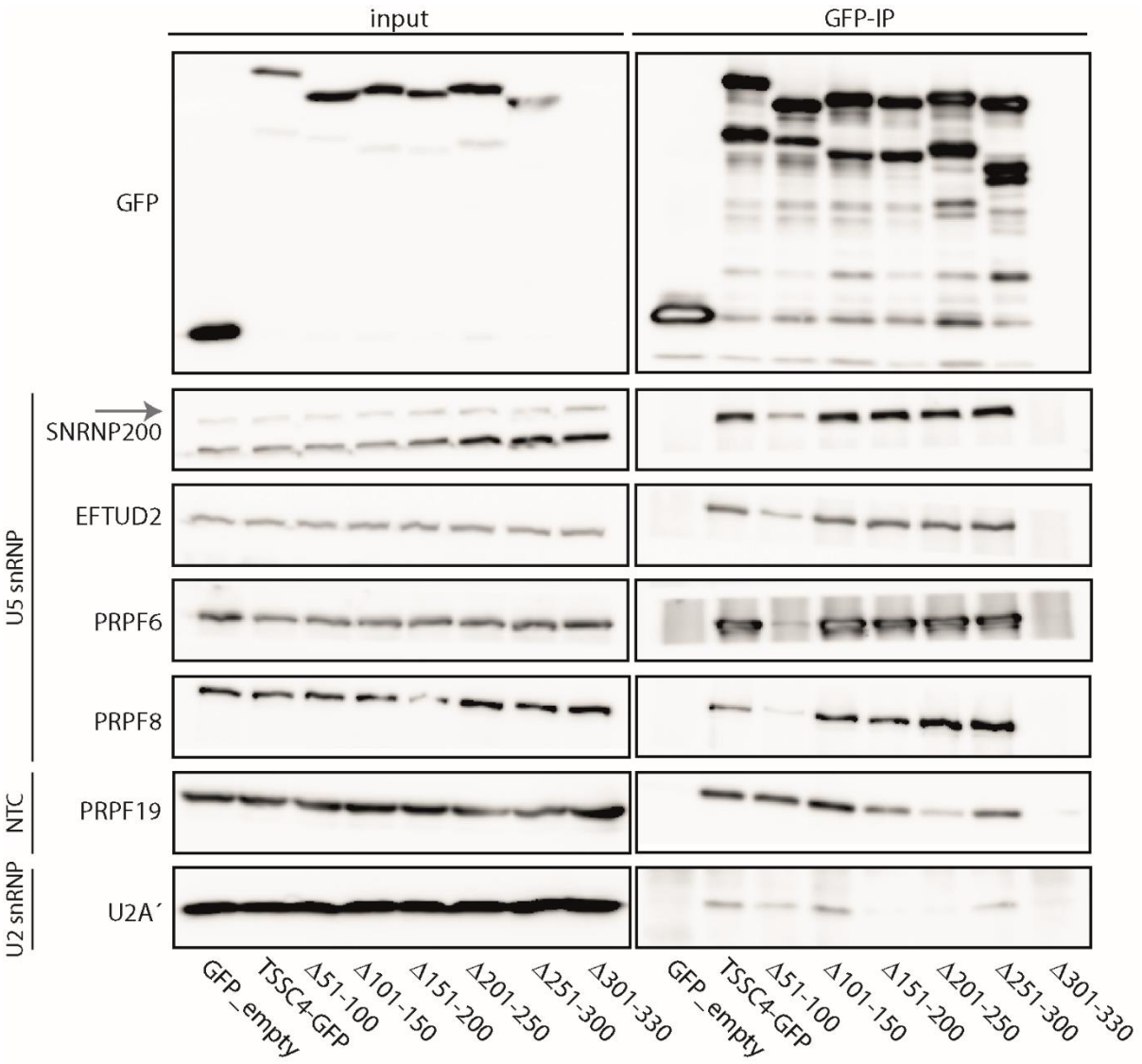

Figure 5.5 Proteins co-precipitated with TSSC4 deletion mutants
HeLa cells were transfected with TSSC4 deletion mutants tagged with GFP, empty GFP vector as a negative control and full-length TSSC4-GFP as a positive control. Cell lysates were prepared and immunoprecipitated with an anti-GFP antibody. Isolated proteins were analysed by Western blotting. Staining for SNRNP200 shows close unspecific band, the specific SNRNP200 band is marked by the grey arrow. NTC – nineteen complex

Deletion mutants show some degradation products, but the full products remain the most abundant. Deletion of amino acids 51-100 disrupted the interaction with U5 snRNP, which can also be seen on the RNA level, but the mutant still interacted with PRPF19. Deletion of amino acids 201-250 gave opposite results, and the mutant lost the interaction with PRPF19 but kept the interaction with U5 snRNP. Weak interaction of U2 snRNP specific U2A′ with TSSC4 was detected, which is lost together with U5 snRNP and PRPF19.

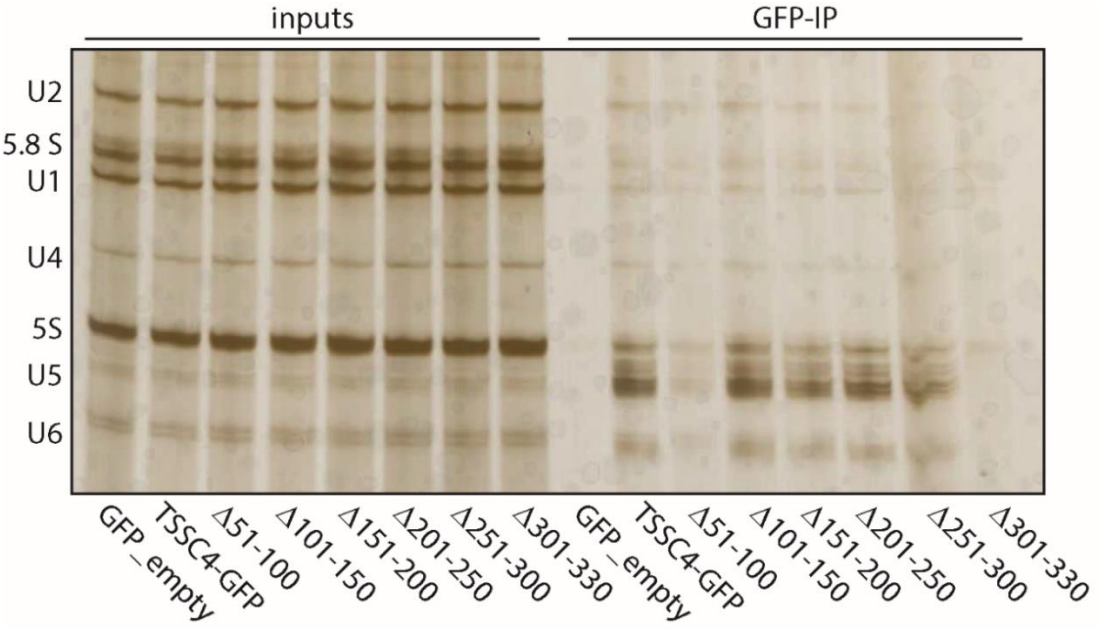

Figure 5.6 RNA co-precipitated with TSSC4 deletion mutants
HeLa cells were transfected with TSSC4 deletion mutants tagged with GFP, empty GFP vector as a negative control and full-length TSSC4-GFP as a positive control. Cell lysates were prepared and immunoprecipitated with an anti-GFP antibody. RNA was isolated by TRIzol reagent and resolved on PAGE-Urea polyacrylamide gel, which was for visualisation of RNA molecules stained by silver. The position of individual snRNAs, together with 5.8S and 5S is shown on the left.

Apart from U5 snRNA, the signal for U2 and U6 snRNAs can be detected in immunoprecipitated samples. Since the interaction of TSSC4 with U2A′ was also detected, it might be possible, that TSSC4 is interacting with post-catalytic spliceosome. The signal for ribosomal RNAs can also be found, which is repeatedly showing in all immunoprecipitated samples. Detection of ribosomal RNAs can be explained by the high abundance of ribosomal RNAs in cells and thus insufficient pre-cleaning, which can cause unspecific results.

To test whether the deletions in TSSC4 could inhibit the nuclear localisation of the protein a thus indirectly influence the interaction with either U5 snRNP or PRPF19, I transfected all constructs to HeLa cells, fixed the cells and analysed the localisation by fluorescence microscopy. Empty GFP was used as a negative control and full-length TSSC4-GFP as a positive control (figure 5.7).

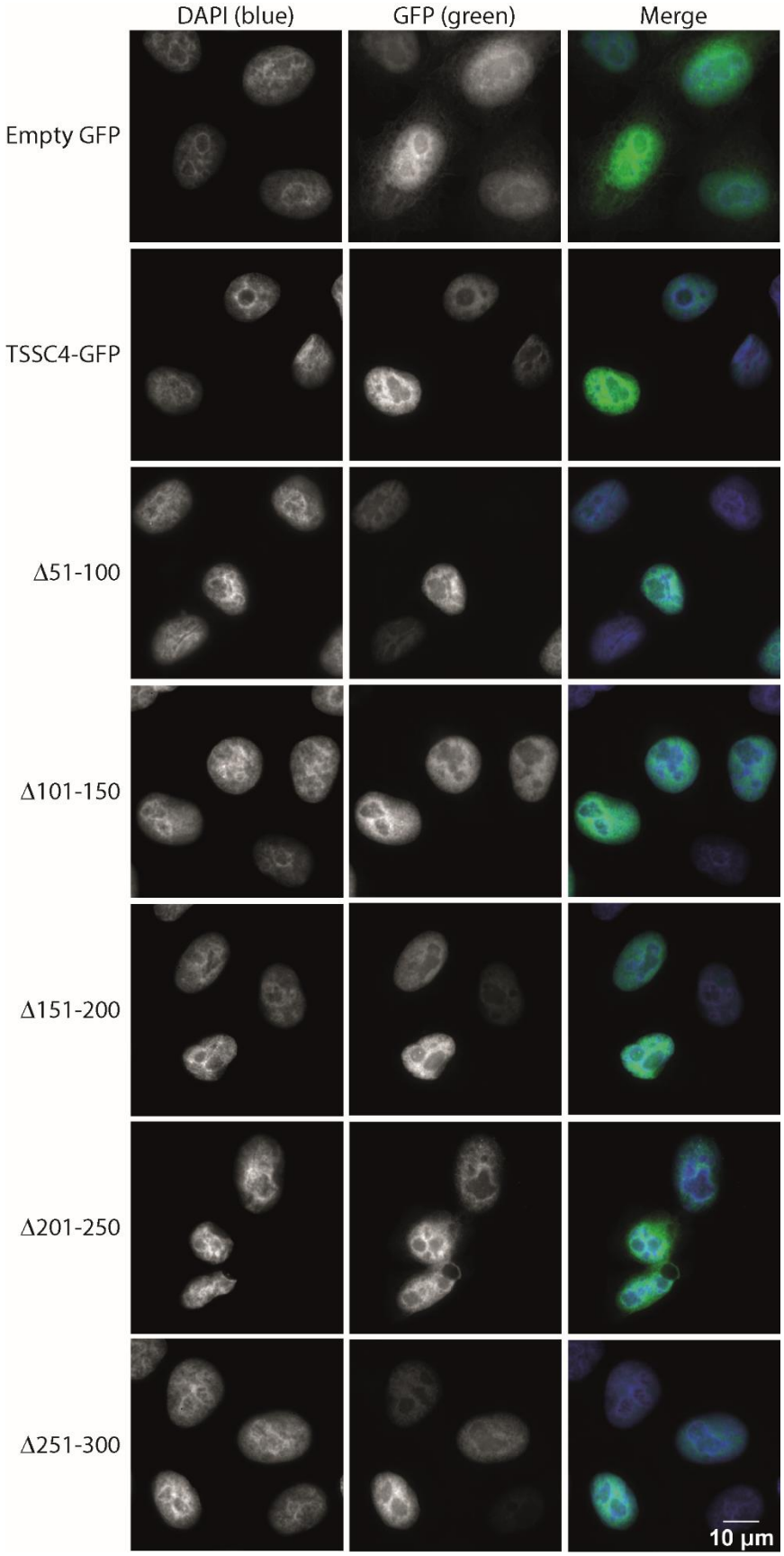

Figure 5.7 Cell localisation of TSSC4 deletion mutants

HeLa cells were transfected with TSSC4 deletion mutants, empty GFP vector as a negative control and full-length TSSC4-GFP as a positive control. Cells were fixed and mounted with Fluoromount containing DAPI. Images were resolved by fluorescence microscopy.

The deletion of amino acids 201-250 results in partial cytoplasmic localisation. The 201-250 region does not contain any predicted nuclear localisation signal (determined by http://nls-mapper.iab.keio.ac.jp/cgi-bin/NLS_Mapper_form.cgi), and I did not observe the cytoplasmic localisation of TSSC4_Δ201-250-GFP in all transfected cells. Besides, even in cells showing partial localisation of TSSC4_Δ201-250-GFP in the cytoplasm, the majority of GFP signal remained mainly in the nucleus and I thus not explain the lower interaction with PRPF19 by the change in cell localisation. In general, nuclear localisation of other TSSC4 deletion mutants remained unchanged, compared to full-length TSSC4.

5.3 The effect of TSSC4 depletion on HeLa cells

To test whether TSSC4 has any role in snRNP biogenesis, I decided to analyse the snRNPs localisation in TSSC4 depleted HeLa cells because it was previously shown, that CB localisation is a good indicator of inhibition of snRNPs assembly (Novotny et al. 2015, Schaffert et al. 2004).

I transfected TSSC4 siRNA and Silencer Negative Control 5 siRNA to HeLa cells and detected localisation of snRNAs by FISH. U2 snRNA was used as a positive control. Cajal bodies were stained using primary antibodies against coilin (figure 5.8).

I observed accumulation of all tri-snRNAs in Cajal bodies, which suggests inhibition of tri-snRNP assembly. Similar phenotype was previously observed upon depletion of U5 snRNP specific PRPF8 and thus inhibition of U5 snRNP assembly (Novotny et al. 2015). To test whether TSSC4 depletion inhibits U5 snRNP assembly, I decided to analyse, whether TSSC4 depletion results in accumulation of U5 snRNP specific proteins, as well as U5 snRNA. Together with U5 snRNP specific proteins, I analysed localisation of PRPF19, component of NTC complex joining the spliceosome during its catalytic activation, which remains associated with U5 snRNP after spliceosome disassembly (Chan et al. 2003, Makarov et al. 2002).

For protein visualisation, I used vector expressing GFP-tagged 52K (prepared and kindly provided by Huranová M., unpublished), stable cell lines expressing GFP-tagged SNRNP200 (Cvackova et al. 2014) and PRPF8 (Malinova et al. 2017) and immunostaining with primary antibodies against PRPF19 and EFTUD2. Cajal bodies were stained with a primary antibody against coilin (figure 5.9).

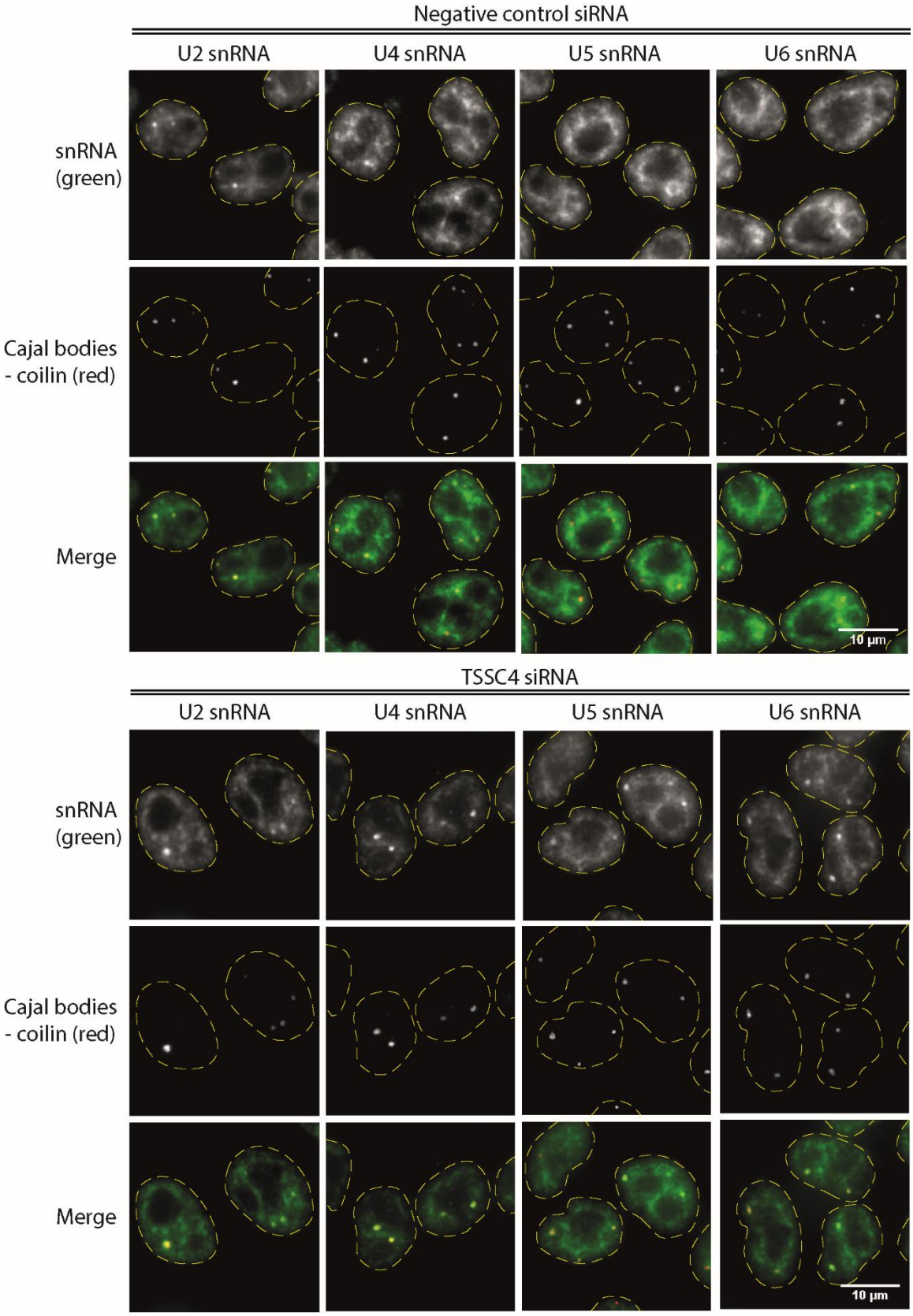

Figure 5.8 Localisation of snRNAs after TSSC4 depletion

HeLa cells were transfected with TSSC4 siRNA or Silencer Negative Control 5 siRNA. Cells were fixed and stained by FISH for specific snRNAs. Cajal bodies were stained by a primary antibody against coilin. Cells were mounted with Fluoromount containing DAPI. Pictures were resolved by fluorescence microscopy. Yellow dashed line is illustrating the edge of the nucleus, based on DAPI staining.

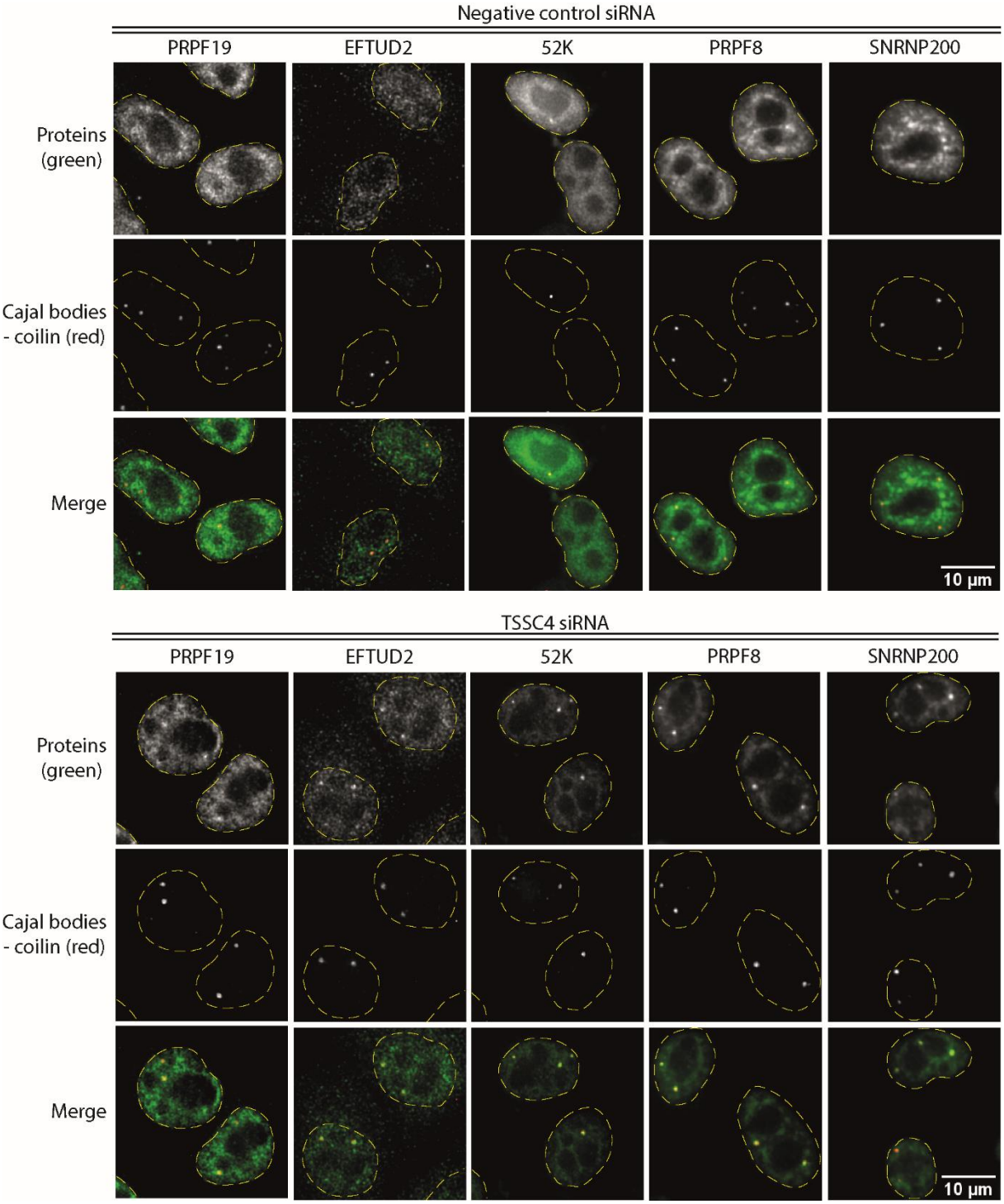

Figure 5.9 Localisation of selected proteins after TSSC4 depletion
HeLa cells were transfected with TSSC4 siRNA or Silencer Negative Control 5 siRNA. Cells were fixed, a vector expressing GFP-tagged 52K, stable cell lines expressing GFP-tagged SNRNP200 and PRPF8 and immunostaining with primary antibodies against PRPF19 and EFTUD2 were used to determine protein localisation. Cajal bodies were stained by a primary antibody against coilin. Cells were mounted with Fluoromount containing DAPI and pictures resolved by fluorescence microscopy. Yellow dashed line is illustrating the edge of the nucleus, based on DAPI staining.

I observed accumulation of all tested U5 snRNP proteins in Cajal bodies after TSSC4 knockdown, which suggests inhibition of tri-snRNP assembly, rather than inhibition of

U5 snRNP assembly. However, because accumulation in Cajal bodies gives only indirect information about the U5 snRNP assembly state, I decided to test U5 snRNP protein composition by immunoprecipitation of the central U5 snRNP specific protein PRPF8 tagged with GFP. I depleted TSSC4 from PRPF8-GFP HeLa stable cell line (Malinova et al. 2017) by siRNA interference, used anti-GFP antibodies for PRPF8-GFP immunoprecipitation and analysed co-precipitated RNA by silver-stained PAGE-Urea polyacrylamide gel (figure 5.10) and proteins by Western blotting (figure 5.11). TSSC4-GFP served as a positive control.

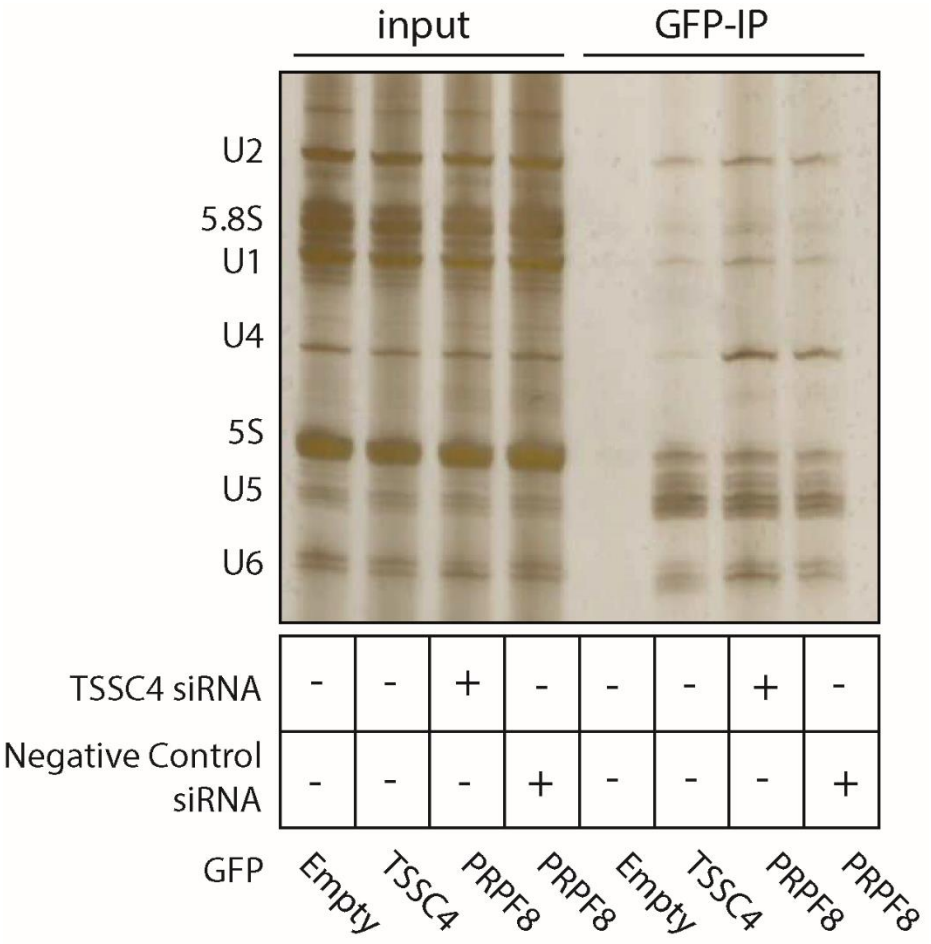

Figure 5.10 Analysis of RNA co-precipitated with PRPF8 in TSSC4 depleted HeLa cells
TSSC4 was depleted form PRPF8-GPF stable HeLa cell line by siRNA interference. Cell lysates were prepared and used for immunoprecipitation of U5 snRNP containing complexes with GFP antibody. Empty GFP vector was used as a negative control and TSSC4-GFP as a positive control. RNA was isolated by TRIzol reagent and resolved on PAGE-Urea polyacrylamide gel, which was for visualisation of RNA molecules stained by silver. The position of individual snRNAs, together with 5.8S and 5S is shown on the left.

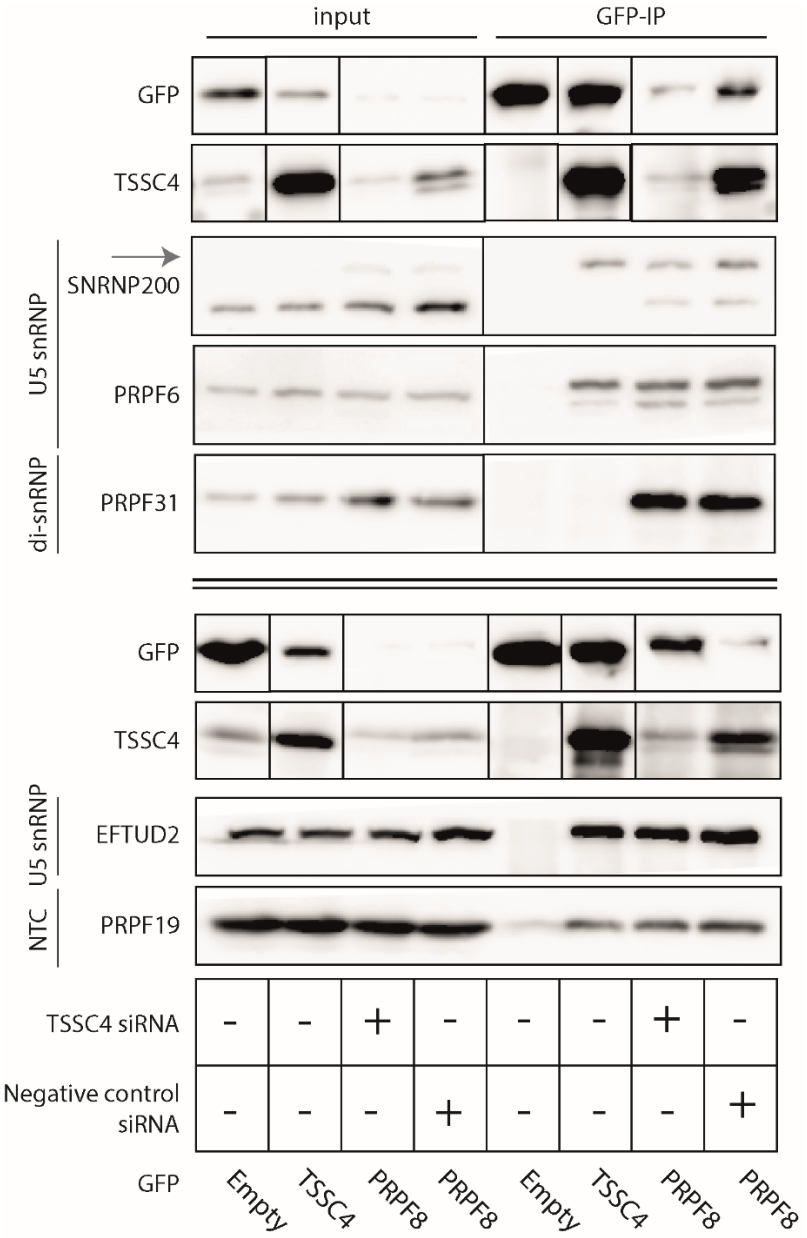

Figure 5.11 Analysis of proteins co-precipitated with PRPF8 in TSSC4 depleted HeLa cells
TSSC4 was depleted form PRPF8-GPF stable HeLa cell line by siRNA interference. Cell lysates were prepared and used for immunoprecipitation of U5 snRNP containing complexes with GFP antibody. Empty GFP vector was used as a negative control and TSSC4-GFP as a positive control. Proteins were isolated and analysed by Western blotting. Staining for SNRNP200 shows close unspecific band, the specific SNRNP200 band is marked by the grey arrow. NTC – nineteen complex

On RNA level, I did not observe any difference after TSSC4 knockdown. On the protein level, GFP signal differs in the knockdowned sample compared to the negative control, which can be explained by inefficient blotting or staining, since the results remain the same independently on this difference. Upon TSSC4 depletion, I repeatedly observed weaker association of PRPF8 with SNRNP200. To test whether CB accumulation of snRNAs (figure 5.8) after TSSC4 depletion can be explained by the loosened association of SNRNP200 with U5 snRNP. I depleted SNRNP200 from HeLa cells by siRNA interference and analysed the

snRNAs localisation by FISH (figure 5.12). Compared to negative control, I did not observe any difference in snRNAs localisation after SNRNP200 depletion, which suggests, that CB accumulation of snRNAs upon TSSC4 depletion is not caused by loosened association of PRPF8 with SNRNP200.

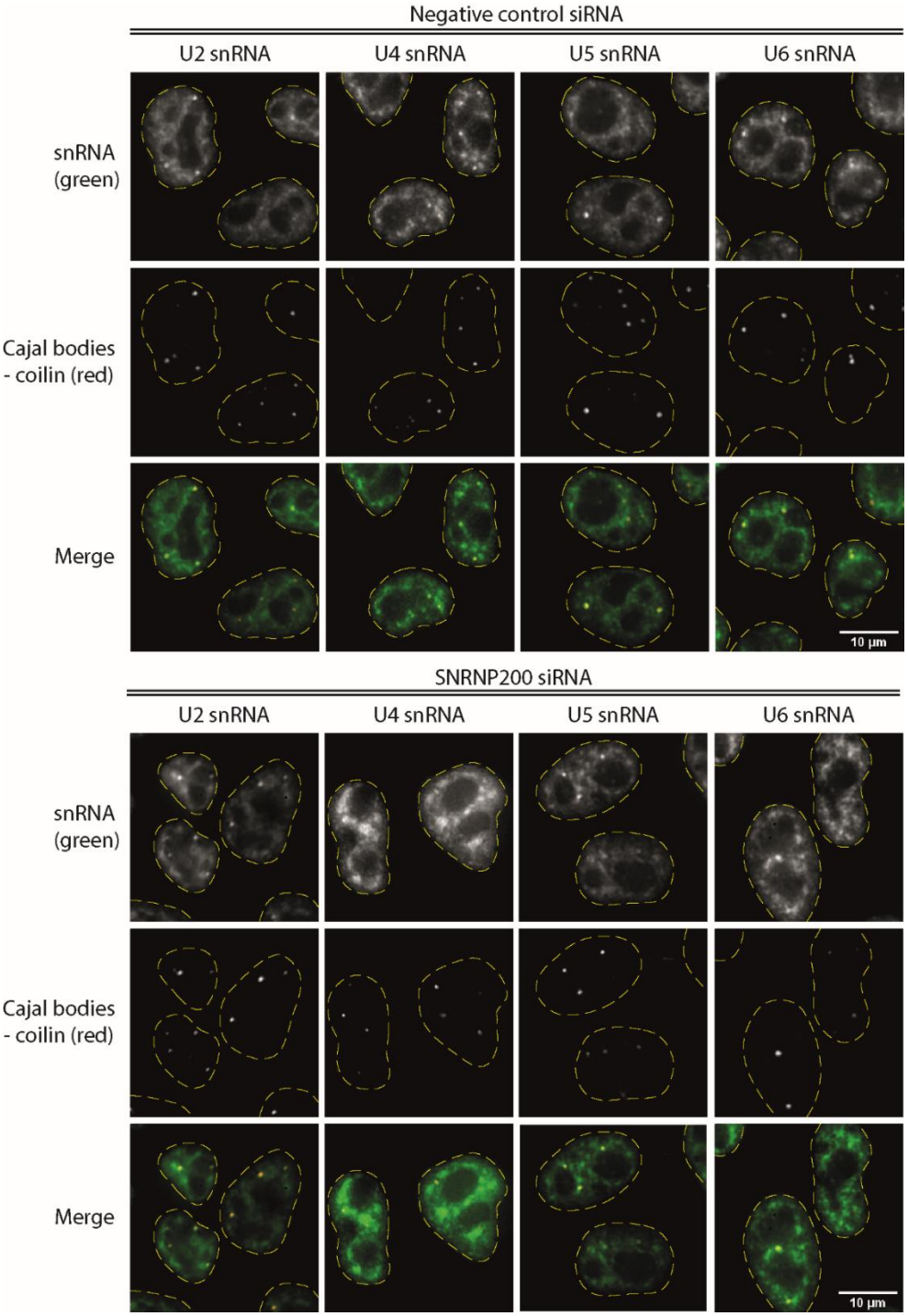

Figure 5.12 Localisation of snRNAs after SNRNP200 depletion

HeLa cells were transfected with SNRNP200 siRNA or Silencer Negative Control 5 siRNA. Cells were fixed and stained by FISH for specific snRNAs. Cajal bodies were stained by a primary antibody against coilin. Cells were mounted with Fluoromount containing DAPI. Pictures were resolved by fluorescence microscopy. Yellow dashed line is illustrating the edge of the nucleus, based on DAPI staining.

5.4 Analysis of tri-snRNP assembly

TSSC4 depletion induced accumulation of tri-snRNP components in CBs, which indicates inhibition of tri-snRNP assembly (Novotny et al. 2015, Schaffert et al. 2004). To test whether TSSC4 functions in tri-snRNP assembly, I analysed the presence of individual snRNPs by gradient ultracentrifugation (Bartels et al. 2003). I separated di-snRNP, mono U5 snRNP and tri-snRNP from nuclear extract of HeLa cells by linear 10-30 % glycerol gradient ultracentrifugation, analysed proteins by Western blotting and RNA by silver-stained PAGE-Urea polyacrylamide gel to determine the position of individual snRNPs (figure 5.13).

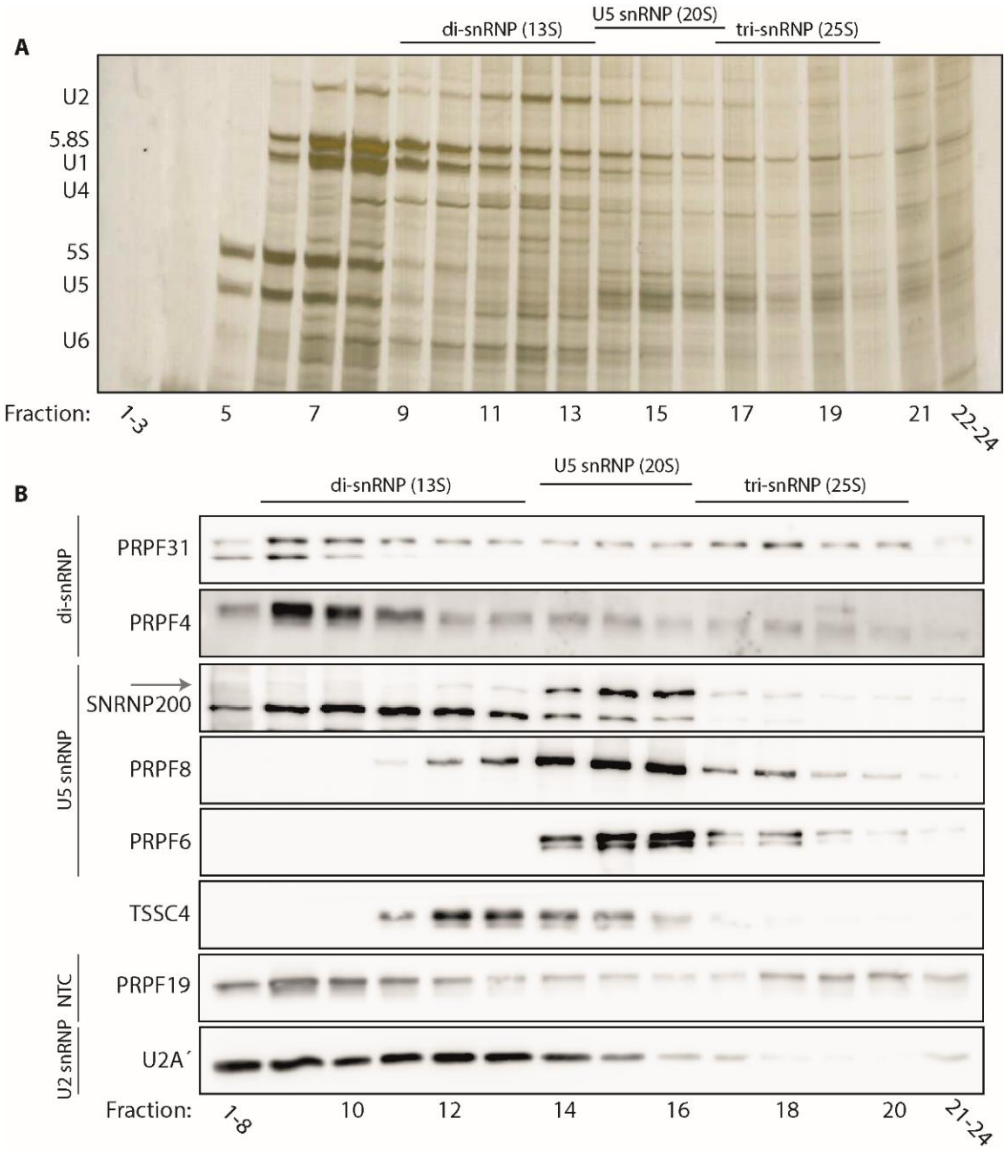

Figure 5.13 Analysis of individual snRNP particles from nuclear extract of HeLa cells
Nuclear extract was isolated from wt HeLa cells and separated on 10-30 % linear glycerol gradient by ultracentrifugation. The gradient was fractioned, and from each fraction, RNA and proteins were isolated. A) RNA was resolved by silver-stained PAGE-Urea polyacrylamide gel which was for visualisation of RNA molecules stained by silver. The position of individual snRNAs, together with 5.8S and 5S is shown on the left. B) Proteins were visualised by Western blotting. Staining for SNRNP200 shows close unspecific band, the specific SNRNP200 band is marked by the grey arrow. NTC – nineteen complex

I observed that TSSC4 is not cosedimenting with mature U5 snRNP, which suggests that TSSC4 is not part of mature U5 snRNP or that TSSC4 is interacting with U5 snRNP only transiently. I further analysed the protein composition of U5 snRNP and assembly level of tri-snRNP by the same approach in TSSC4 HeLa depleted cells (figures 5.14 and 5.15).

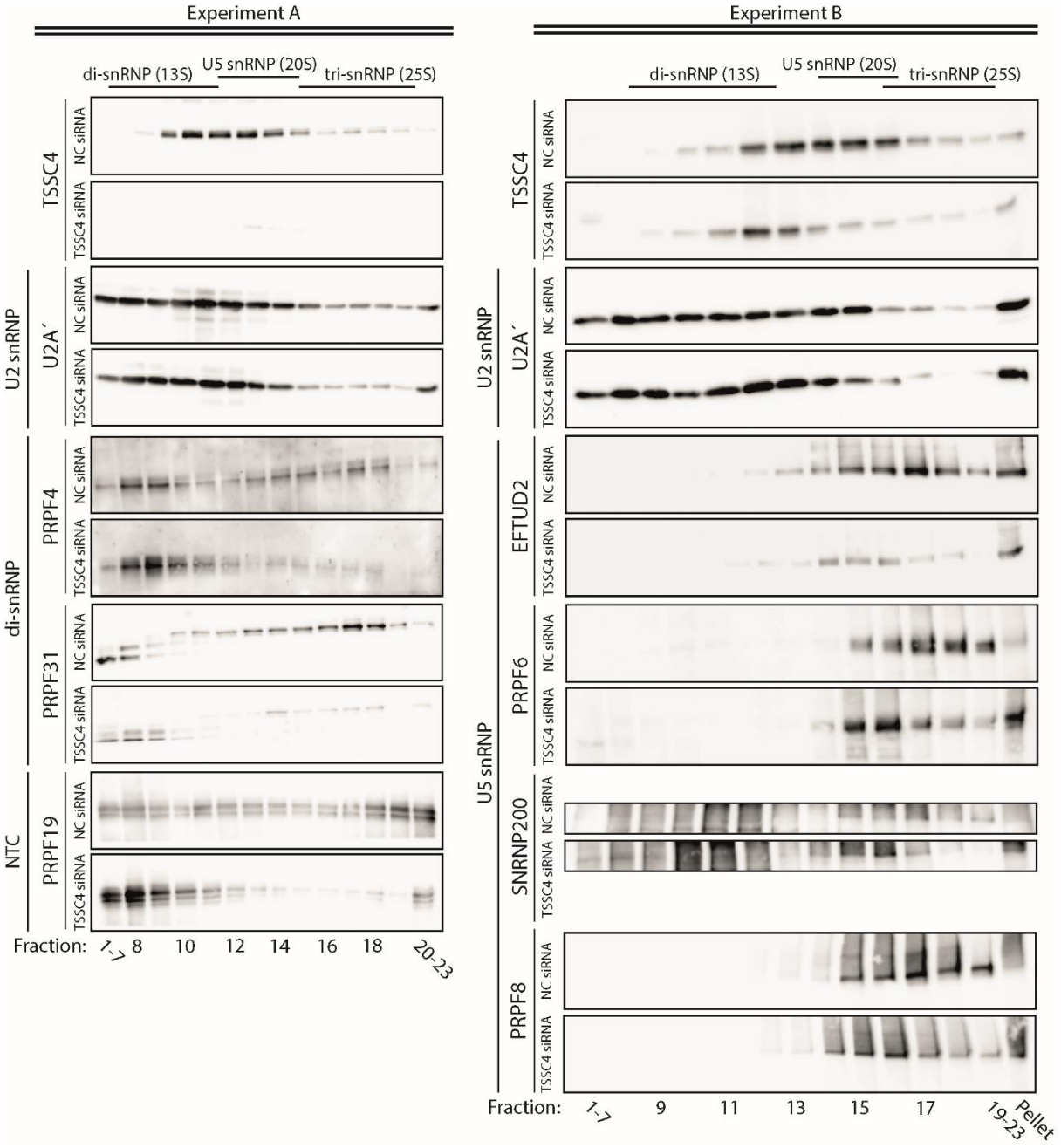

Figure 5.14 Protein composition of U5 snRNP and tri-snRNP from TSSC4 HeLa depleted cells
TSSC4 was depleted from HeLa cells by siRNA interference. Nuclear extract was isolated and separated on a 10-30 % linear glycerol gradient by ultracentrifugation. The gradient was fractioned and proteins were isolated from each fraction. Proteins were visualised by Western blotting. NTC – nineteen complex

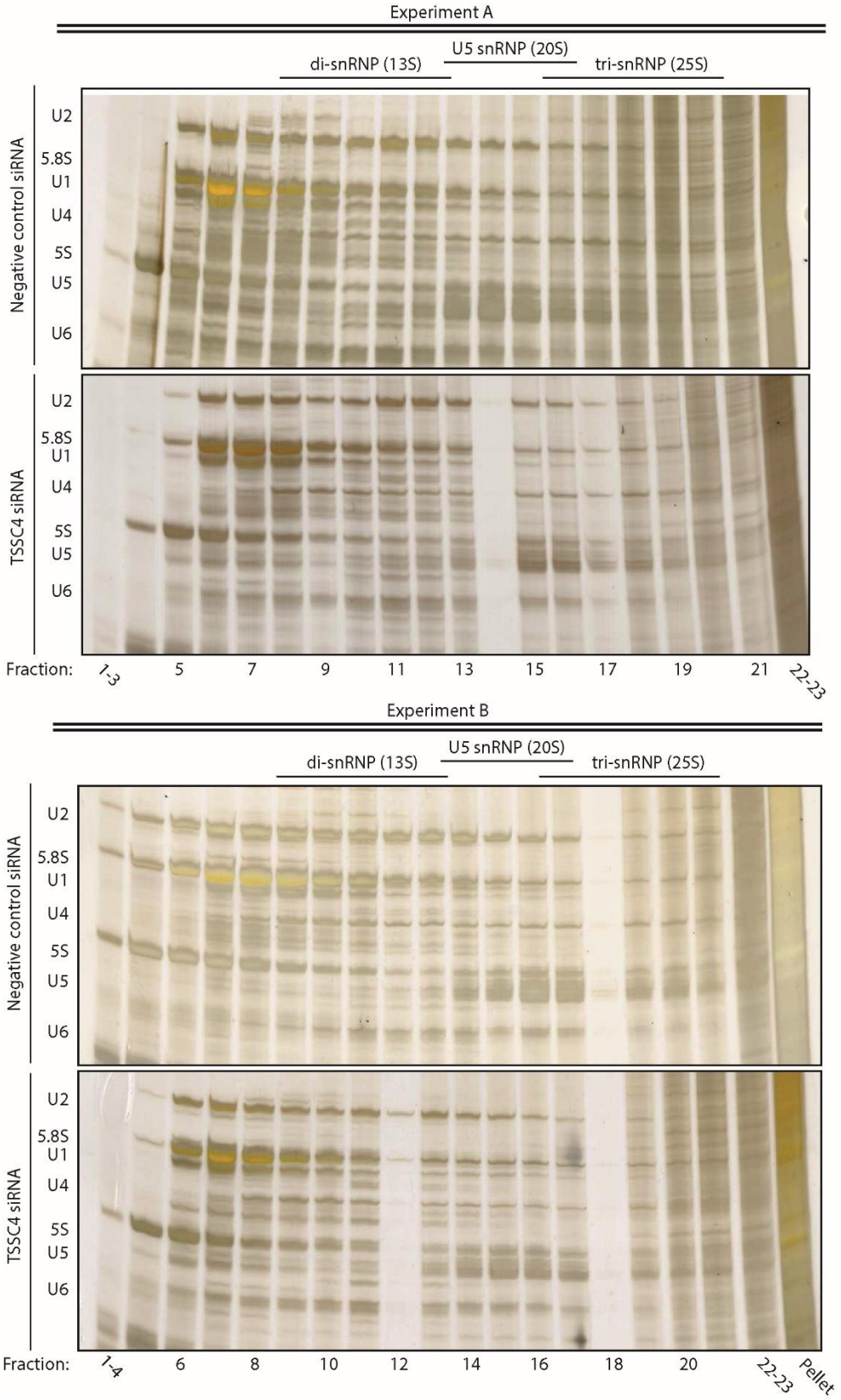

Figure 5.15 Presence and position of individual snRNP specific snRNAs from TSSC4 HeLa depleted cells
TSSC4 was depleted from HeLa cells by siRNA interference. Nuclear extract was isolated and separated on a 10-30 % linear glycerol gradient by ultracentrifugation. The gradient was fractioned and RNA was isolated from each fraction. RNA was resolved by silver-stained PAGE-Urea polyacrylamide gel which was for visualisation of RNA molecules stained by silver. The position of individual snRNAs, together with 5.8S and 5S is shown on the left.

Silver-stained RNA PAGE-Urea polyacrylamide gel was used to determine the position of individual snRNPs. Gel for negative control in experiment A is overloaded and thus hard to analyse, but taken the two experiments together, a weaker signal for tri-snRNAs can be seen, as well as shifting of U5 snRNP to lighter fractions. Both can also be seen in protein levels. These results show that tri-snRNP assembly is inhibited and di-snRNP accumulated upon TSSC4 depletion, which might be the result of misassembled U5 snRNP. I also noticed the presence of TSSC4 in last heavy fraction, which contains the post-catalytic 35S U5 snRNP. U5 snRNP specific proteins are also accumulated in last heavy fraction upon TSSC4 depletion, which might suggest, that TSSC4 could interact with post-catalytic spliceosome and function during U5 snRNP recycling. However, interaction of TSSC4 with post-catalytic spliceosome and function of TSSC4 in U5 snRNP recycling is so far only speculation and needs to be further confirmed.

6 Discussion

TSSC4 was first connected with spliceosomal snRNPs when it was found by mass spectrometry in interaction with PRPF8, a core component of U5 snRNP (Malinova et al. 2017). A few months later, the interaction of TSSC4 with PRPF8 was independently confirmed and further interaction with ZNHIT2, proposed assembly factor of U5 snRNP with TSSC4 was found (Cloutier et al. 2017). It was thus suggested, that TSSC4 may serve as U5 snRNP assembly factor.

We found that TSSC4 is localised to the cell nucleus and confirmed interaction of TSSC4 with U5 snRNP on protein and RNA level. We show that TSSC4 interacting complex does not contain PRPF31, di-snRNP specific protein bridging the interaction with U5 snRNP to form the tri-snRNP (Makarova et al. 2002), which shows, that TSSC4 is not part of the tri-snRNP. Consistently, we did not pull down U4 snRNA with TSSC4-GFP or TSSC4-Flag proteins. We detected interaction of TSSC4 with PRPF19, a component of the NTC complex (Cheng et al. 1993). However, we identified regions of TSSC4 important for U5 snRNP and NTC complex interaction and we show, that interaction of NTC complex with TSSC4 is independent on U5 snRNP. We further observed interaction of TSSC4 with U2 and U6 snRNAs, as well as U2 snRNP specific protein U2A′. Taking together these findings, we hypothesise that TSSC4 could be part of post-catalytic spliceosome.

We also analysed the impact of TSSC4 depletion on HeLa cells. We show, that TSSC4 depletion results in accumulation of all three snRNA components of the tri-snRNP in CBs, indicating the inhibition in snRNP biogenesis (Novotny et al. 2015, Schaffert et al. 2004). We analysed the protein composition of U5 snRNP and we show, that TSSC4 depletion weakens interaction of PRPF8 with SNRNP200. However, we provide evidence, that loosened association of PRPF8 with SNRNP200 does not explain the phenotype of TSSC4 depletion, namely accumulation of snRNAs in CBs.

We analysed the tri-snRNP formation upon TSSC4 depletion and we observed loss of tri-snRNP, as well as accumulation of di-snRNP and possibly post-catalytic 35S U5 snRNP. These results suggest that TSSC4 is important for tri-snRNP formation and potentially U5 snRNP recycling. The inhibition of tri-snRNP assembly is further confirmed by accumulation of 52K in CBs upon TSSC4 depletion. The 52K is a U5 snRNP specific protein not present in tri-snRNP (Laggerbauer et al. 2005), and its localisation in CBs indicates the presence of a complete U5 snRNP not associated with di-snRNP.

Our immunoprecipitation data show that TSSC4 associates with all tested U5-specific proteins, namely PRPF6, PRPF8, EFTUD2 and SNRNP200. However, TSSC4 does not co-migrate with mature U5 snRNP in glycerol gradient. These data thus indicate that TSSC4 associates with incomplete U5 snRNP or alternatively, its interaction with the mature U5 snRNP particle is only transient. It has been shown that TSSC4 interacts with AAR2, known assembly factor of U5 snRNP which suggest, that TSSC4 could participate during U5 snRNP assembly (Gottschalk et al. 2001, Malinova et al. 2017). We show that TSSC4 depletion results in loosened association of two core U5 snRNP components - PRPF8 and SNRNP200. We thus hypothesise that TSSC4 could be a U5 snRNP assembly factor conducive to association of SNRNP200 with U5 snRNP or possibly a stabilisation factor harbouring SNRNP200 within U5 snRNP during spliceosomal rearrangements.

We observed, that TSSC4 depletion results in inhibition of tri-snRNP assembly and accumulation of di-snRNP. Inhibition of tri-snRNP assembly could be caused by misassembly of U5 snRNP. However, we show that TSSC4 is independently on U5 snRNP interacting with PRPF19, a component of the NTC complex. There is a proposed function of NTC complex during tri-snRNP assembly, in which NTC complex could serve as a mediator for ubiquitinases specific for PRPF3 and PRPF31 (Das et al. 2017, Song et al. 2010). It was shown that ubiquitination of di-snRNP specific PRPF3 and PRPF31 enhances the interaction with U5 snRNP specific PRPF8 and thus might potentially stabilise the tri-snRNP (Das et al. 2017, Song et al. 2010). TSSC4 could serve as a mediator for U5 snRNP and NTC complex, which would ensure the proximity of ubiquitinases necessary for PRPF3 and PRPF31 ubiquitination in Cajal bodies.

Interaction of TSSC4, as well as some other poorly identified factors with components of NTC complex was also previously found (Cloutier et al. 2017). NTC complex is integrated to spliceosome during its catalytic activation and stays associated with U5 snRNP after the spliceosome is disassembled, which results in U5 snRNP particle that needs to be recycled by so far unknown mechanism (Chan et al. 2003, Ilagan et al. 2013). It was thus suggested that these factors might be interacting with post-catalytic U5 snRNP (Cloutier et al. 2017). We noticed interaction of TSSC4 with U2 and U6 snRNA suggesting, that TSSC4 might be associated with post-catalytic spliceosome and could have a role in U5 snRNP recycling. Inefficient U5 snRNP recycling could provide an additional explanation for inhibition of tri-snRNP assembly.

7 Conclusions

In this thesis, we confirmed proposed U5 snRNP assembly factor TSSC4 (Cloutier et al. 2017, Malinova et al. 2017) as U5 snRNP specific factor, which is not present in tri-snRNP. In addition to U5 snRNP, we also provide evidence that TSSC4 associates with NTC complex, which guides catalytic activation of the spliceosome (Chan et al. 2003). We also identified TSSC4 domains interacting with U5 snRNP and PRPF19. Since we also observed interaction of TSSC4 with U2 and U6 snRNA, as well as U2 snRNP specific U2A′ we hypothesise, that TSSC4 could associate with the post-catalytic spliceosome.

We show that depletion of TSSC4 from HeLa cells results in accumulation of U5 snRNP in Cajal bodies, nuclear compartments involved in snRNP maturation (Nesic et al. 2004) and we thus suggest, that TSSC4 has a role during U5 snRNP biogenesis. We observed, that upon TSSC4 depletion, U5 snRNP is loosely associated with one of its core components, SNRNP200. TSSC4 might thus be an auxiliary factor for SNRNP200 association with U5 snRNP or, considering the several repositions of SNRNP200 with respect to U5 snRNP during spliceosome rearrangements, TSSC4 might stabilise the interaction of SNRNP200 with U5 snRNP to enable its mobility.

We further present evidence for TSSC4 importance in tri-snRNP assembly. We show, that upon TSSC4 depletion, tri-snRNP is not assembled, which might be direct effect of TSSC4 depletion. However, tri-snRNP assembly inhibition induced by TSSC4 depletion could also be caused by alterations in U5 snRNP and thus its inability to participate in the tri-snRNP assembly, or inefficient U5 snRNP recycling.

We thus identified previously uncharacterized U5 snRNP specific factor, functioning during U5 snRNP assembly or recycling, which is necessary for efficient tri-snRNP assembly.

8 References

Agafonov DE, Kastner B, Dybkov O, Hofele RV, Liu WT, et al. 2016. Molecular architecture of the human U4/U6.U5 tri-snRNP. *Science (New York, N.Y.)* 351: 1416-20

Achsel T, Brahms H, Kastner B, Bachi A, Wilm M, Luhrmann R. 1999. A doughnut-shaped heteromer of human Sm-like proteins binds to the 3'-end of U6 snRNA, thereby facilitating U4/U6 duplex formation in vitro. *The EMBO journal* 18: 5789-802

Allmang C, Kufel J, Chanfreau G, Mitchell P, Petfalski E, Tollervey D. 1999. Functions of the exosome in rRNA, snoRNA and snRNA synthesis. *The EMBO journal* 18: 5399-410

Almeida F, Saffrich R, Ansorge W, Carmo-Fonseca M. 1998. Microinjection of anti-coilin antibodies affects the structure of coiled bodies. *The Journal of cell biology* 142: 899-912

Ansari A, Schwer B. 1995. SLU7 and a novel activity, SSF1, act during the PRP16-dependent step of yeast pre-mRNA splicing. *The EMBO journal* 14: 4001-9

Arenas JE, Abelson JN. 1997. Prp43: An RNA helicase-like factor involved in spliceosome disassembly. *Proceedings of the National Academy of Sciences of the United States of America* 94: 11798-802

Bach M, Winkelmann G, Luhrmann R. 1989. 20S small nuclear ribonucleoprotein U5 shows a surprisingly complex protein composition. *Proceedings of the National Academy of Sciences of the United States of America* 86: 6038-42

Baillat D, Hakimi MA, Naar AM, Shilatifard A, Cooch N, Shiekhattar R. 2005. Integrator, a multiprotein mediator of small nuclear RNA processing, associates with the C-terminal repeat of RNA polymerase II. *Cell* 123: 265-76

Bao P, Hobartner C, Hartmuth K, Luhrmann R. 2017. Yeast Prp2 liberates the 5' splice site and the branch site adenosine for catalysis of pre-mRNA splicing. *Rna* 23: 1770-79

Bartels C, Klatt C, Luhrmann R, Fabrizio P. 2002. The ribosomal translocase homologue Snu114p is involved in unwinding U4/U6 RNA during activation of the spliceosome. *EMBO reports* 3: 875-80

Bartels C, Urlaub H, Luhrmann R, Fabrizio P. 2003. Mutagenesis suggests several roles of Snu114p in pre-mRNA splicing. *The Journal of biological chemistry* 278: 28324-34

Bell M, Schreiner S, Damianov A, Reddy R, Bindereif A. 2002. p110, a novel human U6 snRNP protein and U4/U6 snRNP recycling factor. *The EMBO journal* 21: 2724-35

Berget SM, Moore C, Sharp PA. 1977. Spliced segments at the 5' terminus of adenovirus 2 late mRNA. *Proceedings of the National Academy of Sciences of the United States of America* 74: 3171-5

Bhattacharya R, Perumal K, Sinha K, Maraia R, Reddy R. 2002. Methylphosphate cap structure in small RNAs reduces the affinity of RNAs to La protein. *Gene expression* 10: 243-53

Black DL, Pinto AL. 1989. U5 small nuclear ribonucleoprotein: RNA structure analysis and ATP-dependent interaction with U4/U6. *Molecular and cellular biology* 9: 3350-9

Bogenhagen DF, Brown DD. 1981. Nucleotide sequences in Xenopus 5S DNA required for transcription termination. *Cell* 24: 261-70

Boon KL, Grainger RJ, Ehsani P, Barrass JD, Auchynnikava T, et al. 2007. prp8 mutations that cause human retinitis pigmentosa lead to a U5 snRNP maturation defect in yeast. *Nature structural & molecular biology* 14: 1077-83

Booth BL, Jr., Pugh BF. 1997. Identification and characterization of a nuclease specific for the 3' end of the U6 small nuclear RNA. *The Journal of biological chemistry* 272: 984-91

Carmo-Fonseca M, Pepperkok R, Carvalho MT, Lamond AI. 1992. Transcription-dependent colocalization of the U1, U2, U4/U6, and U5 snRNPs in coiled bodies. *The Journal of cell biology* 117: 1-14

Cloutier P, Poitras C, Durand M, Hekmat O, Fiola-Masson E, et al. 2017. R2TP/Prefoldin-like component RUVBL1/RUVBL2 directly interacts with ZNHIT2 to regulate assembly of U5 small nuclear ribonucleoprotein. *Nature communications* 8: 15615

Company M, Arenas J, Abelson J. 1991. Requirement of the RNA helicase-like protein PRP22 for release of messenger RNA from spliceosomes. *Nature* 349: 487-93

Cozzarelli NR, Gerrard SP, Schlissel M, Brown DD, Bogenhagen DF. 1983. Purified RNA polymerase III accurately and efficiently terminates transcription of 5S RNA genes. *Cell* 34: 829-35

Cuello P, Boyd DC, Dye MJ, Proudfoot NJ, Murphy S. 1999. Transcription of the human U2 snRNA genes continues beyond the 3' box in vivo. *The EMBO journal* 18: 2867-77

Cvackova Z, Mateju D, Stanek D. 2014. Retinitis Pigmentosa Mutations of SNRNP200 Enhance Cryptic Splice-Site Recognition. *Hum Mutat* 35: 308-17

Das R, Zhou Z, Reed R. 2000. Functional association of U2 snRNP with the ATP-independent spliceosomal complex E. *Molecular cell* 5: 779-87

Das T, Park JK, Park J, Kim E, Rape M, et al. 2017. USP15 regulates dynamic protein-protein interactions of the spliceosome through deubiquitination of PRP31. *Nucleic acids research* 45: 4866-80

Didychuk AL, Montemayor EJ, Brow DA, Butcher SE. 2016. Structural requirements for protein-catalyzed annealing of U4 and U6 RNAs during di-snRNP assembly. *Nucleic acids research* 44: 1398-410

Du H, Rosbash M. 2002. The U1 snRNP protein U1C recognizes the 5' splice site in the absence of base pairing. *Nature* 419: 86-90

Dziembowski A, Lorentzen E, Conti E, Seraphin B. 2007. A single subunit, Dis3, is essentially responsible for yeast exosome core activity. *Nature structural & molecular biology* 14: 15-22

Fabrizio P, Dannenberg J, Dube P, Kastner B, Stark H, et al. 2009. The evolutionarily conserved core design of the catalytic activation step of the yeast spliceosome. *Molecular cell* 36: 593-608

Fabrizio P, Laggerbauer B, Lauber J, Lane WS, Luhrmann R. 1997. An evolutionarily conserved U5 snRNP-specific protein is a GTP-binding factor closely related to the ribosomal translocase EF-2. *The EMBO journal* 16: 4092-106

Fica SM, Oubridge C, Wilkinson ME, Newman AJ, Nagai K. 2019. A human postcatalytic spliceosome structure reveals essential roles of metazoan factors for exon ligation. *Science (New York, N.Y.)* 363: 710-14

Fica SM, Tuttle N, Novak T, Li NS, Lu J, et al. 2013. RNA catalyses nuclear pre-mRNA splicing. *Nature* 503: 229-34

Fischer U, Luhrmann R. 1990. An essential signaling role for the m3G cap in the transport of U1 snRNP to the nucleus. *Science (New York, N.Y.)* 249: 786-90

Fischer U, Sumpter V, Sekine M, Satoh T, Luhrmann R. 1993. Nucleo-cytoplasmic transport of U snRNPs: definition of a nuclear location signal in the Sm core domain that binds a transport receptor independently of the m3G cap. *The EMBO journal* 12: 573-83

Fourmann JB, Schmitzova J, Christian H, Urlaub H, Ficner R, et al. 2013. Dissection of the factor requirements for spliceosome disassembly and the elucidation of its dissociation products using a purified splicing system. *Genes & development* 27: 413-28

Frey MR, Bailey AD, Weiner AM, Matera AG. 1999. Association of snRNA genes with coiled bodies is mediated by nascent snRNA transcripts. *Current biology : CB* 9: 126-35

Friesen WJ, Paushkin S, Wyce A, Massenet S, Pesiridis GS, et al. 2001. The methylosome, a 20S complex containing JBP1 and pICln, produces dimethylarginine-modified Sm proteins. *Molecular and cellular biology* 21: 8289-300

Ganot P, Jady BE, Bortolin ML, Darzacq X, Kiss T. 1999. Nucleolar factors direct the 2'-O-ribose methylation and pseudouridylation of U6 spliceosomal RNA. *Molecular and cellular biology* 19: 6906-17

Ghetti A, Company M, Abelson J. 1995. Specificity of Prp24 binding to RNA: a role for Prp24 in the dynamic interaction of U4 and U6 snRNAs. *Rna* 1: 132-45

Gottschalk A, Kastner B, Luhrmann R, Fabrizio P. 2001. The yeast U5 snRNP coisolated with the U1 snRNP has an unexpected protein composition and includes the splicing factor Aar2p. *Rna* 7: 1554-65

Grimm C, Chari A, Pelz JP, Kuper J, Kisker C, et al. 2013. Structural basis of assembly chaperone- mediated snRNP formation. *Molecular cell* 49: 692-703

Hamm J, Mattaj IW. 1990. Monomethylated cap structures facilitate RNA export from the nucleus. *Cell* 63: 109-18

Hausmann S, Shuman S. 2005. Specificity and mechanism of RNA cap guanine-N2 methyltransferase (Tgs1). *The Journal of biological chemistry* 280: 4021-4

Hawkins JD. 1988. A survey on intron and exon lengths. *Nucleic acids research* 16: 9893-908

Hebert MD, Matera AG. 2000. Self-association of coilin reveals a common theme in nuclear body localization. *Molecular biology of the cell* 11: 4159-71

Hermann H, Fabrizio P, Raker VA, Foulaki K, Hornig H, et al. 1995. snRNP Sm proteins share two evolutionarily conserved sequence motifs which are involved in Sm protein-protein interactions. *The EMBO journal* 14: 2076-88

Hoffman BE, Grabowski PJ. 1992. U1 snRNP targets an essential splicing factor, U2AF65, to the 3' splice site by a network of interactions spanning the exon. *Genes & development* 6: 2554-68

Horowitz DS, Abelson J. 1993. Stages in the second reaction of pre-mRNA splicing: the final step is ATP independent. *Genes & development* 7: 320-9

Huang Q, Jacobson MR, Pederson T. 1997. 3' processing of human pre-U2 small nuclear RNA: a base-pairing interaction between the 3' extension of the precursor and an internal region. *Molecular and cellular biology* 17: 7178-85

Huber J, Cronshagen U, Kadokura M, Marshallsay C, Wada T, et al. 1998. Snurportin1, an m3G-cap-specific nuclear import receptor with a novel domain structure. *The EMBO journal* 17: 4114-26

Hutten S, Kehlenbach RH. 2007. CRM1-mediated nuclear export: to the pore and beyond. *Trends in cell biology* 17: 193-201

Chan SP, Kao DI, Tsai WY, Cheng SC. 2003. The Prp19p-associated complex in spliceosome activation. *Science (New York, N.Y.)* 302: 279-82

Chari A, Golas MM, Klingenhager M, Neuenkirchen N, Sander B, et al. 2008. An assembly chaperone collaborates with the SMN complex to generate spliceosomal SnRNPs. *Cell* 135: 497-509

Chen HC, Tseng CK, Tsai RT, Chung CS, Cheng SC. 2013. Link of NTR-mediated spliceosome disassembly with DEAH-box ATPases Prp2, Prp16, and Prp22. *Molecular and cellular biology* 33: 514-25

Chen Z, Gui B, Zhang Y, Xie G, Li W, et al. 2017. Identification of a 35S U4/U6.U5 tri-small nuclear ribonucleoprotein (tri-snRNP) complex intermediate in spliceosome assembly. *The Journal of biological chemistry* 292: 18113-28

Cheng SC, Tarn WY, Tsao TY, Abelson J. 1993. PRP19: a novel spliceosomal component. *Molecular and cellular biology* 13: 1876-82

Chow LT, Gelinas RE, Broker TR, Roberts RJ. 1977. An amazing sequence arrangement at the 5' ends of adenovirus 2 messenger RNA. *Cell* 12: 1-8

Ilagan JO, Chalkley RJ, Burlingame AL, Jurica MS. 2013. Rearrangements within human spliceosomes captured after exon ligation. *Rna* 19: 400-12

Izaurralde E, Lewis J, Gamberi C, Jarmolowski A, McGuigan C, Mattaj IW. 1995. A cap-binding protein complex mediating U snRNA export. *Nature* 376: 709-12

Jady BE, Darzacq X, Tucker KE, Matera AG, Bertrand E, Kiss T. 2003. Modification of Sm small nuclear RNAs occurs in the nucleoplasmic Cajal body following import from the cytoplasm. *The EMBO journal* 22: 1878-88

Kandels-Lewis S, Seraphin B. 1993. Involvement of U6 snRNA in 5' splice site selection. *Science (New York, N.Y.)* 262: 2035-9

Kim SH, Lin RJ. 1996. Spliceosome activation by PRP2 ATPase prior to the first transesterification reaction of pre-mRNA splicing. *Molecular and cellular biology* 16: 6810-9

Kitao S, Segref A, Kast J, Wilm M, Mattaj IW, Ohno M. 2008. A compartmentalized phosphorylation/dephosphorylation system that regulates U snRNA export from the nucleus. *Molecular and cellular biology* 28: 487-97

Klingauf M, Stanek D, Neugebauer KM. 2006. Enhancement of U4/U6 small nuclear ribonucleoprotein particle association in Cajal bodies predicted by mathematical modeling. *Molecular biology of the cell* 17: 4972-81

Konarska MM, Sharp PA. 1986. Electrophoretic separation of complexes involved in the splicing of precursors to mRNAs. *Cell* 46: 845-55

Konkel DA, Tilghman SM, Leder P. 1978. The sequence of the chromosomal mouse beta-globin major gene: homologies in capping, splicing and poly(A) sites. *Cell* 15: 1125-32

Labno A, Warkocki Z, Kulinski T, Krawczyk PS, Bijata K, et al. 2016. Perlman syndrome nuclease DIS3L2 controls cytoplasmic non-coding RNAs and provides surveillance pathway for maturing snRNAs. *Nucleic acids research* 44: 10437-53

Laggerbauer B, Achsel T, Luhrmann R. 1998. The human U5-200kD DEXH-box protein unwinds U4/U6 RNA duplices in vitro. *Proceedings of the National Academy of Sciences of the United States of America* 95: 4188-92

Laggerbauer B, Liu S, Makarov E, Vornlocher HP, Makarova O, et al. 2005. The human U5 snRNP 52K protein (CD2BP2) interacts with U5-102K (hPrp6), a U4/U6.U5 tri-snRNP bridging protein, but dissociates upon tri-snRNP formation. *Rna* 11: 598-608

Lange TS, Gerbi SA. 2000. Transient nucleolar localization Of U6 small nuclear RNA in Xenopus Laevis oocytes. *Molecular biology of the cell* 11: 2419-28

Lau CK, Bachorik JL, Dreyfuss G. 2009. Gemin5-snRNA interaction reveals an RNA binding function for WD repeat domains. *Nature structural & molecular biology* 16: 486-91

Lauber J, Plessel G, Prehn S, Will CL, Fabrizio P, et al. 1997. The human U4/U6 snRNP contains 60 and 90kD proteins that are structurally homologous to the yeast splicing factors Prp4p and Prp3p. *Rna* 3: 926-41

Lesser CF, Guthrie C. 1993. Mutations in U6 snRNA that alter splice site specificity: implications for the active site. *Science (New York, N.Y.)* 262: 1982-8

Licht K, Medenbach J, Luhrmann R, Kambach C, Bindereif A. 2008. 3'-cyclic phosphorylation of U6 snRNA leads to recruitment of recycling factor p110 through LSm proteins. *Rna* 14: 1532-8

Liu S, Mozaffari-Jovin S, Wollenhaupt J, Santos KF, Theuser M, et al. 2015. A composite double-/single-stranded RNA-binding region in protein Prp3 supports tri-snRNP stability and splicing. *eLife* 4: e07320

Liu S, Rauhut R, Vornlocher HP, Luhrmann R. 2006. The network of protein-protein interactions within the human U4/U6.U5 tri-snRNP. *Rna* 12: 1418-30

Lobo SM, Hernandez N. 1989. A 7 bp mutation converts a human RNA polymerase II snRNA promoter into an RNA polymerase III promoter. *Cell* 58: 55-67

Lund E, Dahlberg JE. 1992. Cyclic 2',3'-phosphates and nontemplated nucleotides at the 3' end of spliceosomal U6 small nuclear RNA's. *Science (New York, N.Y.)* 255: 327-30

Madhani HD, Guthrie C. 1992. A novel base-pairing interaction between U2 and U6 snRNAs suggests a mechanism for the catalytic activation of the spliceosome. *Cell* 71: 803-17

Madore SJ, Wieben ED, Pederson T. 1984. Intracellular site of U1 small nuclear RNA processing and ribonucleoprotein assembly. *The Journal of cell biology* 98: 188-92

Maeder C, Kutach AK, Guthrie C. 2009. ATP-dependent unwinding of U4/U6 snRNAs by the Brr2 helicase requires the C terminus of Prp8. *Nature structural & molecular biology* 16: 42-8

Machyna M, Kehr S, Straube K, Kappei D, Buchholz F, et al. 2014. The coilin interactome identifies hundreds of small noncoding RNAs that traffic through Cajal bodies. *Molecular cell* 56: 389-99

Makarov EM, Makarova OV, Urlaub H, Gentzel M, Will CL, et al. 2002. Small nuclear ribonucleoprotein remodeling during catalytic activation of the spliceosome. *Science (New York, N.Y.)* 298: 2205-8

Makarova OV, Makarov EM. 2015. The 35S U5 snRNP Is Generated from the Activated Spliceosome during In vitro Splicing. *PloS one* 10: e0128430

Makarova OV, Makarov EM, Liu S, Vornlocher HP, Luhrmann R. 2002. Protein 61K, encoded by a gene (PRPF31) linked to autosomal dominant retinitis pigmentosa, is required for U4/U6*U5 tri-snRNP formation and pre-mRNA splicing. *The EMBO journal* 21: 1148-57

Malinova A, Cvackova Z, Mateju D, Horejsi Z, Abeza C, et al. 2017. Assembly of the U5 snRNP component PRPF8 is controlled by the HSP90/R2TP chaperones. *The Journal of cell biology* 216: 1579-96

Martin-Tumasz S, Richie AC, Clos LJ, 2nd, Brow DA, Butcher SE. 2011. A novel occluded RNA recognition motif in Prp24 unwinds the U6 RNA internal stem loop. *Nucleic acids research* 39: 7837-47

Martin A, Schneider S, Schwer B. 2002. Prp43 is an essential RNA-dependent ATPase required for release of lariat-intron from the spliceosome. *The Journal of biological chemistry* 277: 17743-50

Masuyama K, Taniguchi I, Kataoka N, Ohno M. 2004. RNA length defines RNA export pathway. *Genes & development* 18: 2074-85

Matera AG, Wang Z. 2014. A day in the life of the spliceosome. *Nature reviews. Molecular cell biology* 15: 108-21

Matera AG, Ward DC. 1993. Nucleoplasmic organization of small nuclear ribonucleoproteins in cultured human cells. *The Journal of cell biology* 121: 715-27

Mathew R, Hartmuth K, Mohlmann S, Urlaub H, Ficner R, Luhrmann R. 2008. Phosphorylation of human PRP28 by SRPK2 is required for integration of the U4/U6-U5 tri-snRNP into the spliceosome. *Nature structural & molecular biology* 15: 435-43

Mattaj IW, Dathan NA, Parry HD, Carbon P, Krol A. 1988. Changing the RNA polymerase specificity of U snRNA gene promoters. *Cell* 55: 435-42

McCloskey A, Taniguchi I, Shinmyozu K, Ohno M. 2012. hnRNP C tetramer measures RNA length to classify RNA polymerase II transcripts for export. *Science (New York, N.Y.)* 335: 1643-6

Meister G, Eggert C, Buhler D, Brahms H, Kambach C, Fischer U. 2001. Methylation of Sm proteins by a complex containing PRMT5 and the putative U snRNP assembly factor pICln. *Current biology : CB* 11: 1990-4

Meister G, Fischer U. 2002. Assisted RNP assembly: SMN and PRMT5 complexes cooperate in the formation of spliceosomal UsnRNPs. *The EMBO journal* 21: 5853-63

Mouaikel J, Narayanan U, Verheggen C, Matera AG, Bertrand E, et al. 2003. Interaction between the small-nuclear-RNA cap hypermethylase and the spinal muscular atrophy protein, survival of motor neuron. *EMBO reports* 4: 616-22

Mroczek S, Krwawicz J, Kutner J, Lazniewski M, Kucinski I, et al. 2012. C16orf57, a gene mutated in poikiloderma with neutropenia, encodes a putative phosphodiesterase responsible for the U6 snRNA 3' end modification. *Genes & development* 26: 1911-25

Narayanan U, Achsel T, Luhrmann R, Matera AG. 2004. Coupled in vitro import of U snRNPs and SMN, the spinal muscular atrophy protein. *Molecular cell* 16: 223-34

Narayanan U, Ospina JK, Frey MR, Hebert MD, Matera AG. 2002. SMN, the spinal muscular atrophy protein, forms a pre-import snRNP complex with snurportin1 and importin beta. *Human molecular genetics* 11: 1785-95

Nesic D, Tanackovic G, Kramer A. 2004. A role for Cajal bodies in the final steps of U2 snRNP biogenesis. *Journal of cell science* 117: 4423-33

Neuman de Vegvar HE, Dahlberg JE. 1990. Nucleocytoplasmic transport and processing of small nuclear RNA precursors. *Molecular and cellular biology* 10: 3365-75

Nottrott S, Urlaub H, Luhrmann R. 2002. Hierarchical, clustered protein interactions with U4/U6 snRNA: a biochemical role for U4/U6 proteins. *The EMBO journal* 21: 5527-38

Novotny I, Blazikova M, Stanek D, Herman P, Malinsky J. 2011. In vivo kinetics of U4/U6.U5 tri-snRNP formation in Cajal bodies. *Molecular biology of the cell* 22: 513-23

Novotny I, Malinova A, Stejskalova E, Mateju D, Klimesova K, et al. 2015. SART3-Dependent Accumulation of Incomplete Spliceosomal snRNPs in Cajal Bodies. *Cell reports*

Novotny I, Podolska K, Blazikova M, Valasek LS, Svoboda P, Stanek D. 2012. Nuclear LSm8 affects number of cytoplasmic processing bodies via controlling cellular distribution of Like-Sm proteins. *Molecular biology of the cell* 23: 3776-85

O'Reilly D, Kuznetsova OV, Laitem C, Zaborowska J, Dienstbier M, Murphy S. 2014. Human snRNA genes use polyadenylation factors to promote efficient transcription termination. *Nucleic acids research* 42: 264-75

Ohno M, Segref A, Bachi A, Wilm M, Mattaj IW. 2000. PHAX, a mediator of U snRNA nuclear export whose activity is regulated by phosphorylation. *Cell* 101: 187-98

Otter S, Grimmler M, Neuenkirchen N, Chari A, Sickmann A, Fischer U. 2007. A comprehensive interaction map of the human survival of motor neuron (SMN) complex. *The Journal of biological chemistry* 282: 5825-33

Palacios I, Hetzer M, Adam SA, Mattaj IW. 1997. Nuclear import of U snRNPs requires importin beta. *The EMBO journal* 16: 6783-92

Park JK, Das T, Song EJ, Kim EE. 2016. Structural basis for recruiting and shuttling of the spliceosomal deubiquitinase USP4 by SART3. *Nucleic acids research* 44: 5424-37

Patel SB, Bellini M. 2008. The assembly of a spliceosomal small nuclear ribonucleoprotein particle. *Nucleic acids research* 36: 6482-93

Pellizzoni L, Yong J, Dreyfuss G. 2002. Essential role for the SMN complex in the specificity of snRNP assembly. *Science (New York, N.Y.)* 298: 1775-9

Plaschka C, Lin PC, Nagai K. 2017. Structure of a pre-catalytic spliceosome. *Nature* 546: 617-21

Plessel G, Fischer U, Luhrmann R. 1994. m3G cap hypermethylation of U1 small nuclear ribonucleoprotein (snRNP) in vitro: evidence that the U1 small nuclear RNA-(guanosine-N2)-methyltransferase is a non-snRNP cytoplasmic protein that requires a binding site on the Sm core domain. *Molecular and cellular biology* 14: 4160-72

Pozzi B, Bragado L, Will CL, Mammi P, Risso G, et al. 2017. SUMO conjugation to spliceosomal proteins is required for efficient pre-mRNA splicing. *Nucleic acids research* 45: 6729-45

Raghunathan PL, Guthrie C. 1998. RNA unwinding in U4/U6 snRNPs requires ATP hydrolysis and the DEIH-box splicing factor Brr2. *Current biology : CB* 8: 847-55

Raker VA, Plessel G, Luhrmann R. 1996. The snRNP core assembly pathway: identification of stable core protein heteromeric complexes and an snRNP subcore particle in vitro. *The EMBO journal* 15: 2256-69

Raska I, Ochs RL, Andrade LE, Chan EK, Burlingame R, et al. 1990. Association between the nucleolus and the coiled body. *Journal of structural biology* 104: 120-7

Roithova A, Klimesova K, Panek J, Will CL, Luhrmann R, et al. 2018. The Sm-core mediates the retention of partially-assembled spliceosomal snRNPs in Cajal bodies until their full maturation. *Nucleic acids research* 46: 3774-90

Ruskin B, Krainer AR, Maniatis T, Green MR. 1984. Excision of an intact intron as a novel lariat structure during pre-mRNA splicing in vitro. *Cell* 38: 317-31

Sadowski CL, Henry RW, Lobo SM, Hernandez N. 1993. Targeting TBP to a non-TATA box cis-regulatory element: a TBP-containing complex activates transcription from snRNA promoters through the PSE. *Genes & development* 7: 1535-48

Selenko P, Sprangers R, Stier G, Buhler D, Fischer U, Sattler M. 2001. SMN tudor domain structure and its interaction with the Sm proteins. *Nature structural biology* 8: 27-31

Shchepachev V, Wischnewski H, Missiaglia E, Soneson C, Azzalin CM. 2012. Mpn1, mutated in poikiloderma with neutropenia protein 1, is a conserved 3'-to-5' RNA exonuclease processing U6 small nuclear RNA. *Cell reports* 2: 855-65

Shimba S, Reddy R. 1994. Purification of human U6 small nuclear RNA capping enzyme. Evidence for a common capping enzyme for gamma-monomethyl-capped small RNAs. *The Journal of biological chemistry* 269: 12419-23

Shumyatsky GP, Tillib SV, Kramerov DA. 1990. B2 RNA and 7SK RNA, RNA polymerase III transcripts, have a cap-like structure at their 5' end. *Nucleic acids research* 18: 6347-51

Schaffert N, Hossbach M, Heintzmann R, Achsel T, Luhrmann R. 2004. RNAi knockdown of hPrp31 leads to an accumulation of U4/U6 di-snRNPs in Cajal bodies. *The EMBO journal* 23: 3000-9

Schaub M, Myslinski E, Schuster C, Krol A, Carbon P. 1997. Staf, a promiscuous activator for enhanced transcription by RNA polymerases II and III. *The EMBO journal* 16: 173-81

Schreib CC, Bowman EK, Hernandez CA, Lucas AL, Potts CHS, Maeder C. 2018. Functional and Biochemical Characterization of Dib1's Role in Pre-Messenger RNA Splicing. *Journal of molecular biology* 430: 1640-51

Schwer B. 2008. A conformational rearrangement in the spliceosome sets the stage for Prp22-dependent mRNA release. *Molecular cell* 30: 743-54

Schwer B, Gross CH. 1998. Prp22, a DExH-box RNA helicase, plays two distinct roles in yeast pre-mRNA splicing. *The EMBO journal* 17: 2086-94

Schwer B, Guthrie C. 1992. A conformational rearrangement in the spliceosome is dependent on PRP16 and ATP hydrolysis. *The EMBO journal* 11: 5033-9

Small EC, Leggett SR, Winans AA, Staley JP. 2006. The EF-G-like GTPase Snu114p regulates spliceosome dynamics mediated by Brr2p, a DExD/H box ATPase. *Molecular cell* 23: 389-99

Smith KP, Carter KC, Johnson CV, Lawrence JB. 1995. U2 and U1 snRNA gene loci associate with coiled bodies. *Journal of cellular biochemistry* 59: 473-85

Song EJ, Werner SL, Neubauer J, Stegmeier F, Aspden J, et al. 2010. The Prp19 complex and the Usp4Sart3 deubiquitinating enzyme control reversible ubiquitination at the spliceosome. *Genes & development* 24: 1434-47

Staley JP, Guthrie C. 1999. An RNA switch at the 5' splice site requires ATP and the DEAD box protein Prp28p. *Molecular cell* 3: 55-64

Stanek D, Neugebauer KM. 2004. Detection of snRNP assembly intermediates in Cajal bodies by fluorescence resonance energy transfer. *The Journal of cell biology* 166: 1015-25

Stanek D, Pridalova-Hnilicova J, Novotny I, Huranova M, Blazikova M, et al. 2008. Spliceosomal small nuclear ribonucleoprotein particles repeatedly cycle through Cajal bodies. *Molecular biology of the cell* 19: 2534-43

Stanek D, Rader SD, Klingauf M, Neugebauer KM. 2003. Targeting of U4/U6 small nuclear RNP assembly factor SART3/p110 to Cajal bodies. *The Journal of cell biology* 160: 505-16

Steinmetz EJ, Conrad NK, Brow DA, Corden JL. 2001. RNA-binding protein Nrd1 directs poly(A)-independent 3'-end formation of RNA polymerase II transcripts. *Nature* 413: 327-31

Stevens SW, Barta I, Ge HY, Moore RE, Young MK, et al. 2001. Biochemical and genetic analyses of the U5, U6, and U4/U6 x U5 small nuclear ribonucleoproteins from Saccharomyces cerevisiae. *Rna* 7: 1543-53

Strzelecka M, Trowitzsch S, Weber G, Luhrmann R, Oates AC, Neugebauer KM. 2010. Coilin-dependent snRNP assembly is essential for zebrafish embryogenesis. *Nature structural & molecular biology* 17: 403-9

Sun JS, Manley JL. 1995. A novel U2-U6 snRNA structure is necessary for mammalian mRNA splicing. *Genes & development* 9: 843-54

Tanaka N, Aronova A, Schwer B. 2007. Ntr1 activates the Prp43 helicase to trigger release of lariat-intron from the spliceosome. *Genes & development* 21: 2312-25

Terns MP, Lund E, Dahlberg JE. 1992. 3'-end-dependent formation of U6 small nuclear ribonucleoprotein particles in Xenopus laevis oocyte nuclei. *Molecular and cellular biology* 12: 3032-40

Tomecki R, Kristiansen MS, Lykke-Andersen S, Chlebowski A, Larsen KM, et al. 2010. The human core exosome interacts with differentially localized processive RNases: hDIS3 and hDIS3L. *The EMBO journal* 29: 2342-57

Trippe R, Guschina E, Hossbach M, Urlaub H, Luhrmann R, Benecke BJ. 2006. Identification, cloning, and functional analysis of the human U6 snRNA-specific terminal uridylyl transferase. *Rna* 12: 1494-504

Trippe R, Sandrock B, Benecke BJ. 1998. A highly specific terminal uridylyl transferase modifies the 3'-end of U6 small nuclear RNA. *Nucleic acids research* 26: 3119-26

Tsai RT, Fu RH, Yeh FL, Tseng CK, Lin YC, et al. 2005. Spliceosome disassembly catalyzed by Prp43 and its associated components Ntr1 and Ntr2. *Genes & development* 19: 2991-3003

Tsai RT, Tseng CK, Lee PJ, Chen HC, Fu RH, et al. 2007. Dynamic interactions of Ntr1-Ntr2 with Prp43 and with U5 govern the recruitment of Prp43 to mediate spliceosome disassembly. *Molecular and cellular biology* 27: 8027-37

Tycowski KT, You ZH, Graham PJ, Steitz JA. 1998. Modification of U6 spliceosomal RNA is guided by other small RNAs. *Molecular cell* 2: 629-38

Ustianenko D, Pasulka J, Feketova Z, Bednarik L, Zigackova D, et al. 2016. TUT-DIS3L2 is a mammalian surveillance pathway for aberrant structured non-coding RNAs. *The EMBO journal* 35: 2179-91

Valcarcel J, Gaur RK, Singh R, Green MR. 1996. Interaction of U2AF65 RS region with pre-mRNA branch point and promotion of base pairing with U2 snRNA [corrected]. *Science (New York, N.Y.)* 273: 1706-9

van Hoof A, Lennertz P, Parker R. 2000. Yeast exosome mutants accumulate 3'-extended polyadenylated forms of U4 small nuclear RNA and small nucleolar RNAs. *Molecular and cellular biology* 20: 441-52

Vasiljeva L, Buratowski S. 2006. Nrd1 interacts with the nuclear exosome for 3 ' processing of RNA polymerase II transcripts. *Molecular cell* 21: 239-48

Wagner JD, Jankowsky E, Company M, Pyle AM, Abelson JN. 1998. The DEAH-box protein PRP22 is an ATPase that mediates ATP-dependent mRNA release from the spliceosome and unwinds RNA duplexes. *The EMBO journal* 17: 2926-37

Wahl MC, Will CL, Luhrmann R. 2009. The spliceosome: design principles of a dynamic RNP machine. *Cell* 136: 701-18

Weber G, Cristao VF, de LAF, Santos KF, Holton N, et al. 2011. Mechanism for Aar2p function as a U5 snRNP assembly factor. *Genes & development* 25: 1601-12

Will CL, Luhrmann R. 2011. Spliceosome structure and function. *Cold Spring Harbor perspectives in biology* 3

Wu Z, Murphy C, Gall JG. 1994. Human p80-coilin is targeted to sphere organelles in the amphibian germinal vesicle. *Molecular biology of the cell* 5: 1119-27

Xu YZ, Newnham CM, Kameoka S, Huang T, Konarska MM, Query CC. 2004. Prp5 bridges U1 and U2 snRNPs and enables stable U2 snRNP association with intron RNA. *The EMBO journal* 23: 376-85

Yan C, Hang J, Wan R, Huang M, Wong CC, Shi Y. 2015. Structure of a yeast spliceosome at 3.6-angstrom resolution. *Science (New York, N.Y.)* 349: 1182-91

Yang H, Moss ML, Lund E, Dahlberg JE. 1992. Nuclear processing of the 3'-terminal nucleotides of pre-U1 RNA in Xenopus laevis oocytes. *Molecular and cellular biology* 12: 1553-60

Yong J, Kasim M, Bachorik JL, Wan L, Dreyfuss G. 2010. Gemin5 delivers snRNA precursors to the SMN complex for snRNP biogenesis. *Molecular cell* 38: 551-62

Yoshimoto R, Kataoka N, Okawa K, Ohno M. 2009. Isolation and characterization of post-splicing lariat-intron complexes. *Nucleic acids research* 37: 891-902

Yu YT, Shu MD, Steitz JA. 1998. Modifications of U2 snRNA are required for snRNP assembly and pre-mRNA splicing. *The EMBO journal* 17: 5783-95

Zamore PD, Green MR. 1989. Identification, purification, and biochemical characterization of U2 small nuclear ribonucleoprotein auxiliary factor. *Proceedings of the National Academy of Sciences of the United States of America* 86: 9243-7

Zaric B, Chami M, Remigy H, Engel A, Ballmer-Hofer K, et al. 2005. Reconstitution of two recombinant LSm protein complexes reveals aspects of their architecture, assembly, and function. *The Journal of biological chemistry* 280: 16066-75

Zhan X, Yan C, Zhang X, Lei J, Shi Y. 2018a. Structure of a human catalytic step I spliceosome. *Science (New York, N.Y.)* 359: 537-45

Zhan X, Yan C, Zhang X, Lei J, Shi Y. 2018b. Structures of the human pre-catalytic spliceosome and its precursor spliceosome. *Cell research* 28: 1129-40

Zhang Q, Harding R, Hou F, Dong A, Walker JR, et al. 2016. Structural Basis of the Recruitment of Ubiquitin-specific Protease USP15 by Spliceosome Recycling Factor SART3. *The Journal of biological chemistry* 291: 17283-92

Zhuang Y, Weiner AM. 1986. A compensatory base change in U1 snRNA suppresses a 5' splice site mutation. *Cell* 46: 827-35